


6-2016

The Growth and Ecology of Upper Cambrian Microbialite Biostromes from the Notch Peak Formation in Utah

Ken P. Coulson

Follow this and additional works at: <http://scholarsrepository.llu.edu/etd>

 Part of the [Geology Commons](#), and the [Paleontology Commons](#)

Recommended Citation

Coulson, Ken P., "The Growth and Ecology of Upper Cambrian Microbialite Biostromes from the Notch Peak Formation in Utah" (2016). *Loma Linda University Electronic Theses, Dissertations & Projects*. 367.
<http://scholarsrepository.llu.edu/etd/367>

This Dissertation is brought to you for free and open access by TheScholarsRepository@LLU: Digital Archive of Research, Scholarship & Creative Works. It has been accepted for inclusion in Loma Linda University Electronic Theses, Dissertations & Projects by an authorized administrator of TheScholarsRepository@LLU: Digital Archive of Research, Scholarship & Creative Works. For more information, please contact scholarsrepository@llu.edu.

LOMA LINDA UNIVERSITY
School of Medicine
in conjunction with the
Faculty of Graduate Studies

The Growth and Ecology of Upper Cambrian Microbialite Biostromes from the Notch
Peak Formation in Utah

by

Ken P. Coulson

A Dissertation submitted in partial satisfaction of
the requirements for the degree
Doctor of Philosophy in Earth Science

June 2016

© 2016

Ken P. Coulson
All Rights Reserved

Each person whose signature appears below certifies that this dissertation in his/her opinion is adequate, in scope and quality, as a dissertation for the degree Doctor of Philosophy.

Chairperson

Leonard R. Brand, Professor of Biology and Paleontology

Stanley M. Awramik, Adjunct Professor of Geology

Danilo Boskovic, Assistant Professor of Geochemistry

H. Paul Buchheim, Professor of Geology

Ronald Nalin, Adjunct Assistant Professor of Geology

Kevin E. Nick, Associate Professor of Geology

ACKNOWLEDGEMENTS

Thanks to my advisor Dr. Leonard Brand for providing me the opportunity to study some of the world's best stromatolites! Thanks also for organizing our fruitful field trips, and keeping a keen interest in my progress. Thanks to Dr. Stan Awramik and Dr. Paul Buchheim for providing insightful ideas to help further my research, as well as time taken out of busy schedules to look over manuscripts. Thanks to Dr. Kevin Nick for suggesting very helpful editorial revisions made to several different manuscript iterations. Thanks also for taking time out, even when extremely busy, to answer a vast array of research-related questions. Thanks to Dr. Ronald Nalin for showing a real and keen interest in my research, for spending many hours with me pouring over thin-sections, and for providing some thought-provoking ideas that have helped tremendously. Thanks to Dr. Art Chadwick for assistance with fieldwork. If it wasn't for Dr. Chadwick's persistence, there is no way we would have gotten two one-hundred pound stromatolites off the mountain and into the truck! Thanks to Dr. Jongsun Hong who has been a tremendous source of inspiration for the content contained in chapter three. Thanks to my colleague and friend Matt McLain for prayerful encouragement and support. Thanks to my mentor and friend Dr. John Whitmore, for providing me a critically-based, scientific foundation. Thanks to all my committee members who gave up valuable time to assist in the completion of this work. This work was partially supported by a Geological Society of America Research Grant, and a AAPG, John H. and Colleen Silcox named research grant. Thanks to Loma Linda University for ongoing financial support.

Thanks to my wonderful, Godly wife, Beth, who has enabled me to pursue this milestone. Truly, she has borne a weighty load looking after our three little girls while

I've either been in the field, at a conference, in class or studying. And finally, I would like to thank the Lord for providing me the undeserved opportunity to study His creation and marvel in its complexity.

CONTENT

Approval Page.....	iii
Acknowledgements.....	iv
List of Figures.....	viii
List of Abbreviations.....	x
Abstract.....	xi
Chapter	
1. Introduction.....	1
Microbialite Definition.....	1
Microbialite Classification.....	6
Microbialite Growth Processes.....	6
Geological Background.....	7
The House Range Embayment.....	8
The Hellnmaria Microbialites.....	9
Synopsis for Chapters 2 and 3.....	12
Chapter 2.....	12
Chapter 3.....	13
References.....	17
2. Microbialite Elongation by Means of Coalescence: An Example from the Middle Furongian (Upper Cambrian) Notch Peak Formation of Western Utah.....	20
Abstract.....	20
Introduction.....	21
Geologic Background.....	24
Methods.....	29
Results.....	30
Hellnmaria Microbialites.....	30
Bed 9 Descriptions.....	33
Petrographic Data.....	42
SEM, EDS, XRD and Grain-size Analysis of Insoluble Residues.....	46
Discussion.....	49

Interpretation of Petrographic and Sedimentological Data.....	49
The Importance of Coalescence.....	50
Constructing a Model.....	56
Conclusions.....	59
References.....	61
3. Lithistid Sponge-Microbial Reef-building Communities Construct Laminated Upper Cambrian (Furongian) ‘Stromatolites’.....	65
Abstract.....	65
Introduction.....	66
Geologic Background.....	67
Methods.....	73
Results.....	74
Overview of Bed 11.....	74
Spicule Networks in Zone 1.....	77
Fenestral Networks in Zone 2.....	85
Discussion.....	91
Sponge-microbial ‘Stromatolites.’.....	91
Metazoan Reefs: Underrepresented or Overlooked?.....	92
Conclusions.....	98
References.....	100
4. Conclusions.....	104
Appendices	
A. Wackestone—Grainstone Interval.....	107
B. Additional Methods.....	108
C. Cross-bedding.....	110
D. SEM Images of Insoluble Residues.....	112
E. Hydrodynamics Affects Morphology.....	113
F. Nutrient Diffusion.....	115

FIGURES

Figures	Page
Chapter 1	
1. Map of the Great Basin Region	2
2. Microbialite Classification.....	4
3. House Range Embayment.....	10
4. Middle and Upper Cambrian Metazoan Reefs.....	15
Chapter 2	
1. Geologic Setting of Research Area.....	25
2. Stratigraphy and Biostratigraphy	27
3. Vertical Thickness of Bed 9 Over Research Area	31
4. Synoptic Relief. Long Axes Orientations	34
5. Change in Morphology in Vertical Section.	37
6. Mosaic of the Strongly Elongate Layer	40
7. Petrographic Data.....	44
8. Interpretation for Bed 9.....	47
9. Various Examples of Modern and Ancient Elongate Microbialites	51
Chapter 3	
1. Geologic Setting of Research Area.....	69
2. Stratigraphy and Biostratigraphy.	71
3. Macro and Meso-Scale Features of ‘Stromatolites’ in Zone 1	75
4. Macro and Meso-Scale Features of ‘Stromatolites’ in Zone 2	78
5. Sponge Distribution and Morphology.	81
6. Spicule Networks from Zone 1.....	83

7.	Deteriorated Spicule Networks From Zone 1.	87
8.	Fenestral and Peloidal Networks From Zone 2.....	89

Appendices

1.	Thickening Wackestone—Granstone Interval.....	107
2.	Cross-bedding.	111
3.	SEM of Insoluble Residues.....	112
4.	Hydrodynamics Affects Morphology.	114
5.	Nutrient Diffusion.	116

ABBREVIATIONS

EPS	Extracellular Polymeric Substance
HRE	House Range Embayment
SEM	Scanning Electron Microscopy
XRD	X-ray Diffraction
EDS	Energy Dispersive X-ray Spectrometry
LLH	Laterally Linked Hemispheriods
SH	Stacked Hemispheriods
YNP	Yellowstone National Park

ABSTRACT OF THE DISSERTATION

The Growth and Ecology of Upper Cambrian Microbialite Biostromes from the Notch Peak Formation in Utah

by

Ken P. Coulson

Doctor of Philosophy, Graduate Program in Earth Science

Loma Linda University, June 2016

Dr. Leonard Brand, Chairperson

Exposure of carbonate rocks within the uplifted mountains of southwestern Utah presents a unique opportunity to study the growth, morphology and ecology of two upper Cambrian microbialite reefs located within the Hellmaria Member of the Notch Peak Formation. The first reef contains meter-length, strongly elongate microbialites that grew in a deep, subtidal marine environment. These elongate microbialites formed as a result of coalescence of round ‘algal’ heads, a process known to produce compound microbialite structures in shallow water, but seldom explored as a key factor in the elongation of deep, subtidal forms that grew in ancient environments. The second reef contains lithistid sponge-microbial ‘stromatolites,’ a new type of metazoan bio-structure that has only been described from the Carboniferous and Triassic periods. This discovery has important implications when reconstructing middle to upper Cambrian reef-building communities, as these periods are assumed to have a very low diversity of metazoan reefal components. Taken together, both reefs shed light on the paleoecology and paleoenvironment of upper Cambrian microbialite reef-building communities.

CHAPTER ONE

INTRODUCTION

Some of the world's most impressive upper Cambrian microbialite reefs are found in the Great Basin region on the west coast of the United States (Fig. 1). Exposure of upper Cambrian carbonate rocks within the uplifted mountains of southwestern Utah, presents a unique opportunity to study some of these Cambrian microbialite reefs that appear stacked in multiple beds in and around the northern House Range (Fig. 1). Hintze et al. (1988) and Miller et al. (2003) provided a cursory account of some of these microbialites while describing the local stratigraphy, but a formal investigation into their genesis, growth and morphology has only now been published with the writing of this dissertation. Two beds were chosen from a total of 11 beds found within the upper half of the Hellnmaria Member of the Notch Peak Formation, for the purpose of answering specific questions related to their paleoenvironment and ecology. Several important conclusions have been developed from this research which will aid future microbialite-workers and carbonate sedimentologists interpret similar paleoenvironments.

Microbialite Definition

Generally, microbialites are defined as: "Organosedimentary deposits that have accreted as a result of a benthic microbial community trapping and binding detrital sediment and/or forming the locus of mineral precipitation (Burne and Moore, 1987, p. 241-242)." The term "microbialite" is an umbrella term that comprises four different subgroups: stromatolites, thrombolites, dendrolites and leiolites (Fig. 2). The latter will not be discussed any further.



Fig. 1. The Great Basin region. Red star indicates location of the House Range, southwestern Utah. Author: Karl Musser. Image used under Creative Commons Attribution-Share Alike 3.0 Unported lic. Image can be downloaded from: <https://commons.wikimedia.org/wiki/File:Greatbasinmap.png>

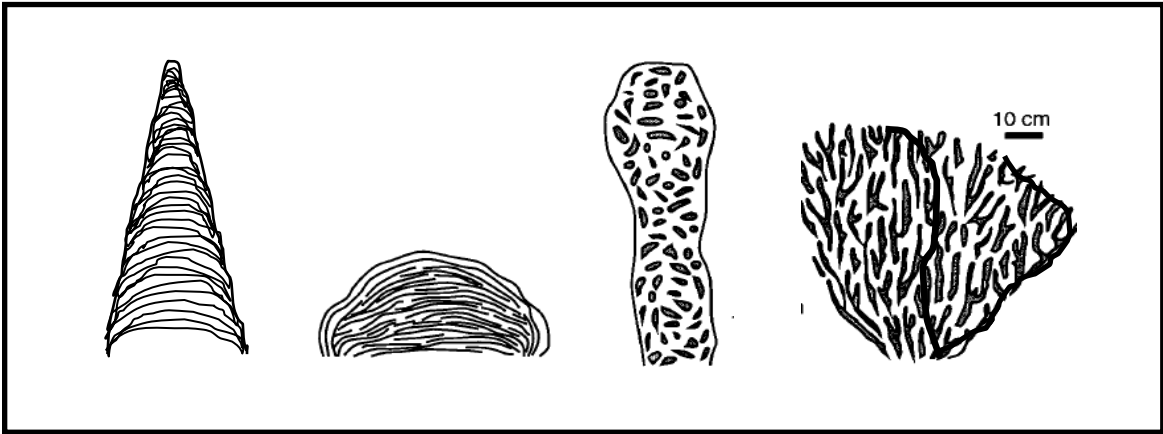


Fig. 2. Microbialite classification. From left to right: conical, domal, columnar, and branching-columnar *macrostructure*. Internal *mesostructure* dictates nomenclature. From left to right: conical stromatolite, domal stromatolite, columnar thrombolite and branching-columnar dendrolite. Illustrations adapted from Shapiro and Awramik (2000, p. 6).

Microbialite Classification

Microbialites are classified using one or a combination of just four macrostructural shapes: conical, domal, columnar, and branching-columnar (Fig. 2). Differentiating between stromatolite, thrombolite and dendrolite occurs at the *meso*structural scale; at this level, the investigator is interested in the texture or fabric *within* the macrostructural shape (Fig. 2); Stromatolites have discrete laminations, thrombolites have a distinct clotted fabric, and dendrolites have a branch or flame-like fabric. These distinctions will need to be kept in mind during the flow of discussion, as nomenclature may change from one paragraph to the next without further explanation.

Microbialite Growth Processes

Microbialites accrete at a sub-laminar to laminar level using one of three general processes. 1) There is a purely mechanical interaction between benthic, microbial communities and detrital grains of sediment. Here, the sticky EPS sheaths of microbes trap and bind sediment grains (Burne and Moore, 1987). 2) Precipitation of calcite by purely biological factors due to chemical changes associated with photosynthesis (Dupraz and Visscher, 2005; Berelson et al., 2011). 3) Precipitation of calcite by purely inorganic factors due to changes in environmental and/or chemical factors (Serebryakov and Semikhatov, 1974).

A fourth factor that as yet remains unaddressed in the microbialite community is the recent discovery of laminated sponge-microbial 'stromatolites' (Luo and Reitner, 2014, 2015; this dissertation). There presently exists an ambiguity as to what these

structures should be called. Are they stromatolites, 'stromatolites,' laminated sponge-microbialites, or something else?

Geological Background

The western continental margin of Laurentia is thought to have formed during the Late Proterozoic rifting of Rodinia. According to Miller et al. (2003, p. 58), lower Paleozoic strata of the eastern Great Basin were deposited on a subsiding carbonate platform that provided over 4500 m of early Paleozoic accommodation space. Superimposed throughout these sediments are large-scale, second-order sequences that deposited the Cambrian/Ordovician Orr and Notch Peak Formations as well as the Ordovician House Limestone (Miller et al., 2003) in what is now southwestern Utah (Fig. 1 in chapter 2). Central to this discussion is the microbialite-bearing Notch Peak Formation which has been divided into three mappable members: the Hellnmaria, Red Tops and Lava Dam (Fig. 2A in chapter 2). All three members are traceable from within the House and Confusion Ranges in western-central Utah to the Wah Wah Mountains in the south (Hintze et al., 1988). According to Palmer, the Notch Peak Formation was deposited during the third interval of the Sauk mega-sequence (Palmer, 1981). Miller et al. (2003) broke the Sauk III interval into 14 smaller sequences (See illustration in Miller et al. 2003, p. 27). The Hellnmaria Member of the Notch Peak Formation includes the upper half of sequence 1, and all of sequences 2-4 in Miller et al. (2003).

Conodont biostratigraphic correlations by Miller et al. (2003, p. 27) assign the microbialite-bearing beds of the upper Hellnmaria Member to the *Proconodontus tenuiserratus* through *Proconodontus muelleri* zones. This places the upper Hellnmaria

Member in the late Cambrian Sunwaptan Stage of the Millardan Series (middle Furongian) (Fig. 2A in chapter 2). According to Miller et al. (2003), the lower to middle parts of the Hellnmaria Member chiefly consist of thin-bedded to laminated dark lime mudstones, that change to intraclastal, ooid and oncoidal packstones and grainstones towards the top (Miller et al., 2003, p. 30). At its type section, only the upper 154 m of the 366 m thick Hellnmaria Member contains microbialite-bearing beds that are completely absent from the lower interval (Fig. 2A in chapter 2). Miller et al. (2003) interpret the Hellnmaria Member as an overall sea-level highstand that shallows significantly towards its top. This shallowing-upwards succession is terminated by the Red Tops Lowstand (Miller et al., 2003, p. 27), where clean, largely homogeneous, fine to medium-grained stromatolitic limestones and dolostones are abruptly truncated by a coarse-grained calcarenite deposit.

The House Range Embayment

The House Range Embayment (HRE) was an “asymmetrical [fault-controlled] trough that deepened [in a southeasterly direction] and widened as it extended—400 km westward... (Rees, 1986, p. 1054).” The southeast end of the embayment represented a basin-like, deep-water environment while the northwest boundary represented its shallow-water continuation (Fig. 3). This embayment acted like a locally steepened carbonate ramp within the larger distally steepened carbonate platform of the east Laurentian passive margin. The literature is replete with descriptions of the HRE and associated facies-related processes that both prograded and retrograded up and down the ramp in response to varied allocyclic and/or autocyclic controls (Kepper, 1972; Rees,

1986; Brady and Keopnick, 1979; Miller et al., 2003; Halgedahl et al., 2009). According to Rees (1986), the Notch Peak microbialites are situated within the ancient HRE trough, just to the north of the southern fault boundary. This may be significant since the southern fault is described as discrete, with deeper water facies found to its north, within the HRE trough, and shallow water deposits found to its south, upon the Laurentian platform proper (Rees, 1986). The geographic area within the research may, therefore, be located on a mini steepened ramp dipping northwest down into the HRE trough. A northwesterly thickening of the wackestone-grainstone interval located between beds 10 and 11 (Fig 2B in chapter 2) seems to support this interpretation (Appendix A).

The Hellnmaria Member Microbialites

Hintze et al. (1988) bundle all microbialites into a single package of strata that spans the upper 154 m of the Hellnmaria Member (Fig. 2A in chapter 2). I re-measured this segment of the type section (Fig. 2B in chapter 2) being especially attentive to specific microbialite beds, bed thicknesses and general microbialite characteristics. I found eleven distinct microbialite-bearing beds separated by intervening wackestone-grainstone intervals that span the upper 154 m of the Hellnmaria Member. All eleven beds are morphologically unique, although substantial overlap does exist from one bed to the next. Beds 9 and 11 are the focus of this dissertation.

Bed 9 is a microbialite-bearing unit exhibiting a remarkable change in morphology when seen in vertical section. Microbialites change from small, round,

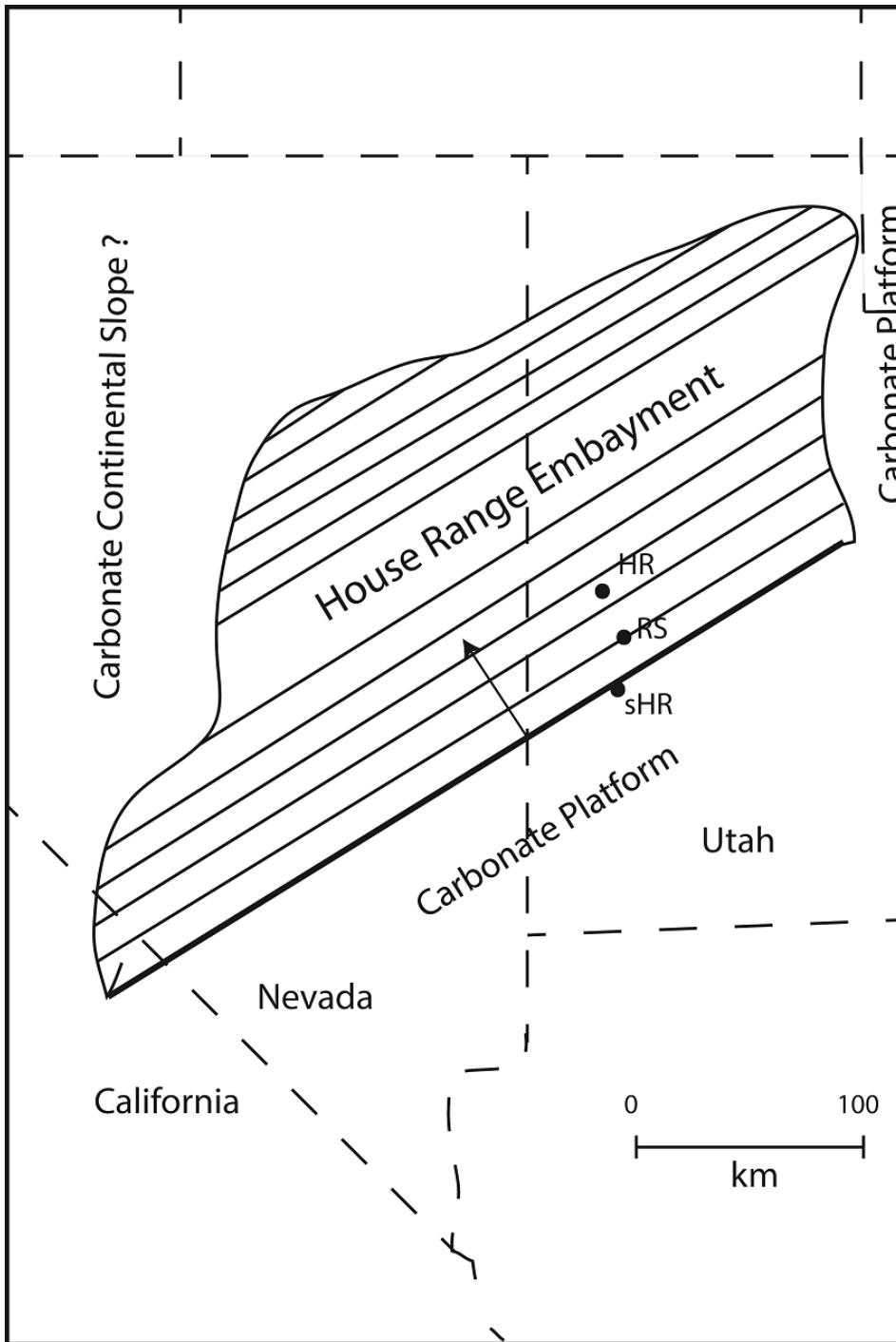


Fig. 3. House Range Embayment adapted from Rees (1986). sHR = southern House Range, Steamboat Pass area. HR = House Range, Marjum Pass area. RS = Research Site. Arrow indicates approximate orientation for elongate microbialite long-axes (perpendicular to southern HRE fault boundary). Notice that research site is only located about 8-10 km to the north of the southern HRE boundary.

decimeter-sized forms to large, elongate structures many m in length, branching back to round profiles at the top of the bed.

Bed 11 is a 1 to 3 m thick microbialite-bearing unit that contains a tightly packed field of round to sub-round microbialites covering a large geographic area of approximately 20 km². Microbialite meso-scale fabric is best described as stromatolitic, and many forms have a large core composed of mini-stromatolites. Diameters vary from about 40 – 70 cm, and are very well exposed in plan-view at multiple locations. Heights vary from a few dm to about 70 cm and in cross-section widen slightly towards the top.

Synopsis for Chapters 2 and 3

Chapter 2

Elongate microbialites represent important paleoenvironmental indicators for interpreting many sedimentary facies associated with ancient peritidal environments (Hoffman, 1967; Logan et al., 1974; Serebryakov and Semikhatov, 1974; Playford et al., 2013).

Most workers agree that the primary factors involved in the elongation of strongly elongate microbialites are hydrodynamics, microbially influenced trapping and binding of sediment, and/or precipitation of peloidal cement, and intertidally generated abrasion and mechanical scour over sheet-like microbial mats. Some of these processes, however, are inadequate for explaining the construction of strongly elongate structures in deep, subtidal, or wave-restricted environments.

Chapter 2 examines the deep-subtidal, elongate microbialites of bed 9, and suggests that these strongly elongate structures formed as a result of coalescence, a process known to produce compound microbialite structures in shallow water, but seldom

explored as a key factor in the elongation of deep, subtidal forms that grew in ancient environments.

My aims in chapter 2 are: 1) To evaluate the Notch Peak elongate microbialites, demonstrating the importance of elongate-related coalescence in the construction of these forms. 2) To suggest that some of the processes involved in the construction of modern elongate analogues do not correlate with the Notch Peak elongate forms. And 3) To propose some useful criteria from which to approach the subject of microbialite morphogenesis in general.

Chapter 3

The evolution of Cambrian reefs has traditionally been interpreted in terms of two general reef-building stages; the archaeocyath-calicimicrobe consortium that dominated the early Cambrian, followed by a largely microbial stage that dominated the middle to late Cambrian, subsequent to the archaeocyath decline in the late early Cambrian (Klappa and James, 1980; James and Gravestock, 1990; Shapiro and Rigby, 2004; Li et al., 2015). An increasing number of recent papers, however, are demonstrating that metazoan reef-builders may have been more prevalent during these periods than was previously thought (Johns et al., 2007; Hong et al., 2014; Adachi et al., 2015) (Fig. 4).

In chapter 3, I contribute to this growing number of middle and upper Cambrian reefal discoveries by examining bed 11, an upper Cambrian sponge-microbial reef located at the top of the Hellnmaria Member. This reef is unlike other coeval metazoan reefs, in that it contains small-scale, weakly fused lithistid sponges that encrusted automicritic laminae taking on a similar lamina-like morphology. Coeval sponge-microbial reefs are typically dominated by frame-building anthaspidellids that are

randomly scattered throughout the sponge-microbial buildups (Shapiro and Rigby, 2004; Kruse and Zhuravlev, 2008; Hong et al., 2012). The overall meso-scale fabric of the Notch Peak associations, however, are stromatolitic, and therefore represent a significant departure from coeval sponge-microbial reefal architecture. Similar sponges have recently been found in Carboniferous and Triassic ‘stromatolites’ (Luo and Reitner 2014, 2015). Taken together, these factors could easily lead to the misidentification of metazoan components in other microbial buildups at other locations around the world.

My aims in this chapter are: 1) To suggest that as yet unclassified lithistid sponges, together with microbial reef-building communities, mutually constructed laminated ‘stromatolites.’ 2) To propose that these metazoan ‘stromatolites’ have largely gone unnoticed due to the sponge’s lamina-like morphology, size and preservation potential. And 3) To compare well preserved sponge spicule networks with deteriorated spicule networks and fenestral networks, for the purpose of providing some petrographic and taphonomic criteria that may help identify sponge-microbial associations in similar rocks.

Ordovician	Lower	Tremadocian	Microbial, and lithistid sponge-microbial buildups				
		Cambrian	Furongian	Stage 10	A. sponge-microbial buildups	Nevada, USA	1
Stage 9	A. sponge-microbial buildups			Colorado, USA	2		
	A. sponge-microbial buildups			Texas, USA	3		
	D. sponge-microbial buildups			east China	4		
	D. sponge-microbial buildups			Utah, USA	5		
Paibian	A. sponge-microbial buildups		Nevada, USA	6			
Epoch 3	Guzhangian		A. sponge-microbial buildups	Northern Iran	7		
			A. sponge-microbial buildups				
	Drumian		A. sponge-microbial buildups	NT Australia	8		
			D. sponge-microbial buildups	east China	9		
Stage 5			Korea	10			
Epoch 2	Stage 4	A. sponge/H. sponge-microbial buildups				NT Australia	11
		Archaeocyathid-calcimicrobial buildups					
	Stage 3						
Terreneuvian	Stage 2						
	Fortunian	Predominantly stromatolitic buildups					
Precambrian							

Fig. 4. Recent middle to upper Cambrian fossilized reef discoveries. Modified and expanded from Hong et al. (2012). A. sponge = Anthaspidellid sponge; D. Sponge = Demosponge; H. Sponge = Heteractinid sponge. 1. Johns et al. (2007); 2. Johns et al. (2007); 3. Johns et al. (2007); 4. Lee et al. (2010), Chen et al. (2014), Lee et al. (2014); 5. Present study; 6. Shapiro and Rigby (2004); 7. Kruse and Zhuravlev (2008); 8. Kruse and Reitner (2014); 9. Park et al. (2011); Adachi et al. (2015); 10. Hong et al. (2012); 11. Kruse and Reitner (2014). Bold print highlights contribution of this research.

References

- ADACHI, N., KOTANI, A., EZAKI, Y., and LIU, J., 2015, Cambrian Series 3 lithistid sponge-microbial reefs in Shandong Province, North China: reef development after the disappearance of archaeocyaths: *Lethaia*, v. 48, Issue 3, p. 405–416.
- ANDRES, M.S., and REID, P.R., 2006, Growth morphologies of modern marine stromatolites: a case study from Highborne Cay, Bahamas: *Sedimentary Geology*, v. 185, p. 310–328.
- BERELSON, W.M., CORSETTI, F.A., PEPE-RANNEY, C., HAMMOND, D.E., BEAUMONT, W., and SPEAR, J.R., 2011, Hot spring siliceous stromatolites from Yellowstone National Park: assessing growth rate and laminae formation: *Geobiology*, v. 9, p. 411 – 424.
- BRADY, M. J., and KOEPNICK, R. B., 1979, A Middle Cambrian Platform-to-basin Transition, House Range, West Central Utah: *Brigham Young University Geology Studies*, v. 26, p. 1–7.
- BURNE, R.V., and MOORE, L.S., 1987, Microbialites: organosedimentary deposits of benthic microbial communities: *PALAIOS*, v. 2, p. 241–254.
- CHEN, J., LEE, J.-H., and WOO, J., 2014, Formative mechanisms, depositional processes, and geological implications of Furongian (late Cambrian) reefs in the North China Platform: *Palaeogeography, Palaeoclimatology, Palaeoecology*, v. 414, p. 246–259.
- DUPRAZ, C., and VISSCHER, P.T., 2005, Microbial lithification in marine stromatolites and hypersaline mats: *Trends in Microbiology*, v. 13, no. 9, p. 429 – 438.
- HALGEDAHL, S. L., JARRARD, R. D., BRETT, C. E., and ALLISON, P. A., 2009, Geophysical and geological signatures of relative sea level change in the upper Wheeler Formation, Drum Mountains, West-Central Utah: A perspective into exceptional preservation of fossils: *Palaeogeography, Palaeoclimatology, Palaeoecology*, v. 277, p. 34–56.
- HINTZE, L.F., TAYLOR, M.E., and MILLER, J.F., 1988, Upper Cambrian—Lower Ordovician Notch Peak Formation in Western Utah: U.S. Geological Survey, Professional Paper, no. 1393, p. 1–29.
- HOFFMAN, P., 1967, Algal microbialites: use in stratigraphic correlation and paleocurrent determination: *Science*, v. 157, p. 1043–1045.
- HONG, J., CHO, S.-H., CHOH, S.-J., WOO, J., and LEE, D.-J., 2012, Middle Cambrian siliceous sponge–calcimicrobe buildups (Daegi Formation, Korea): Metazoan buildup constituents in the aftermath of the Early Cambrian extinction event: *Sedimentary Geology*, v. 253–254, p. 47–57.

- HONG, J., CHOH, S.-J., and LEE, D.-J., 2014, Tales from the crypt: Early adaptation of cryptobiontic sessile metazoans: *PALAIOS*, v. 29, p. 95–100.
- JAMES, N.P., and GRAVESTOCK, D., 1990, Lower Cambrian shelf and shelf margin buildups, Flinders Ranges, South Australia: *Sedimentology*, v. 37, p. 455–480.
- JOHNS, R.A., DATTILO, B.F., and SPINCER, B., 2007, Neotype and redescription of the Upper Cambrian Anthaspidellid sponge, *Wilbernicyathus donegani* Wilson, 1950: *Journal of Paleontology*, v. 81, p. 435–444.
- KEPPER, J. C., 1972, Paleoenvironmental Patterns in Middle to Lower Upper Cambrian Interval in Eastern Great Basin: *The American Association of Petroleum Geologists*, v. 56, no. 3, p. 503–527.
- KLAPPA, C.F., and JAMES, N.P., 1980, Small lithistid sponge bioherms, early Middle Ordovician Table Head Group, western Newfoundland: *Bulletin of Canadian Petroleum Geology*, v. 28, p. 425–451.
- KRUSE, P.D., and REITNER, J.R., 2014, Northern Australian microbial metazoan reefs after the mid-Cambrian mass extinction: *Memoirs of the Association of Australasian Paleontologists*, v. 45, p. 31–53.
- KRUSE, P.D., and ZHURAVLEV, A.Y., 2008, Middle–Late Cambrian *Rankenella*–*Girvanella* reefs of the Mila Formation, northern Iran: *Canadian Journal of Earth Sciences*, v. 45, p. 619–639.
- LEE, J.-H., CHEN, J., and Chough, S.K., 2010, Paleoenvironmental implications of an extensive maceriate microbialite bed in the Furongian Chaomidian Formation, Shandong Province, China: *Palaeogeography, Palaeoclimatology, Palaeoecology*, v. 297, p. 621–632.
- LEE, J.-H., CHEN, J., CHOH, S.-J., LEE, D.-J., HAN, Z., and CHOUGH, S.K., 2014, Furongian (late Cambrian) sponge-microbial maze-like reefs in the North China Platform: *PALAIOS*, v. 29, p. 27–37.
- LI, Q., LI, Y., and KIESSLING, W., 2015, Early Ordovician lithistid sponge-*Calathium* reefs on the Yangtze Platform and their paleoceanographic implications: *Palaeogeography, Palaeoclimatology, Palaeoecology*, v. 425, p. 84–96.
- LOGAN, B.W., 1961, Cryptozoon and associate stromatolites from the recent, Shark Bay, Western Australia: *Journal of Geology*, v. 69, no. 5, p. 517–533.
- LOGAN, B.W., HOFFMAN, P., and GEBELEIN, C.D., 1974, Algal mats, cryptalgal fabrics, and structures, Hamelin Pool, Western Australia, in Logan, B.W., Read, J.F., Hagan, G.M., Hoffman, P., Brown, R.G., Woods, P.J., and Gebelein, C.D., eds., *Evolution and Diagenesis of Quaternary Carbonate Sequences, Shark Bay*,

- Western Australia: American Association of Petroleum Geologists, Mem. 13, p. 140–194.
- LUO, C., and REITNER, J., 2015, ‘Stromatolites’ built by sponges and microbes –a new type of Phanerozoic bioconstruction: *Lethaia*, Doi: 10.1111/let.12166.
- MILLER, J.F., EVANS, K.R., LOCH, J.D., ETHINGTON, R.L., STITT, J.H., HOLMER, L., and POPOV, L.E., 2003, Stratigraphy of the Sauk III interval (Cambrian-Ordovician) in the Ibez area, western Millard County, Utah and central Texas: Brigham Young University Geological Studies, v. 47, p. 23–118.
- PALMER, A.R., 1981, Subdivision of the Sauk Sequence, *in* Taylor, M.E., ed., Short Papers for the Second Symposium on the Cambrian System: U.S. Geological Survey Open-File Report 81-743, p. 160–162.
- PARK, T.Y., WOO, J., LEE, D.-J., LEE, D.-C., LEE, S.-B., HAN, Z., CHOUGH, S.K., and CHOI, D.K., 2011, A stem-group cnidarian described from the mid-Cambrian of China and its significance for cnidarian evolution: *Nature Communications*, v. 2, 442. doi:10.1038/ncomms 1457.
- PLAYFORD, P.E., 1980, Environmental controls on the morphology of modern microbialites at Hamelin Pool, Western Australia: Geological Survey of Western Australia, Annual Report, p. 73 – 77.
- PLAYFORD, P.E., COCKBAIN, A.E., BERRY, P.F., ROBERTS, A.P., HAINES, P.W., and BROOKS, B.P., 2013, The geology of Shark Bay: Geological Survey of Western Australia, Bull. 146, p. 1–281.
- REES, M. N., 1986, A fault-controlled trough through a carbonate platform: The Middle Cambrian House Range embayment: *Geological Society of America Bulletin*, v. 97, p. 1054–1069.
- SEREBRYAKOV, S.N., and SEMIKHATOV, M.A., 1974, Riphean and recent stromatolites: a comparison: *American Journal of Science*, v. 274, p. 556–574.
- SHAPIRO, R. S., and AWRAMIK, S. M., 2000, Microbialite Morphostratigraphy as a Tool for Correlating Late Cambrian—Early Ordovician Sequences: *The Journal of Geology*, v. 108, p. 171–180.
- SHAPIRO, R.S., and RIGBY, J.K., 2004, First occurrence of an in situ Anthaspidellid sponge in a dendrolite mound (Upper Cambrian; Great Basin, USA): *Journal of Paleontology*, v. 78, p. 645–650.

CHAPTER TWO

**MICROBIALITE ELONGATION BY MEANS OF COALESCENCE: AN
EXAMPLE FROM THE MIDDLE FURONGIAN (UPPER CAMBRIAN) NOTCH
PEAK FORMATION OF WESTERN UTAH.**

By

Ken P. Coulson and Leonard Brand of Loma Linda University, Loma Linda, CA 92350,
and Art Chadwick of South Western Adventist University, Keene, TX 76059.

Submitted for Publication, *Facies Journal*, January 12, 2016.

Accepted April 6, 2016

Abstract

Strongly elongate microbialites having axial ratios greater than 4:1 and sometimes exceeding 10:1, are currently forming in modern, shallow-subtidal to intertidal environments. Construction of these elongate forms is greatly dependent on hydrodynamics, microbially influenced trapping and binding of sediment, and/or precipitation of peloidal cement, and intertidally generated abrasion and mechanical scour over sheet-like microbial mats. Some of these processes, however, are inadequate for explaining the construction of strongly elongate structures in deep-subtidal or wave-restricted environments. Since elongate morphogenesis is an important factor in paleoenvironmental reconstructions, ancient examples of elongate-related growth sequences should be documented and compared with modern analogues. This paper explores such a growth sequence from a 13 meter thick, middle Furongian (upper

Cambrian) microbialite bed in western Utah that records a morphological succession of deep, subtidal microbialites in vertical section over a large geographical area.

Microbialites change from round, decimeter-sized forms to large, elongate structures many meters in length, reverting back to round, centimeter-sized shapes at the top of the bed. We suggest that these elongate microbialites formed as a result of coalescence, a process known to produce compound microbialite structures in shallow water, but seldom explored as a key factor in the elongation of deep, subtidal forms that grew in ancient environments.

Introduction

Elongate microbialites represent important paleoenvironmental indicators for interpreting many sedimentary facies associated with ancient peritidal environments (Hoffman, 1967; Logan et al., 1974; Serebryakov and Semikhatov, 1974; Young and Long, 1976; Playford, 1980; Playford et al., 2013; Mariotti et al., 2014). Most researchers agree that the primary factors involved in microbialite formation are microbially induced trapping and binding of sediments, and/or precipitation of peloidal cements, and that structure elongation is a result of hydrodynamics and mechanical scour.

Microbialite accretion occurs due to the trapping and binding of detrital grains (Logan et al., 1964; Cloud and Semikhatov, 1969; Logan et al., 1974; Semikhatov et al., 1978; Playford, 1980; Burne and Moore, 1987) within the mucilaginous Extracellular Polymeric Substance (EPS) of cyanobacteria (Dupraz and Visscher, 2005; Berelson et al., 2011). These particles are then cemented by microbially influenced precipitation of calcite, lithifying and preserving the structure so that it can act as a substrate for further

growth (Reid et al., 2000; Bosak et al., 2013). Microbially influenced precipitation of calcite may also act as the principal mode of microbialite accretion, especially in ancient forms (Serebryakov and Semikhatov, 1974). Specific to the process of elongation is the direction of microbial growth. Actualistic studies from Shark Bay, Western Australia, the Bahamas and Bermuda, have shown that microbialite surfaces exposed to up-current flow, tend to over-steepen and accrete sediment in that direction, producing a streamlined structure parallel to flow (Logan, 1961; Logan et al., 1964; Gebelein, 1969; Logan et al., 1974; Playford and Cockbain, 1976; Playford, 1980; Dravis, 1983; Dill et al., 1986; Shapiro, 1990; Playford et al., 2013). Gebelein, for example (1969, p. 65), demonstrated that marine stromatolitic biscuits growing in Bermuda over-steepen and thicken in two directions during bi-directional flow as long as sediment supply is equal in both directions. In contrast, surfaces protected from sediment influx will not thicken at those locations.

Scour by mechanical abrasion within microbialite interspaces is a well understood process that has also been observed sculpting elongate and ellipsoid microbialites in Shark Bay and in the Bahamas at both Highbourne Cay and Lee Stocking Island (Logan et al., 1964; Logan et al., 1974; Hoffman, 1976; Playford, 1980; Dravis, 1983; Dill et al., 1986; Shapiro, 1990; Andres and Reid, 2006; Playford et al., 2013). Bosak et al. (2013) have summarized this process well, detailing the importance of moving, sediment-laden water which not only prevents mat growth between individual microbialites, but also acts as an abrasive, eroding fragments from microbialite walls, especially the lower extremities, and depositing them between columns and/or ridges.

Of course, other factors are involved in microbialite growth and elongation such as: sunlight and illumination angle, bed surface topography, type of substrate, size of detrital particles, and varieties of micro and macro biota (Playford, 1980; Feldmann and McKenzie, 1998; Ginsburg and Planavsky, 2008; Bosak et al., 2013), but hydrodynamics, microbially influenced trapping and binding of sediment, and/or precipitation of peloidal cement, and intertidally generated abrasion and mechanical scour over sheet-like microbial mats seem to be the major mechanisms through which modern, elongate microbialite arrangements are constructed. Some of these processes, however, are inadequate for explaining the construction of strongly elongate structures in deep, subtidal, or wave-restricted environments.

This paper examines deep-subtidal, elongate microbialites from a 13 meter thick, middle Furongian microbialite bed from the Notch Peak Formation in western Utah. We suggest that the strongly elongate microbialites within this bed formed as a result of coalescence, a process known to produce compound microbialite structures in shallow water, but seldom explored as a key factor in the elongation of deep, subtidal forms that grew in ancient environments.

Our aims in this paper are: 1) To evaluate the Notch Peak elongate microbialites, demonstrating the importance of elongate-related coalescence in the construction of these forms. 2) To suggest that some of the processes involved in the construction of modern elongate analogues do not correlate with the Notch Peak elongate forms. 3) To propose some useful criteria from which to approach the subject of microbialite morphogenesis in general.

Geologic background

The western continental margin of Laurentia is thought to have formed during the Late Proterozoic rifting of Rodinia. According to Miller et al. (2003, p. 58), lower Paleozoic strata of the eastern Great Basin were deposited on a subsiding carbonate platform that provided over 4500 m of early Paleozoic accommodation space. Superimposed throughout these sediments are large-scale, second-order sequences that deposited the Cambrian/Ordovician Orr and Notch Peak Formations as well as the Ordovician House Limestone (Miller et al., 2003) in what is now southwestern Utah (Fig. 1). Central to this discussion is the microbialite-bearing Notch Peak Formation which has been divided into three mappable members: the Hellnmaria, Red Tops and Lava Dam (Fig. 2A). All three members are traceable from within the House and Confusion Ranges in western-central Utah to the Wah Wah Mountains in the south (Hintze et al., 1988). According to Palmer, the Notch Peak Formation was deposited during the third interval of the Sauk mega-sequence (Palmer, 1981). Miller et al. (2003) broke the Sauk III interval into 14 smaller sequences (See illustration in Miller et al., 2003, p. 27). The Hellnmaria Member of the Notch Peak Formation includes the upper half of sequence 1, and all of sequences 2-4 in Miller et al. (2003) and has been interpreted in terms of an overall sea-level highstand.

Conodont biostratigraphic correlations by Miller et al. (2003, p. 27) assign the microbialite-bearing beds of the upper Hellnmaria Member to the *Proconodontus tenuiserratus* through *Proconodontus muelleri* zones.

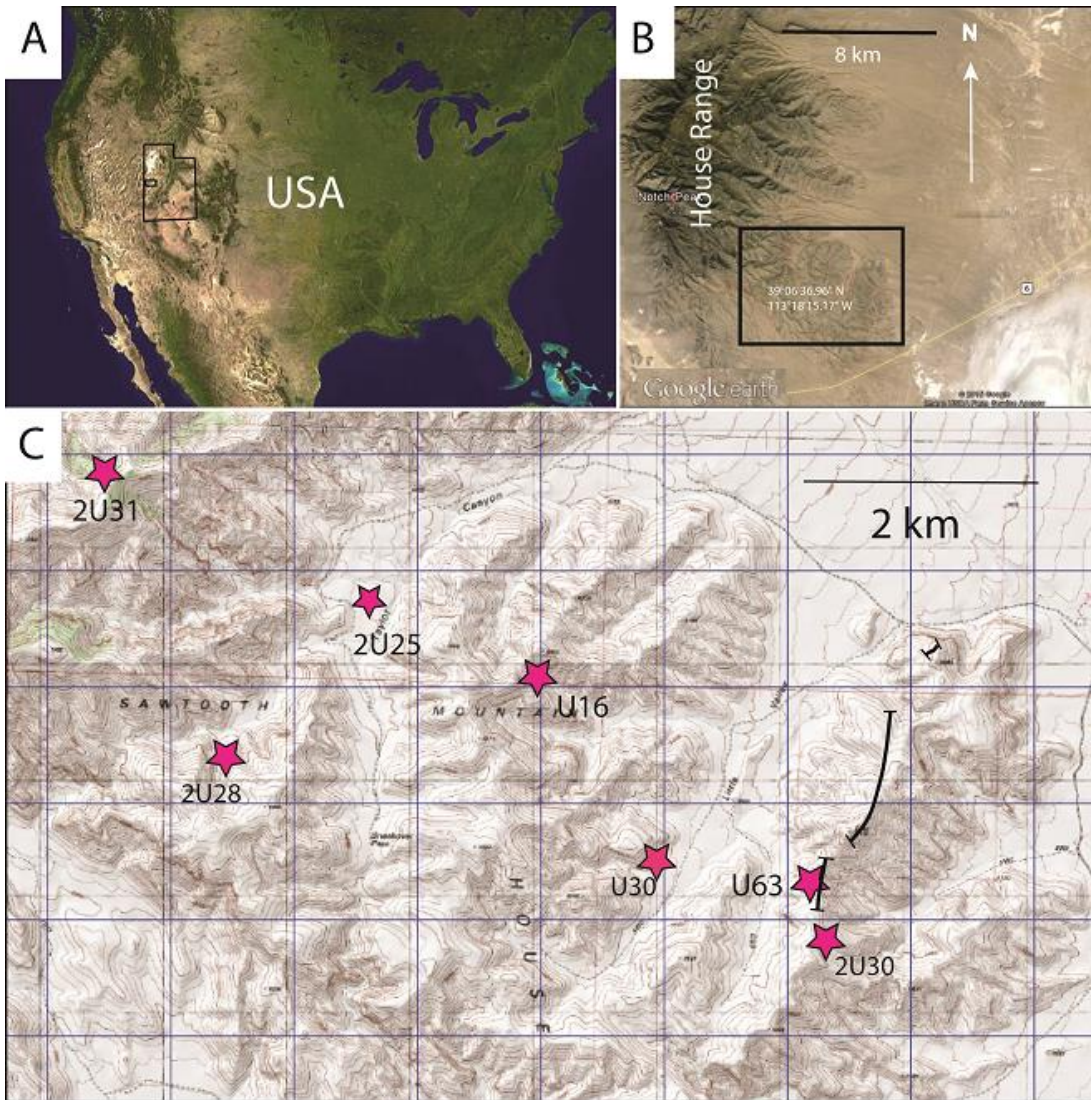


Fig. 1. Geological setting of research area. A) Satellite image of the USA showing state of Utah. Image Public Domain. Small black rectangle enlarged in B. B) Image adapted from Google Earth showing research area. Black rectangle enlarged in C. C) Image of research area provided by MyTopo indicating outcrop locations. Outcrops and UTM coordinates are as follows from NW to SE: 2U31, 296590 4332862; 2U28, 297509 4330507; 2U25, 299088 4331582; U16, 299798 4331367; U30, 301002 4329694; U63, 302195 4329234; 2U30, 302234 4329081. Type section (Hintze et al., 1988) runs through U63 (All 3 black lines).

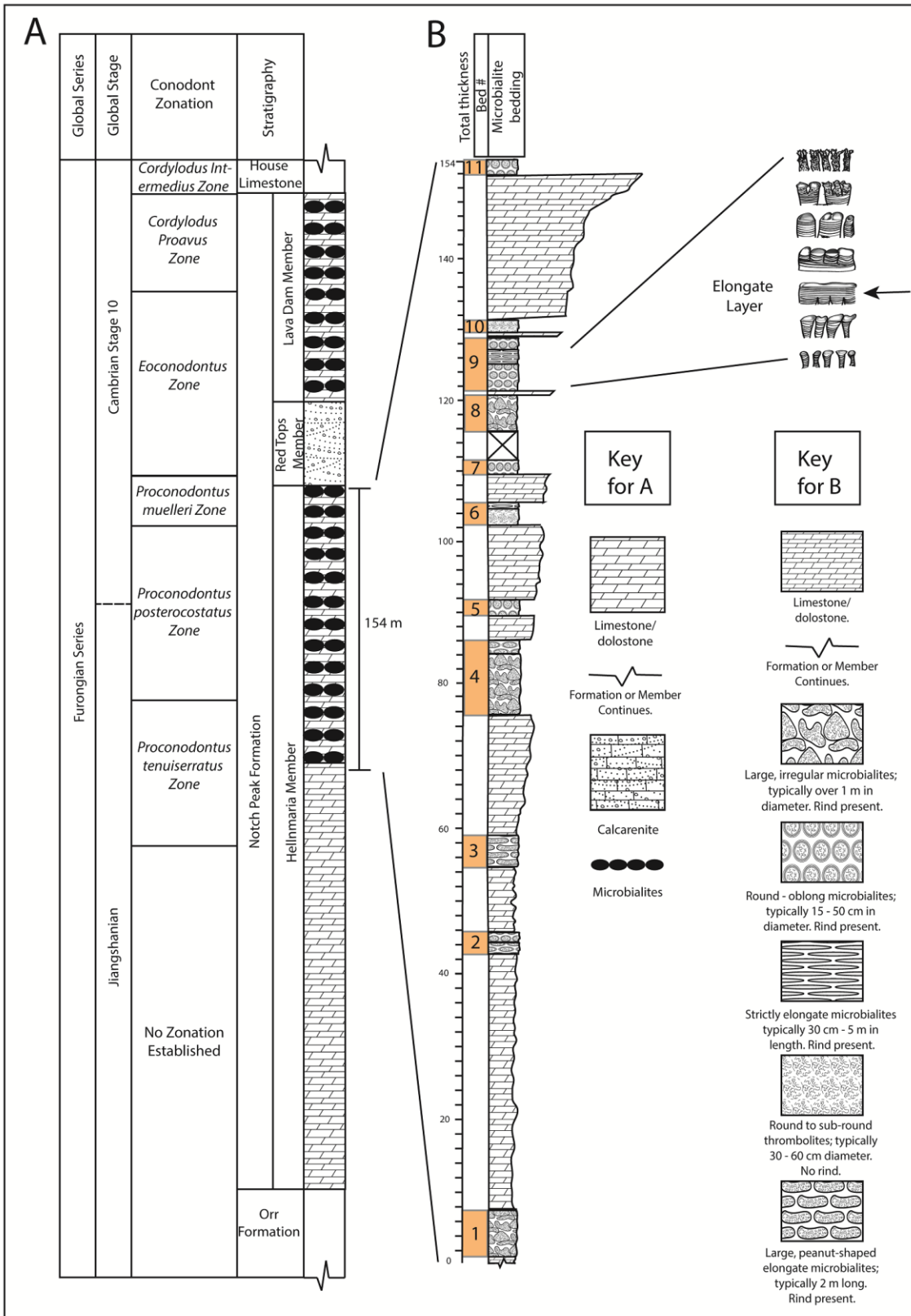


Fig. 2. Stratigraphy and biostratigraphy. A) Stratigraphic column of the Notch Peak Formation, adapted and simplified from Hintze et al. (1988), and conodont zonation adapted from Miller et al. (2003). Notice that in the Hellnmaria Member, microbialites are only found in the top 154 m. B) Stratigraphic column for top 154 m of the Hellnmaria Member of the Notch Peak Formation measured at the type section (only beds 9,10 and 11 could be correlated across the research area. Bed thicknesses vary depending on outcrop). Although each bed differs from the next, all eleven beds can be categorized using six basic facies. Illustrations of microbialites appear as plan-view representations, since at most outcrops this was the exposed surface available for inspection. Tapered limestone/dolostone sections communicate a general coarsening upward trend.

This places the upper Hellnmaria Member in the late Cambrian Sunwaptan Stage of the Millardan Series (middle Furongian) (Fig. 2A). According to Miller et al. (2003), the lower to middle parts of the Hellnmaria Member chiefly consist of thin-bedded to laminated dark lime mudstones, that change to intraclastal, ooid and oncoidal packstones and grainstones towards the top (Miller et al., 2003, p. 30). At its type section, only the upper 154 m of the 366 m thick Hellnmaria Member contains microbialite-bearing beds that are completely absent from the lower interval (Fig. 2A). Miller et al. (2003) interpret the Hellnmaria Member as an overall sea-level highstand that shallows significantly towards its top. This shallowing-upwards succession is terminated by the Red Tops Lowstand (Miller et al., 2003, p. 27), where clean, largely homogeneous, fine to medium-grained stromatolitic limestones and dolostones are abruptly truncated by a coarse-grained calcarenite deposit.

Methods

Seven sections of the middle Furongian, Hellnmaria Member were measured, described and analyzed (Fig. 1) so as to record and interpret the vertical change in microbialite morphologies found in a single bed (Bed 9 in fig. 2B).

In order to collect microbialite core samples we used a gas powered Stihl drill fitted with a diamond studded 3.2 cm core bit, and a gas powered Shaw-backpack drill fitted with a diamond studded 5.1 cm core bit. Cores varied in length from 2 to 15 cm, and were removed from several different locations, although most samples were obtained from a single outcrop. Where possible, large rock samples were also obtained from various microbialite beds. These rock samples were slabbed, lapped and polished at

Loma Linda University. We took ten core samples from bed 9, five from the interspace zones and five from within the corresponding microbialites. These cores were used as a source for both thin-sections and insoluble residues.

Thin-sections and rock samples were analyzed using microscopy, Scanning Electron Microscopy (SEM), X-ray diffraction (XRD) and Energy Dispersive X-ray Spectroscopy (EDS). See Appendix B for extended Methods.

Results

Hellnmaria Microbialites

The description from Hintze et al. (1988) bundles all microbialites into a single package of strata that spans the upper 154 m of the Hellnmaria Member (Fig. 2A). We re-measured this segment of the type section (Fig. 2B) being especially attentive to specific microbialite beds, bed thicknesses and general microbialite characteristics. We found eleven distinct microbialite-bearing beds separated by intervening wackestone-grainstone intervals that span the upper 154 m of the Hellnmaria Member (Fig. 2B). All eleven beds are morphologically unique, although substantial morphological overlap does exist from one bed to the next. Only beds 9, 10 and 11 could be correlated over the entire research area.

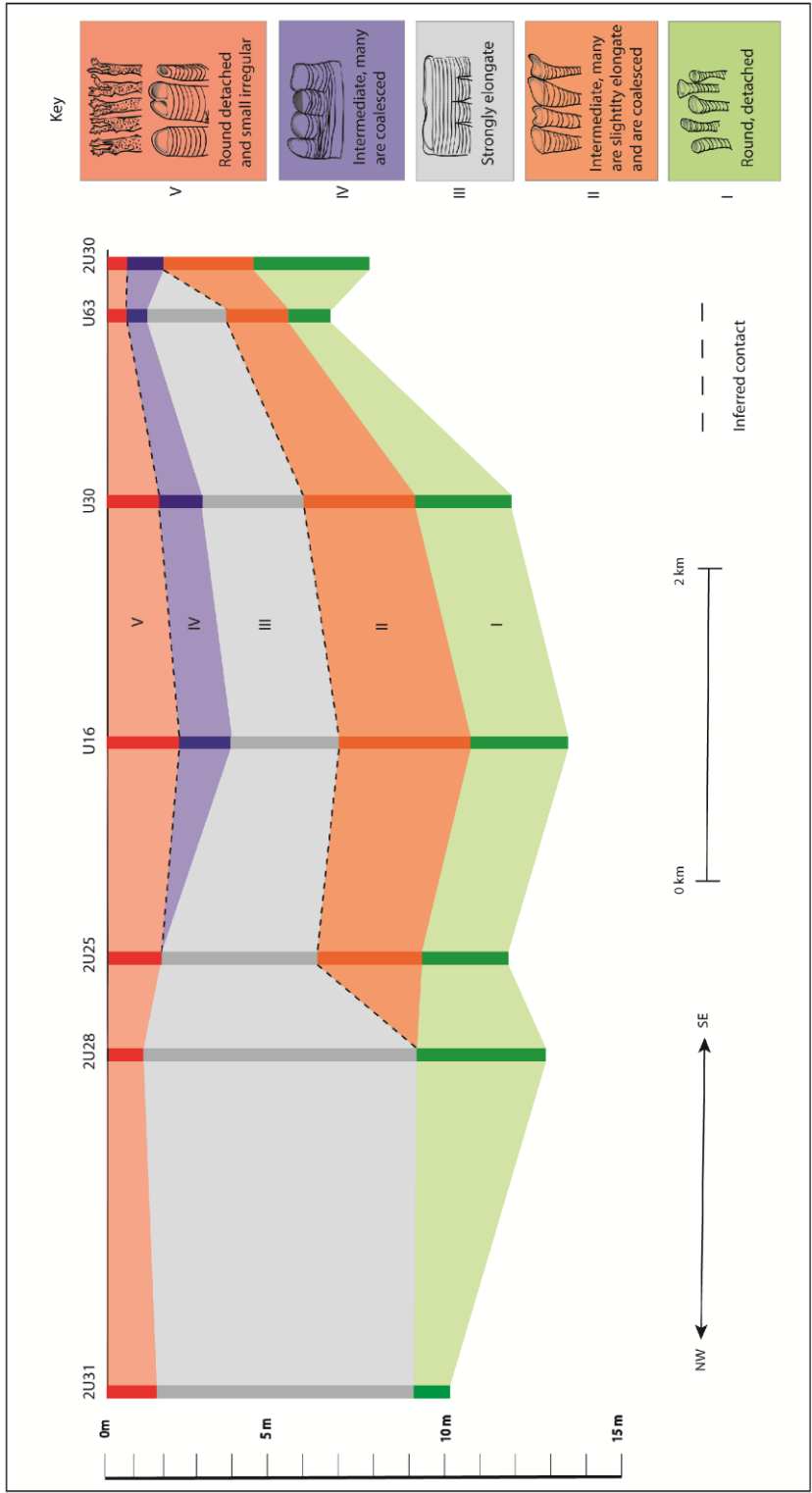


Fig. 3. Diagram depicting vertical thickness of bed 9 at each of the seven outcrops (outcrop number above each section), but being especially attentive to the thickness and horizontal correlation for each morphology. Roman numerals and colors for forms in key correspond to those in the diagram. Datum line is set to the top of the bed. We drew a line between 2U31 and 2U30 (in a general NW/SE direction) and then projected the other five outcrops onto that line. Notice that intermediate forms (II and IV) pinch out northwest of 2U25. At these northwesterly locations, morphologies change within just a few cm. Notice that the strongly elongate layer pinches out towards the southeast at 2U30.

Bed 9 is a microbialite-bearing bed exhibiting an acute change in morphology when seen in vertical section. Microbialites change from small, round, dm-sized forms to large, elongate structures many m in length, returning to more or less round profiles at the top of the bed. We were able to correlate these morphologies across seven outcrop locations spanning a total area of about 30 km² (Fig. 3).

Bed 9 Descriptions

Bed 9 is a heavily dolomitized peloidal/bioclastic wackestone that contains packstone/grainstone domains within the interspace channels of the elongate morphologies. Disconformities exist at the top of the bed as well as its base. Only a few, local, discontinuous disconformities were observed within the bed which therefore suggests a single entity composed of changing morphologies. Unlike some of the other microbialite beds, where weathering tends to erode rock vertically, bed 9 at almost every outcrop weathers to an oblique surface. A benefit of such weathering is the production of a surface of exposure that cuts diachronously through the bed, revealing a continuous stratigraphic succession of several microbialite layers in oblique plan view. This allowed us to walk up section and document the temporal evolution of the microbialite morphologies.

Current-induced sedimentary features are absent from bed 9, although some very fine cross-bedding is present to a small degree at the bottom of the wackestone interval intercalated between beds 10 and 11 (Fig. 2B and fig. 4A).

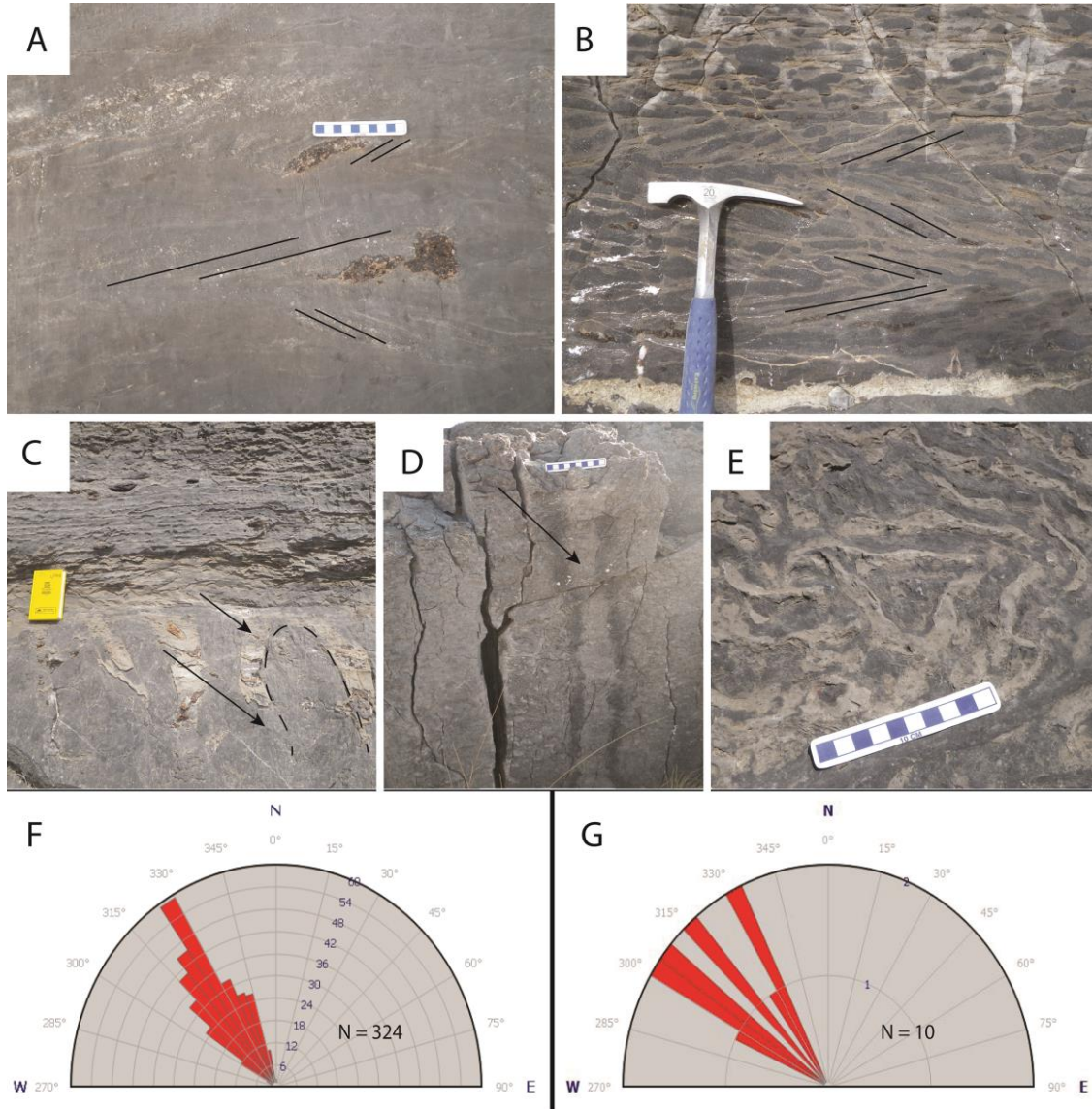


Fig. 4. Cross-bedding, synoptic relief, narrow interspace zones, microbialite interiors, and rose diagrams. A) Bioclastic wackestones just above bed 10 (Fig. 2B) sometimes exhibit fine-grained, bi-modal cross-bedding. B) Coarse-grained cross-beds located just below bed 11 (Fig. 2B). Bi-modal cross-bedding indicates current directions from the northwest and southeast. C) Cross-section of coarse-grained infill (short arrow) which overlies synsedimentary micritic infill (long arrow) within microbialite interspace records original synoptic relief (a single microbialite is outlined). Microbialites are planed off by the same coarse-grained material as in the interspace at the short arrow. D) Cross-sectional view through elongate layer shows consistent interspace width from top to bottom (arrow) (Note: this image comes from elongate forms found in bed 3 [Fig. 2B] which exhibit similar interspace dimensions as those in bed 9). E) Channel-like patterns become distinct as a function of weathering in elongate forms. Coarser-grained material stands in relief against finer-grained material. F) 324 long axis bearings taken for the strongly elongate microbialites found in bed 9 clearly demonstrate a strong signal favoring a 140/320° orientation. G) Elongate forms in bed 3 (Fig. 2B) share a similar signal. Cm-scale. Field book is about 18 cm in height.

Half meter thick cross-beds, composed of a very well sorted, coarse grainstone were correlated for about 100 m at the top of the same wackestone interval at the U16 outcrop location (Appendix C) (Fig. 2B and fig. 4B). This cross-bedded grainstone bed was also found at another location about 3 km away. In all three cases, dip directions indicated paleocurrent flowing from the northwest and southeast.

The round microbialites at the base of bed 9 are columnar forms that widened slightly as they grew vertically. Diameters vary between 10 and 50 cm (Fig. 5A), although heights for the structures could not be determined. Synoptic relief likewise was difficult to ascertain, but since relief for round forms found in bed 10 average a few to 20 cm (Fig. 4C), we tentatively suggest this to be the case for this and other layers as well. In thin-section, the dark rind located around the microbialite perimeter displayed mm-thick laminations.

Moving slightly up section, microbialites change in shape to become oblong to slightly elongate. Many of these forms exhibit alignment and incipient coalescence (Fig. 5B – D). Small groups of round to slightly oblong and/or slightly elongate forms are also in alignment and often coalesce (Fig. 5E and F) just a few tens of cm below the strongly elongate layer. Individual groups of these aligned microbialites are always orientated at $\approx 140/320^\circ$. These latter, intermediate forms, give way to strongly elongate structures just a few tens of cm further up-section (Fig. 5G and fig. 6), that likewise have a consistent $\approx 140/320^\circ$ bearing across the entire research area (Fig. 4F). This particular trait was noted for elongate structures in other microbialite beds (Fig. 4G).

The strongly elongate layer thickens in a northwesterly direction ranging from about 1.5 m in the southeast to almost 8 m in the northwest (Fig. 3).

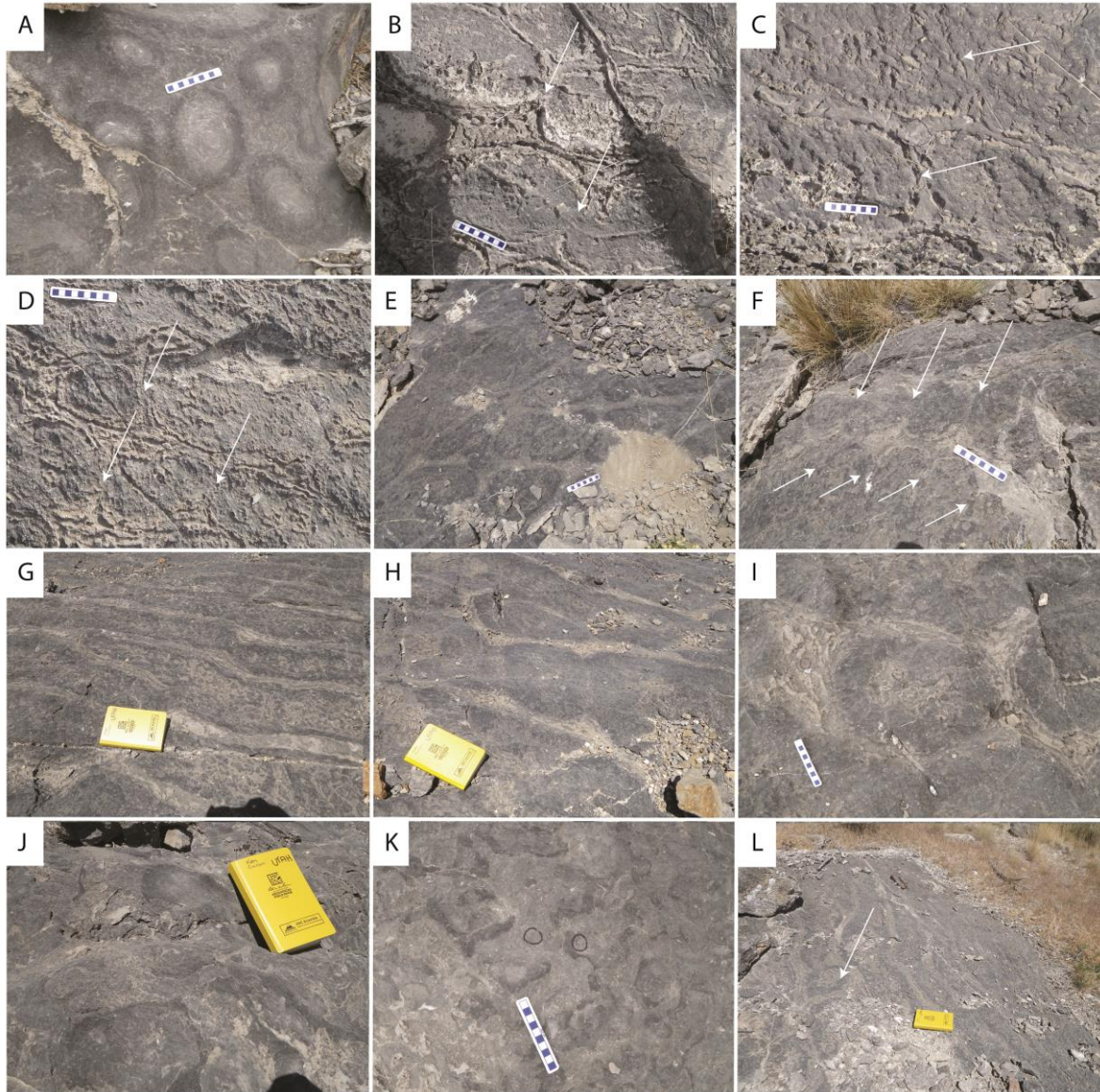


Fig. 5. Change in microbialite morphology, as seen in plan-view, moving up-section from the bottom of bed 9 to the top. A) Fully detached round to oblong forms are located at the base of the bed. B - D) Oblong to slightly elongate forms show incipient alignment and coalescence (arrows indicate sutures). All long axes are orientated at $\approx 140/320^\circ$. E and F) Groups of aligned and coalesced microbialites orientated at $\approx 140/320^\circ$. Notice the shared interspace channel. G) Strongly elongate forms. H) Elongate forms begin to detach and become wider. I) Fully detached, large round to sub-round forms. J) Fully detached round microbialites begin to shrink and become more irregular at the perimeter. K) Extremely irregular forms with diameters of less than about 10 cm appear at the top of most outcrops. L) Some round forms persist throughout the round to elongate transition. The arrow shows one of these round microbialites in the midst of the strongly elongate layer, although it coalesces at the tip of an elongate form. Cm-scale. Field book is about 18 cm in height.

Long axis length averages around 3 m at most locations, but reduces in size towards the southeast, scaling down to only about 1.5 m at outcrop U63. Outcrops located southeast of U63 are almost devoid of the elongate form, instead containing more oblong or intermediate shapes with axial ratios of about 2:1 (Fig. 3). Short axis length for the elongate form remains fairly consistent at the southeasterly locations with an average width of around 25 cm (Fig. 6A – C), although the microbialites widen to around 60 cm at the locations northwest of 2U25 (Fig. 3 and Fig. 6D). We measured height for the elongate forms at two locations to well over 4 m. Strongly elongate forms did not seem to widen as the structures grew vertically. Looking at two elongate forms in cross-section reveals an interspace zone that is consistent in width from the top to the bottom (Fig. 4D). In 3D, these elongate forms would look somewhat tabular. All of the elongate forms are characterized by a dark rind at the microbialite perimeter, similar to that for the round forms below, but laminations cannot be distinguished even in thin-section. The centers of the microbialites are set apart from the external rind by an arrangement of patterns that become quite distinct due to weathering (Fig. 4E).

A few dm further up section, strongly elongate forms detach into sub-round forms coalesced at the longer axis (Fig. 5H). These attached forms finally give way to fully detached forms with diameters averaging about 30 cm (Fig. 5I) dividing into much smaller forms with ≈ 5 cm diameters at the top of the bioherm (Fig. 5J and K). Once detached, the perimeter of the round forms becomes extremely irregular. We were unable to determine height or synoptic relief for any of these forms. Throughout the change from round to elongate and back to round again, thickness of interspaces between microbialites remains relatively consistent at around 3 - 8 cm. Interspace thicknesses for elongate

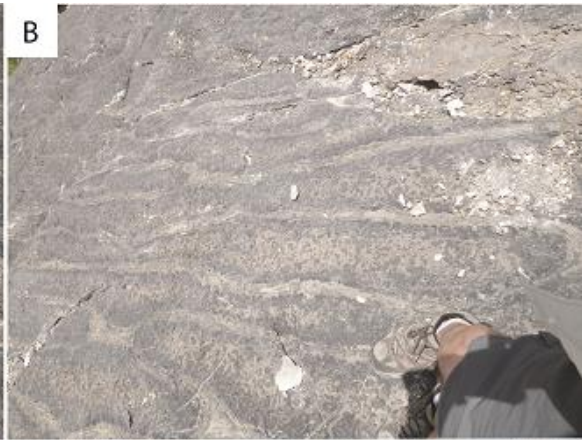
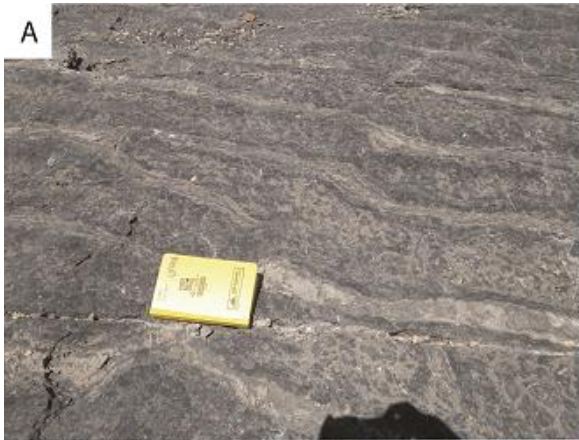


Fig. 6. Elongate forms from four different locations. A – C) Locations southeast of 2U25 (Fig. 3) have narrow interspaces that average 3 - 8 cm in width. The length of the short axis is also quite consistent at about 25 cm. D) Elongate forms become wider northwest of 2U25. Outline shows a single structure that dips obliquely away from the camera. Long axis orientation ($\approx 140/320^\circ$) is the same at all four locations. Field book is 18 cm in height. Cm-scale is displayed.

forms in the northwesterly outcrops averages around 5 - 10 cm (Fig. 6). All of these structures are best described as columnar microbialites.

Petrographic Data

Interspace sediments for the round microbialites at the base of bed 9 (Fig. 3, Roman numeral I) are characterized by abundant micrite (Fig 7A). Trilobite bioclasts are randomly located throughout the matrix, constitute $\approx 25\%$ of the allochems and are ≈ 250 μm to ≈ 3 mm in length. Small packstone pockets of medium to large-sized intraclasts up to ≈ 1.5 mm in size are also present. All of the allochems are angular and poorly sorted. This material is best described as a bioclastic wackestone with some intraclastal packstone domains. Inside the microbialites, the bindstone is composed of laminated, fenestral-rich micrite containing less than 5% bioclasts. The fenestrae have an orientation coincident and parallel to that of the laminations and are filled with sparry calcite.

Interspace sediments for the elongated forms (Fig. 3, Roman numerals II and III) are composed of moderate to well-sorted, well-rounded, sub-spherical, micritized intraclasts ≈ 250 μm to 0.5 mm in diameter, and make up $\approx 80\%$ of the allochems (Fig. 7B). Trilobite fragments constitute less than 20% of the allochems, and are typically less than 0.5 mm in length. Some intraclastic packstone domains are randomly scattered throughout the matrix. Intergranular spaces are filled with sparry calcite. These interspace sediments are best described as intraclastal grainstones with some intraclastic packstone domains. Due to dolomitization within the microbialite interior it is difficult to discern the original fabric, but from what we can resolve we suggest that the microbialite interior was a bioclastic wackestone when deposited.

The interspace sediments for the large round microbialites, as well as the smaller forms with irregular perimeters (Fig. 3, Roman numerals IV and V) are composed of $\approx 20\%$ trilobite bioclasts, $\approx 250\ \mu\text{m}$ to several mm in length (Fig. 7C). Intraclasts ≈ 0.5 to ≈ 2 mm in diameter appear in isolated packstone pockets and constitute $\approx 30\%$ of the allochems. All of the allochems are angular and poorly sorted. Inside the microbialites, the bindstone is rich in micrite, contains $\approx 20\%$ randomly scattered trilobite bioclasts, and $\approx 20\%$ intraclasts that appear in isolated intraclastal packstone domains. One to 2 mm sized fenestrae also appear throughout the matrix and make up $\approx 30\%$ of the overall fabric. Interspace and microbialite sediments are best described as bioclastic wackestones.

The microbialite-free interval located just below bed 9 (Fig. 2B) is a very well sorted peloidal packstone with mm-thick mudstone laminae intercalated throughout (Fig. 7D). Bioclasts constitute less than 5% of the allochems.

Another microbialite-free interval located just above bed 10 (Fig. 2B) is a burrowed bioclastic wackestone that is rich in erratically distributed monaxon sponge spicules (Fig. 7E). The sediments in this interval grade into very coarse-grained, cross-bedded grainstones directly below the contact with bed 11 (Fig. 7F).

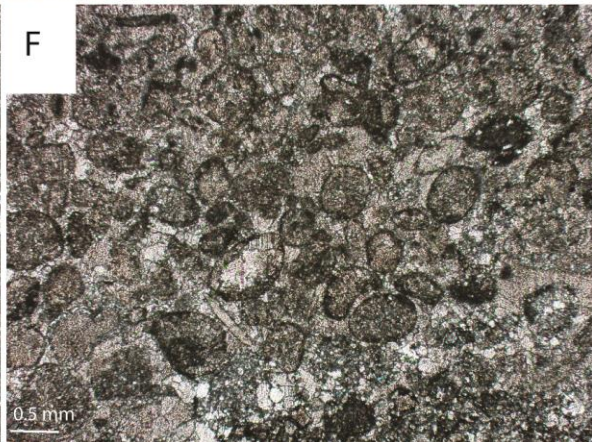
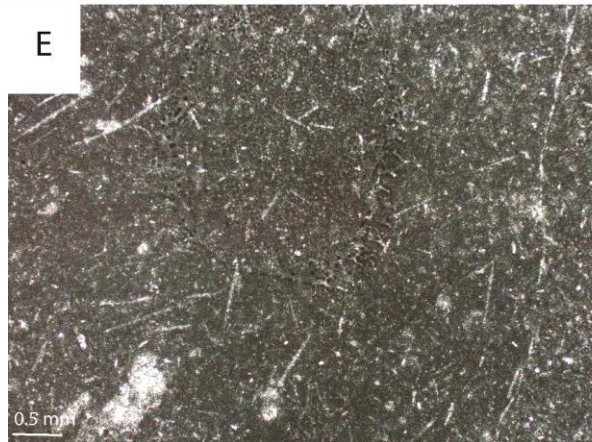
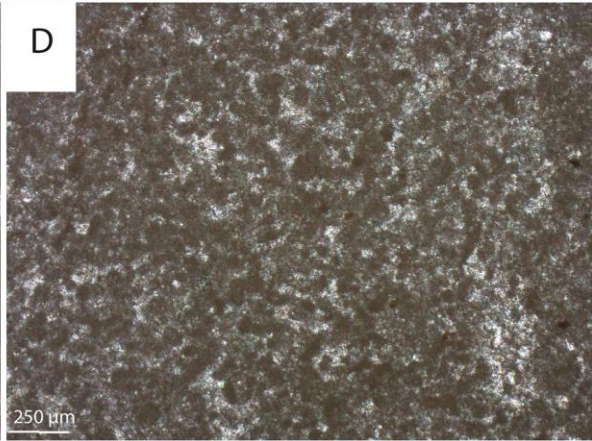
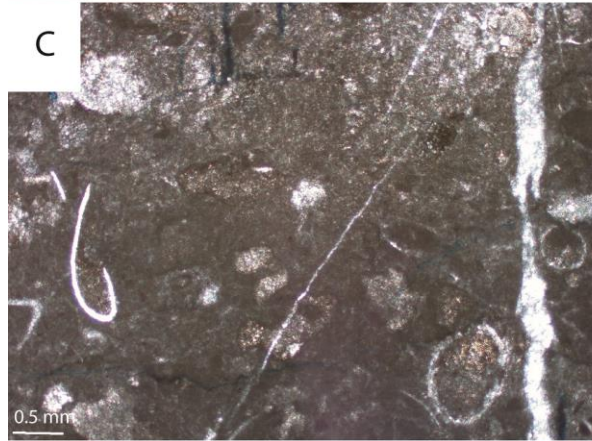
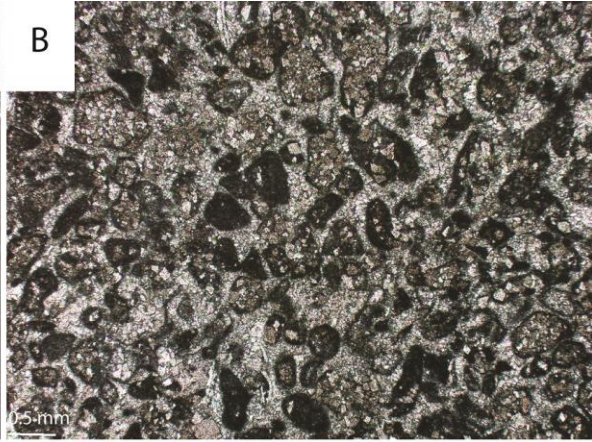
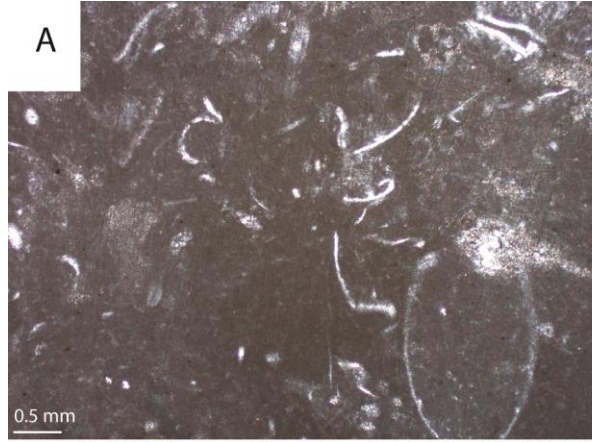


Fig. 7. Petrographic data for bed 9 microbialite interspaces, as well as for intervals below bed 9 and above bed 10. A) Interspace zone for round forms at the base of the bed are best described as bioclastic wackestones. B) Intraclastic grainstones best describe the overall fabric of interspace zones for the oblong to elongate forms. C) A return to the round motif is accompanied by a return to similar bioclastic wackestones as in A. D) The interval just below bed 9 is a peloidal packstone with mudstone laminae occurring throughout. E) The interval just above bed 10 (Fig. 2B) is a bioclastic wackestone containing ubiquitous monaxon sponge spicules. F) The interval just above bed 10 grades into a mature grainstone right at the top of the interval, just below bed 11 (Fig 2B).

SEM, EDS, XRD and Grain Size Analysis of Insoluble Residues

We found that siliciclastic percentages are consistently higher in the rounder (including round irregular) microbialites compared to those forms that exhibited elongation (Fig. 8C). This is the case whether the residues come from within the interspaces or from within the microbialites.

SEM analysis demonstrates that the average insoluble residue grain sizes vary from about 5 – 40 μm in diameter. The largest grain we found in all the samples is only 0.5 mm in diameter; the smallest is less than 1 μm . We determined that these siliciclastics are best described as very fine silts. Composition of the insoluble residues was determined using EDS and bulk sample XRD. These analyses show that the constituents making up most of the insoluble residues are a combination of authigenic chert, detrital quartz, detrital potassium feldspar and a combination of either detrital or authigenic clay. Most of the chert residues range in size from a few mm to almost a cm in diameter, and as such were easily removed and excluded from the final detrital residue percentages. Bulk sample XRD indicates that the feldspar is microcline (KAlSi_3O_8), and that the clays are either muscovite ($\text{KAl}_2(\text{AlSi}_3\text{O}_{10})(\text{F,OH})_2$), or chlorite ($(\text{Mg, Fe})_3(\text{Si, Al})_4\text{O}_{10}$), although a combination of other clays could also be present. Detrital quartz makes up about 40% of the siliciclastic content, the feldspars also about 40% and the clays about 20%. See Appendix D for SEM insoluble residue images.

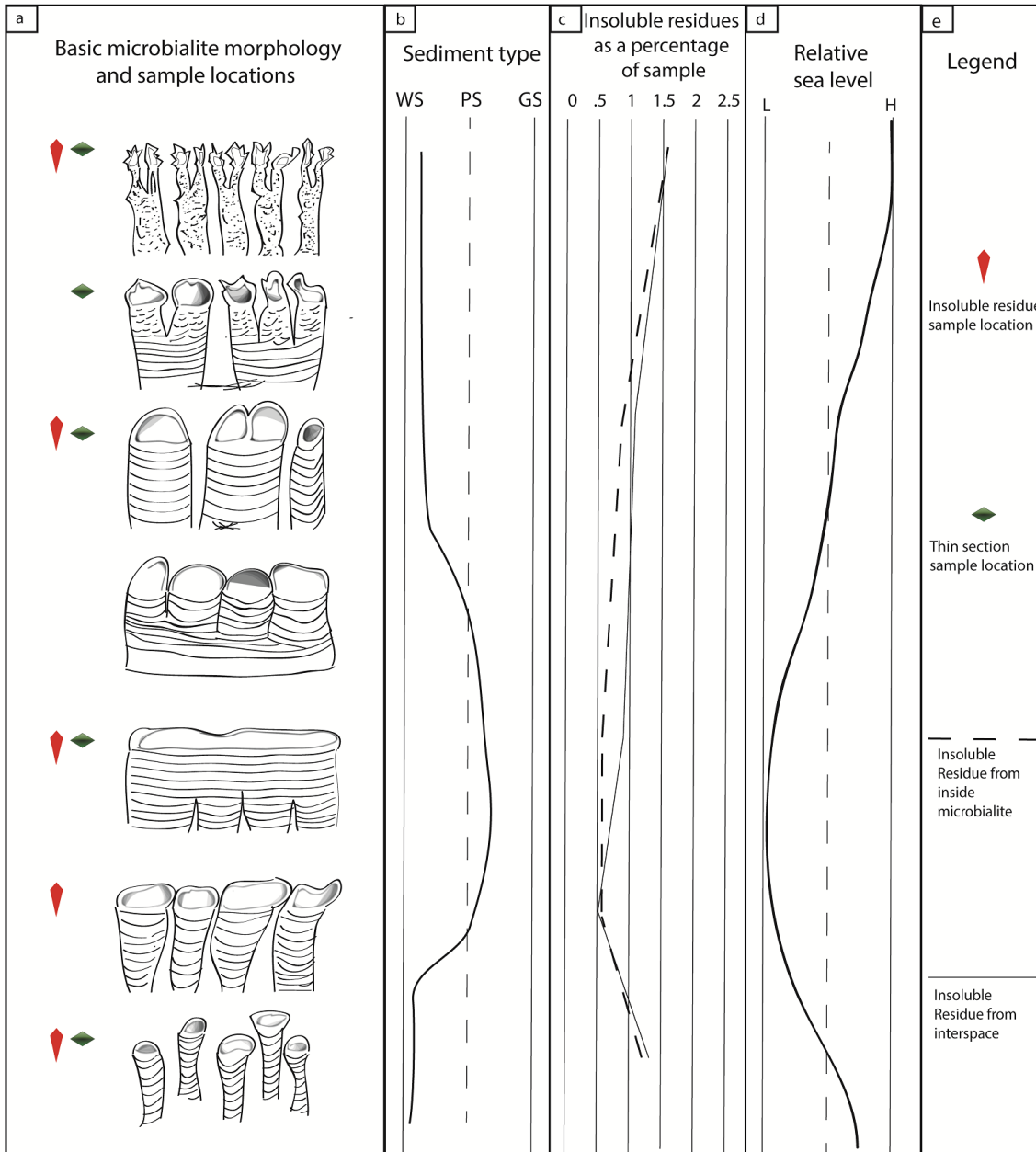


Fig. 8. Microbialite morphology, associated petrographic data and interpretation for bed 9. A) Macro-scale microbialite morphology showing changes in shape through time. B) Dominant lithology: wackestone, packstone or grainstone, as seen in thin section. C) Insoluble residues, consisting of very fine silts, were obtained from microbialite interspaces (solid line) and from within the corresponding microbialites (dotted line). Notice that both sets of data follow the same general curve. Lesser amounts of insoluble residues are interpreted to mean that they were kept in suspension, an interpretation that correlates with thin-section data in B. D) Relative change in sea-level.

Discussion

Interpretation of Petrographic and Sedimentological Data

The round microbialites at the base of bed 9 (Fig. 3, Roman numeral I) grew in an environment that was conducive to the accumulation of micrite (Fig. 8B). Although some packstone lenses bear testimony to occasional, higher energy conditions, the overall micritic nature of this bioclastic wackestone, along with relatively higher quantities of clay to fine, silt-sized insoluble residues, indicate deposition in a low energy, subaqueous environment, probably below fair-weather wave base, but above storm wave base. We suggest these round forms, and thus the establishment of bed 9, initiated and grew on a peloidal packstone at the sediment/water interface where current action was minimal (Gebelein, 1969; Ginsburg and Planavsky, 2008; Petroff et al., 2010).

The oblong to elongate microbialites grew in a slightly different environment (Fig. 3, Roman numerals II and III). The presence of moderately to well-sorted, well-rounded, sub-spherical intraclasts, combined with the absence of much of the micrite within the interspaces (Fig. 8B), suggests a relative sea-level fall (Fig. 8D) and the introduction of a directional, subaqueous current regime that abraded and shaped the microbialites. Reduced quantities of clay, to fine, silt-sized insoluble residues found both within the microbialites and within the associated interspaces, supports a more energetic paleoenvironmental interpretation which kept these grains in suspension (Fig. 8C).

The intraclastic grainstones of the oblong to elongate layers change to bioclastic wackestones in the morphologies located towards the top of the bed (Fig. 3, Roman numerals IV – V). These bioclastic wackestones are similar to those for the microbialites of the round layer at the base of the bed and are, therefore, interpreted to represent the

same kind of low energy environment. In accordance with an increase in micrite, there is a concomitant increase in fine, silt-sized insoluble residues (Fig. 8C). We suggest that as accommodation space increased, microbialite morphology retrograded back through the round to elongate transitions outlined above. This phase began with elongate forms separating at distinct boundaries (Fig. 5H) before finally separating into individual structures (Fig. 5I). Unlike the round forms at the base of the bed, however, which widened as they grew vertically, these forms became more irregular, and split into smaller morphologies (Fig. 5J and K).

The Importance of Coalescence

Several hypotheses have been proposed for the evolution of strongly elongate microbialites. Some of the best modern examples are currently growing in the intertidal and shallow subtidal zones at Shark Bay in Australia, and Highbourne Cay in the Bahamas, and owe their primary, strongly elongate structures to various abrasive-related processes interacting with sheet-like microbial mats.

Logan et al. (1974, p. 185) demonstrate how microbial mats growing over tidal flats can evolve into ridges and adjacent rill structures due to the abrasive action of wave-scour perpendicular to the shoreline. Continual agitation within rills precludes the establishment of microbial communities, while on the ridges they thrive (Fig. 9A). These processes ultimately contribute to the construction of strongly elongate forms.

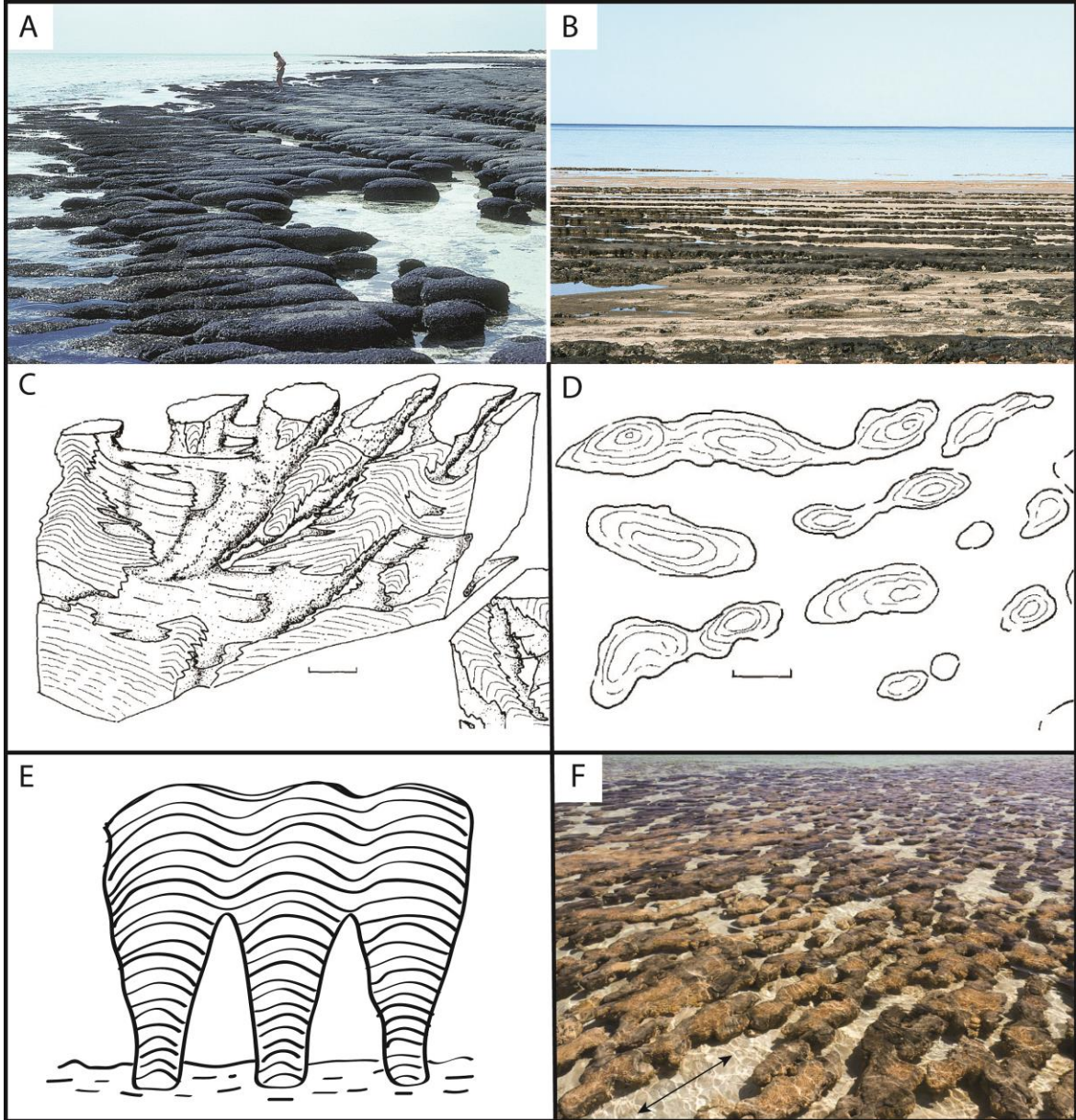


Fig. 9. Various examples of modern and ancient elongate microbialites. A) Microbial mats growing over tidal flats can evolve into ridges and adjacent rill structures due to the abrasive action of wave-scour perpendicular to the shoreline. B) “Seif” stromatolites. C) Pseudo-columns are coalesced into an elongate structure. Note ‘algal bridges’ crossing columns. D) Plan-view of a similar structure from C. Notice that laminations are no longer specific to individual columns. Scale bars for C and D = 3 cm. E) Individual columns coalesce to become a compound structure. Adapted from Logan et al. (1964). F) Elongate stromatolites at Shark Bay, formed from the coalescence of discrete columns (‘algal heads’). Arrow indicates directions of wave translation. Images in A and B courtesy of the Geological Survey of Western Australia, Department of Mines and Petroleum. © State of Western Australia 2016. Images in (C and D) courtesy Bertrand-Sarfati, J., and Awramik, S. M., 1992. Stromatolites of the Mescal Limestone (Apache Group, middle Proterozoic, central Arizona): Taxonomy, biostratigraphy, and paleoenvironments. *Geol. Soc. Am. Bull.* 104, 1138 – 1155. Image in (F) courtesy of Brendon Doran, 2kiwis.nz.

Andres and Reid (2006) document similar structures growing in shallow water at Highbourne Cay, the Bahamas, which likewise owe their elongate morphology to wave-scour perpendicular to shoreline. Playford (1980) and Playford et al. (2013) invoke wind-induced helical vortices in the construction of “seif” stromatolites which formed parallel to the prevailing winds at Shark Bay (Fig. 9B), although recently this hypothesis has been challenged (Mariotti et al., 2014). Mariotti et al. (2014), seeking to interpret the same structures appeal to differential shear stresses related to standing wave hydrodynamics. Logan et al. (1974) also describe shallow-subtidal elongate forms that owe their primary morphology to substrate inheritance; the mats growing on ancient coquina ridges carved from the substrate.

Perhaps the most effective, but least explored explanation for the evolution of large, m-scaled elongate structures is the coalescence of numerous smaller, usually round or oblong ‘algal’ heads. Bertrand-Sarfati and Awramik (1992) described coalescing, cm-sized pseudo-columns from the Mescal Limestone, a middle Proterozoic, subtidal stromatolite-bearing unit in central Arizona. They interpret the resulting elongate structures to have formed from episodic, but persistent currents that initiated coalescence between pseudo-columns. This is one of the few instances where coalescence is clearly depicted, showing ‘algal bridges’ linking pseudo-columns in the direction of paleo-current (Fig. 9C and D). Serebryakov and Semikhatov (1974, p. 564, 565) infer that Neoproterozoic columnar forms evolved into strongly elongate structures as a result of coalescence. Bunting (1986) similarly infers this for strongly elongate Proterozoic forms in Australia. These are some of the few examples where coalescence is employed, either

specifically or incidentally, as a key factor in the elongation of ancient forms. Coalescence is often mentioned, but only as it relates to linkage in neighboring forms. The most thorough description of microbialite coalescence in modern environments comes from Logan et al. (1964). In order to classify morphological variations within stromatolites at Shark Bay and apply those variations to specific environments, these authors proposed a nomenclature based on the arrangements of the hemispheroid. The two most pertinent arrangements are styled “laterally linked hemispheroids (LLH)” and “stacked hemispheroids (SH)” by Logan et al. (1964, p. 78). Noteworthy is the combination of these two arrangements, a formula that is written as: $SH \rightarrow LLH$, to indicate columnar precursors (SH) that coalesced at their top surface (LLH), thus changing them from a columnar form to a compound form (Fig. 9E). These classifications reflect observations made in the field; Logan et al. (1974) demonstrate that some types of elongate stromatolites growing in Shark Bay are in fact a composite form constructed from round or oblong ‘algal’ heads (Fig. 9F), and that coalescence did in fact occur in the direction of and as a direct result of wave translation (Logan et al., 1974, p. 172). Unlike the coalescence described by Bertrand-Sarfati and Awramik (1992), which seems to develop from the bottom up, Shark Bay coalescence develops due to crowding at the top of the structures. Once two adjacent forms are linked, binding mats continue the process by filling out the inter-columnar areas *below* the coalescing stromatolite head (Logan et al., 1974, p. 164).

Coalesced stromatolites growing at Lee Stocking Island appear to challenge the observations just outlined above; instead of coalescing in rows parallel to flow, these forms coalesce *perpendicular* to flow. Shapiro (1990) describes these greater than 30 m

long structures as wall-like, coalesced at the heads, and growing in troughs between sinusoidal sand waves. If coalesced stromatolites such as this were found in the geologic record, they could be misinterpreted as elongate stromatolites that have coalesced *parallel* to current flow, leading to a false sense for the overall paleoenvironmental interpretation. This example shows the importance of the substrate as a control for coalescent microbialites. The physical location of these long, coalesced stromatolites, correlates with the sinusoidal sand waves that parallel one another perpendicular to current flow (across the channel). The troughs between the sand waves contain abundant hardground-rubble that consists of large conch shells, rip-up clasts, coral and other similar items. Shapiro (1990, p. 211) estimates that over 90% of the objects are covered in microbial mats. Since microbial mats tend to initiate and grow on hard substrates (Young, 1973; Andres and Reid, 2006; Ginsburg and Planavsky, 2008), it is no surprise to find groups of coalesced stromatolites competing for space on the only hard substrate available. Once removed from the troughs, the only available space for growth consists of unsuitable mobilized sand.

Logan (1961) and Logan et al. (1964, 1974) went a step further, demonstrating that coalescence is actually dependent on the dense arrangement of closely packed microbialites, and that the substrate is only important in so far as it promotes this close-packing relationship. Logan (1961, p. 527) observed that desiccated, stromatolitic fragments tend to spall and/or concentrate near or at the high-water level of the intertidal zone in Shark Bay, resulting in more potential nuclei per unit area within this region than for that located in a more seaward location. As a result, denser patches of stromatolites are more common at or near high-water level. Logan et al. (1974, p. 164 and 180)

demonstrated that these dense patches are typically located in headland areas where diffracted wave-fronts produce turbulence, and that the degree of local interference around a particular patch correlated to the way in which that patch coalesced. For example, stromatolites coalesced in a single direction produced very narrow elongate structures parallel to flow, and were typically found in the least diffracted zones where wave translation remained unobstructed by turbulence (Fig. 9F). Ellipsoid patches coalesced in the direction of wave translation, yet still coalesced to a lesser degree perpendicular to wave translation due to the presence of turbulent, choppy water.

Constructing a Model

We propose a bi-directional hydrodynamic system that favored a $\approx 140/320^\circ$ bearing based on bimodal cross-bed dip directions at the top of the wackestone/grainstone interval just below bed 11 (Fig. 2B and Fig. 4B). As this bi-directional system was introduced to the environment, microbialite growth became more aggressive in both directions of flow (See Appendix E for the importance of directional hydrodynamics). Since the microbialites were tightly packed with respect to each other, coalescence occurred parallel to flow constructing linear groups of laterally linked forms. The obconical shape of these microbialites suggests coalescence most likely proceeded from the top down, similar to the coalesced 'algal' heads at Shark Bay (Fig. 5B-F and Fig. 9F). Strongly elongate structures naturally followed (Fig. 5G). Semikhatov et al. (1978, p. 1002) suggest that the degree of linkage between adjacent microbialites depends on factors such as bottom turbulence, sediment movement and proximity to adjacent microbialites. These same factors were stressed by Logan (1961) and Logan et al. (1964;

1974). These observations strongly suggest that interspace channels with only cm of available space between adjacent microbialites, in conjunction with directional hydrodynamics, make conditions ideal for processes related to coalescence and subsequent elongation.

Relying too much on modern analogues proves problematic with respect to the role of mechanical scour. Although abrasion is evident from the nature of deposited material within elongate interspace zones, it is also evident that this abrasion differed from that which presently sculpts elongate forms in Shark Bay and the Bahamas. Interspace zones between the Notch Peak forms are extremely narrow, on the order of just a few cm to about 8 cm in width (although as much as 10 cm at the most northwesterly locations), and are exceptionally consistent down the length of the long axes over an extensive area (Fig. 6). Interspace areas for elongate forms at both Shark Bay and the Bahamas, however, are extremely wide, measured in dm to m, are irregular down the long axes, and are filled with very coarse detrital grains (Fig. 9A, B and F). Petroff et al. (2010) have shown that narrow, uniform interspaces reflect the creation of a nutrient gradient due to the photosynthetic activities of microbes in modern elongated microbialites growing in Yellowstone National Park (See also Appendix F). Bosak et al. (2013), however, suggest that the biological processes responsible for these narrow interspace zones may not be good analogues for similar ancient counterparts.

The best explanation for the presence of very narrow, consistent interspaces between elongate microbialites is most likely environmental, and reflects a contrast between shoaling internal and surface waves. Internal waves propagate sub-aqueously along stratified density boundaries within the water column. Much like shoaling surface

waves, internal waves break and dissipate energy as shoreward moving bores (same as ‘surf fronts’ in the intertidal zone) that travel over internal ‘beach’ zones. Bourgault et al. (2008) measured the turbulent energy dissipation rate (ϵ) of breaking internal waves at 4×10^{-6} W/kg within the internal ‘swash zone.’ The rate of turbulent dissipation within the swash zone at the surface, however, has been measured at 10^{-1} W/kg (Feddersen 2011). This suggests that wave-generated turbulence is much greater in the intertidal zone than on subtidal ‘beach’ zones. Chaotic eddies of shoreward-moving, sediment-laden surf therefore seem a natural mechanism for sculpting wide, irregular interspaces between modern elongate microbialites in intertidal zones. Abrasive sculpting is still important in the deeper subtidal regions, but most of the scouring would result from less turbulent, shoreward moving *internal* wave bores that can travel across the sea-floor at velocities as high as 40 cm/s (Cacchione et al. 2002).

The size, shape and abrasive potential of entrained detrital grains are also important microbialite-sculpting factors that need to be considered. Siliciclastic beach sands are often extremely coarse and highly abrasive; this is in contrast to the detrital sediments associated with the Notch Peak microbialites that are mainly composed of clay to fine silt-sized carbonate grains. It seems, then, that the most intuitive solution for explaining narrow, consistent interspaces between the Notch Peak elongate microbialites is the presence of much smaller, less abrasive detrital grains, combined with processes related to shoaling internal waves.

Conclusions

The existence of a uniquely preserved suite of upper Cambrian microbialite morphologies capturing many phases of elongate-related processes in vertical succession, serves as a useful case study from which to compare strongly elongate microbialites found in other ancient environments (Hoffman, 1967; Young, 1973; Campbell and Cecile, 1975; Hoffman, 1976; Young and Long, 1976; Button and Vos, 1977; Eriksson, 1977). Apart from demonstrating elongation by coalescence, this example provides some general principles that can be universally applied to the study of microbialite morphogenesis:

- I. Coalescence is the most effective mechanism for constructing strongly elongate microbialites, parallel to flow, in deep-subtidal or wave restricted settings where intertidal scouring processes are weak. Other elongate-related processes do create strongly elongate structures, but in these cases the elongate forms are intertidal or very shallow subtidal structures that owe their primary morphology to a combination of sheet-like microbial growth combined with intertidal mechanical wave scour.
- II. Elongate morphologies, according to both modern and ancient analogues, are always formed in the presence of directional hydrodynamics where the long axes parallel the direction of flow, irrespective of whether those forms are constructed in a subtidal, intertidal or supratidal setting. The hypothesis put forward by Mariotti et al. (2014) as well as the example discussed by Shapiro (1990) are exceptions. If, as in the latter case, elongate microbialites are found

to have formed perpendicular to flow, then this might indicate some kind of substrate control that overprinted the hydrodynamic component.

III. A close-packing relationship is necessary for elongation by means of coalescence to occur. Since most Proterozoic and early Paleozoic microbialites are closely packed, this mechanism, in conjunction with (I), is an interpretive possibility for these other ancient examples.

IV. Modern examples of sculpting by mechanical wave scour in the intertidal zone are not good analogues from which to interpret some ancient examples.

Extremely narrow and consistent interspaces found in the Notch Peak growth series are best explained by abrasion related to the propagation of less turbulent internal wave bores which entrain smaller, less abrasive detrital grains than do intertidal surface waves propagating across siliciclastic beach zones.

References

- ANDRES, M.S., and REID, P.R., 2006, Growth morphologies of modern marine stromatolites: a case study from Highborne Cay, Bahamas: *Sedimentary Geology*, v. 185, p. 310–328.
- BERELSON, W.M., CORSETTI, F.A., PEPE-RANNEY, C., HAMMOND, D.E., BEAUMONT, W., and SPEAR, J.R., 2011, Hot spring siliceous stromatolites from Yellowstone National Park: assessing growth rate and laminae formation: *Geobiology*, v. 9, p. 411 – 424.
- BERTRAND-SARFATI, J., and AWRAMIK, S.M., 1992, Stromatolites of the Mescal Limestone (Apache Group, middle Proterozoic, central Arizona): taxonomy, biostratigraphy, and paleoenvironments: *Geological Society of America, Bulletin*, v. 104, p. 1138 – 1155.
- BOSAK, T., KNOLL, A.H., and PETROFF, A.P., 2013, The meaning of stromatolites: *Annual Review of Planetary Sciences*: v. 41, p. 21 – 44.
- BOURGAULT, D., KELLEY, D.E., and GALBRAITH, P.S., 2008, Turbulence and boluses on an internal beach: *Journal of Marine Research*, v. 66, no 5, p. 563 – 588. DOI: 10.1357/002224008787536835
- BUNTING, J.A., 1986, Geology of the eastern part of the Nabberu Basin Western Australia: *Geological Survey of Western Australia, Bulletin*, v. 131, p. 1 – 130.
- BURNE, R.V., and MOORE, L.S., 1987, Microbialites: organosedimentary deposits of benthic microbial communities: *PALAIOS*, v. 2, p. 241–254.
- BUTTON, A., and VOS, R., 1977, Subtidal and intertidal clastic and carbonate sedimentation in a macrotidal environment: an example from the lower Proterozoic of South Africa: *Sedimentary Geology*, v. 18, p. 175 – 200.
- CACCHIONE, D.A., PRATSON, L.F., and OGSTON, A.S., 2002, The shaping of continental slopes by internal tides: *Science*, v. 296, p. 724 – 727. DOI: 1126/science.1069803
- CAMPBELL, F.H.A., and CECILE, M.P., 1975, Report on the geology of the Kilohigok Basin, Goulburn Group, Bathurst Inlet, N. W. T: *Geological Survey of Canada, Professional Paper*. 75-1, p. 297 – 306.
- CLOUD, P.E., and SEMIKHATOV, M.A., 1969, Proterozoic stromatolite zonation: *American Journal of Science*, v. 267, p. 1017 – 1061.
- DILL, R.F., SHINN, E.A., JONES, A.T., KELLY, K., and STEINEN, R.P., 1986, Giant subtidal stromatolites forming in normal salinity waters: *Nature*, v. 324, p. 55 – 58.

- DRAVIS, J.J., 1983, Hardened subtidal stromatolites, Bahamas: *Science*, v. 219, no. 4583, p. 385 – 386.
- DUPRAZ, C., and VISSCHER, P.T., 2005, Microbial lithification in marine stromatolites and hypersaline mats: *Trends in Microbiology*, v. 13, no. 9, p. 429 – 438.
- ERIKSSON, K.A., 1977, Tidal flat and subtidal sedimentation in the 2250 M. Y. Malmani Dolomite, Transvall, South Africa: *Sedimentary Geology*, v. 18, p. 223 – 244.
- FEDDERSEN, F., 2011, Observations of the surf-zone turbulent dissipation rate: *Journal of Physical Oceanography*, v. 42, p. 386 – 399. DOI:10.1175/JPO-D-11-082.1
- FELDMANN, M., and MCKENZIE, J.A., 1998, Stromatolite-thrombolite associations in a modern environment, Lee Stocking Island, Bahamas: *PALAIOS*, v. 13, p. 201 – 212.
- GEBELEIN, C.D., 1969, Distribution, morphology and accretion rate of recent subtidal algal microbialites, Bermuda: *Journal of Sedimentary Geology*, v. 39, p. 49 – 60.
- GINSBURG, R.N., and PLANAVSKY, N.J., 2008, Diversity of Bahamian microbialite substrates, *in* Dilek, T., Furnes, H., Muelenbachs, K., eds., *Links Between Geological Processes, Microbial Activities and Evolution of Life: Modern Approaches in Solid Earth Sciences*, Vol 4. Springer, New York, p. 177 – 195.
- HINTZE, L.F., TAYLOR, M.E., and MILLER, J.F., 1988, Upper Cambrian—Lower Ordovician Notch Peak Formation in Western Utah: U.S. Geological Survey, Professional Paper, no. 1393, p. 1–29.
- HOFFMAN, P., 1967, Algal microbialites: use in stratigraphic correlation and paleocurrent determination: *Science*, v. 157, p. 1043–1045.
- HOFFMAN, P., 1976, Stromatolite morphogenesis in Shark Bay, Western Australia, *in* Walter, M.R., ed., *Developments in Sedimentology: Stromatolites*, Vol 20. Elsevier, Amsterdam, p. 261 – 271.
- LOGAN, B.W., 1961, Cryptozoon and associate stromatolites from the recent, Shark Bay, Western Australia: *Journal of Geology*, v. 69, no. 5, p. 517–533.
- LOGAN, B.W., REZAK, R., and GINSBURG., R.N., 1964, Classification and environmental significance of algal stromatolites: *Journal of Geology*, v. 72, no. 1, p. 68 – 83.
- LOGAN, B.W., HOFFMAN, P., and GEBELEIN, C.D., 1974, Algal mats, cryptalgal fabrics, and structures, Hamelin Pool, Western Australia, *in* Logan, B.W., Read, J.F., Hagan, G.M., Hoffman, P., Brown, R.G., Woods, P.J., and Gebelein, C.D., eds., *Evolution and Diagenesis of Quaternary Carbonate Sequences, Shark Bay, Western Australia*: American Association of Petroleum Geologists, Mem. 13, p. 140–194.

- MARIOTTI, G., PERRON, J.T., and BOSAK, T., 2014, Feedbacks between flow, sediment motion and microbial growth on sand bars initiate and shape elongated stromatolite mounds: *Earth and Planetary Science Letters*, v. 397, p. 93 – 100.
- MILLER, J.F., EVANS, K.R., LOCH, J.D., ETHINGTON, R.L., STITT, J.H., HOLMER, L., and POPOV, L.E., 2003, Stratigraphy of the Sauk III interval (Cambrian-Ordovician) in the Ibex area, western Millard County, Utah and central Texas: *Brigham Young University Geological Studies*, v. 47, p. 23–118.
- PALMER, A.R., 1981, Subdivision of the Sauk Sequence, *in* Taylor, M.E., ed., *Short Papers for the Second Symposium on the Cambrian System: U.S. Geological Survey Open-File Report 81-743*, p. 160–162.
- PETROFF, A.P., SIM, M.S., MASLOV, A., KRUPENIN, M., ROTHMAN, D.H., and BOSAK, T., 2010, Biophysical basis for the geometry of conical microbialites: *Proceedings of the National Academy of Science, U. S. A.*, v. 107, p. 9956-9961.
- PLAYFORD, P.E., 1980, Environmental controls on the morphology of modern microbialites at Hamelin Pool, Western Australia: *Geological Survey of Western Australia, Annual Report*, p. 73 – 77.
- PLAYFORD, P.E., and COCKBAIN, A.E., 1976, Modern algal stromatolites at Hamlin Pool, a hypersaline barred basin in Shark Bay, Western Australia, *in* Walter, M.R., ed., *Developments in Sedimentology: Stromatolites, Vol 20*. Elsevier, Amsterdam, p. 261 – 271
- PLAYFORD, P.E., COCKBAIN, A.E., BERRY, P.F., ROBERTS, A.P., HAINES, P.W., and BROOKS, B.P., 2013, The geology of Shark Bay: *Geological Survey of Western Australia, Bull.* 146, p. 1–281.
- REID, R.P., VISSCHER, P.T., DECHO, A.W., STOLZ, J.F., BEBOUT, B.M., DUPRAZ, C., MACINTYRE, I.G., STEPPE, T.F., and DESMARAIS, D.J., 2000, The role of microbes in accretion, lamination and early lithification of modern marine stromatolites: *Nature*, v. 406, p. 989 – 992.
- SEMIKHATOV, M.A., GEBELEIN, C.D., CLOUD, P., AWRAMIK, S.M., and BENMORE, W.C., 1978, Microbialite morphogenesis—progress and problems: *Canadian Journal of Earth Sciences*, v. 16, p. 992 – 1015.
- SEREBRYAKOV, S.N., and SEMIKHATOV, M.A., 1974, Riphean and recent stromatolites: a comparison: *American Journal of Science*, v. 274, p. 556–574.
- SHAPIRO, R., 1990, Morphological variations within a modern stromatolite field, Lee Stocking Island, Exuma Cays, Bahamas, *in* Bain, R.J., ed., *Fifth Symposium on the Geology of the Bahamas, San Salvador, Bahamian Field Station*, p. 209 – 220.

YOUNG, G.M., 1973, Stratigraphy, paleocurrents and stromatolites of Hadrynian (Upper Cambrian) rocks of Victoria Island, Artic Archipelago, Canada: *Precambrian Research*, v. 1, p. 13 – 41.

YOUNG, G.M., and LONG, D.G.F., 1976, Microbialites and basin analysis: an example from the upper Proterozoic of northwestern Canada: *Palaeogeography, Palaeoclimatology, Palaeoecology*, v. 19, p. 303 – 318.

CHAPTER THREE
LITHISTID SPONGE-MICROBIAL REEF-BUILDING COMMUNITIES
CONSTRUCT LAMINATED, UPPER CAMBRIAN (FURONGIAN)
‘STROMATOLITES.’

Ken P. Coulson and Leonard Brand of Loma Linda University, Loma Linda, CA 92350.

Submitted for Publication, *Palaios Journal*, March 2, 2016.

Abstract

Lamina-like, weakly fused sponge spicule networks are intercalated between convex stromatolitic laminae in an upper Cambrian (Furongian) reef. Sponges are small, millimeter to centimeter-sized lithistids that encrusted automicritic laminae and in turn were encrusted by microbial biofilms, eventually leading to columnar, crudely laminated ‘stromatolites.’ Weakly fused desmas, now preserved as drusy calcite, possess an arcuate geometry along the medial to distal ray axes. Marginal decay and separation of calcified sponge tissue from these spicules produced curved, filament-like cavities that now obscure the former presence of spicules when viewed in cross-section. Further deterioration produced unrecognizable peloidal networks. These peculiarities may have contributed to the poor preservation of spicule networks in about 95% of the reef; an area covering at least 20 km². These observations have important implications when reconstructing middle to upper Cambrian reef-building communities. Until recently, these periods were assumed to be virtually devoid of calcified metazoan reefal components. An increasing number of recent papers, however, are demonstrating that metazoan reef-builders may have been more prevalent during these periods than was previously thought.

This paper adds a unique element to this consensus by demonstrating that lithistid sponge-microbial reef-building communities constructed laminated ‘stromatolites.’ This suggests that metazoan reef-builders may have had a flourishing ecology within upper, and perhaps middle Cambrian reefs, but due to the laminated morphology, size and preservation potential of sponges such as these, they have largely gone unnoticed in microbial buildups.

Introduction

The evolution of Cambrian reefs has traditionally been interpreted in terms of two general reef-building stages; the archaeocyath-calicimicrobe consortium that dominated the early Cambrian, followed by a largely microbial stage that dominated the middle to late Cambrian, subsequent to the archaeocyath decline in the late early Cambrian (Klappa and James, 1980; Kobluk, 1988; James and Gravestock, 1990; Brunton and Dixon, 1994; Shapiro and Rigby, 2004; Kruse and Zhuravlev, 2008; Adachi et al., 2011; Li et al., 2015). An increasing number of recent papers, however, are demonstrating that metazoan reef-builders may have been more prevalent during these periods than was previously thought (Johns et al., 2007; Hong et al., 2012, 2014; Chen et al., 2014; Lee et al., 2014; Adachi et al., 2015). We seek to add to this growing number of middle and upper Cambrian reefal discoveries, by examining an upper Cambrian sponge-microbial reef from the Hellnmaria Member of the Notch Peak Formation in southwestern Utah. This reef is unlike other coeval metazoan reefs, in that it contains small-scale, weakly fused lithistid sponges that encrusted automicritic laminae using a similar lamina-like morphology. Coeval sponge-microbial reefs are typically dominated by frame-building anthaspidellids that are randomly scattered throughout the sponge-microbial buildups

(Shapiro and Rigby, 2004; Kruse and Zhuravlev, 2008; Hong et al., 2012). The overall meso-scale fabric of the Notch Peak associations, however, are stromatolitic, and therefore represent a significant departure from coeval sponge-microbial reefal architecture. The remains of similar, lamina-like sponges have recently been found intercalated between microbial automicrites in Carboniferous and Triassic ‘stromatolites’ (Luo and Reitner, 2014; 2015). Taken together, these factors could easily lead to the misidentification of metazoan components in other microbial buildups at other locations around the world.

The aims in the paper are: 1) To suggest that as yet unclassified lithistid sponges, together with microbial reef-building communities, mutually constructed laminated ‘stromatolites.’ 2) To propose that these sponge-microbial ‘stromatolites’ have largely gone unnoticed due to the sponge’s lamina-like morphology, size and preservation potential. And 3) To compare well preserved sponge spicule networks with deteriorated spicule networks and fenestral networks, for the purpose of providing some petrographic and taphonomic criteria that may help identify sponge-microbial associations in similar rocks.

Geologic Background

The western continental margin of Laurentia is thought to have formed during the Late Proterozoic rifting of Rodinia. According to Miller et al. (2003, p. 58), lower Paleozoic strata of the eastern Great Basin were deposited on a subsiding carbonate platform that provided over 4500 m of early Paleozoic accommodation space. Superimposed throughout these sediments are large-scale, second-order sequences that deposited the Cambrian/Ordovician Orr and Notch Peak Formations as well as the

Ordovician House Limestone (Miller et al. 2003) in what is now southwestern Utah (Fig. 1). Central to this discussion is the microbialite-bearing Notch Peak Formation which has been divided into three mappable members: the Hellnmaria, Red Tops and Lava Dam (Fig. 2A). All three members are traceable from within the House and Confusion Ranges in western-central Utah to the Wah Wah Mountains in the south (Hintze et al. 1988). According to Palmer, the Notch Peak Formation was deposited during the third interval of the Sauk mega-sequence (Palmer, 1981). Miller et al. (2003) broke the Sauk III interval into 14 smaller sequences (See illustration in Miller et al. 2003, p. 27). The Hellnmaria Member of the Notch Peak Formation includes the second half of sequence 1, and all of sequences 2-4 in Miller et al. (2003) and has been interpreted in terms of an overall sea-level highstand.

Conodont biostratigraphic correlations by Miller et al. (2003, p. 27) assign the microbialite-bearing beds of the upper Hellnmaria Member to the *Proconodontus tenuiserratus* through *Proconodontus muelleri* zones. This places the upper Hellnmaria Member in the late Cambrian Sunwaptan Stage of the Millardan Series (middle Furongian) (Fig. 2). According to Miller et al. (2003), the lower to middle parts of the Hellnmaria Member chiefly consist of thin-bedded to laminated dark lime mudstones, that change to intraclastal, ooid and oncoidal packstones and grainstones towards the top (Miller et al., 2003, p. 30). At its type section, only the upper 154 m of the 366 m thick Hellnmaria Member contains microbialite-bearing beds that are completely absent from the lower interval (Fig. 2A). Miller et al. (2003) interpret the Hellnmaria Member as an overall sea-level highstand that shallows significantly towards its top. This shallowing-

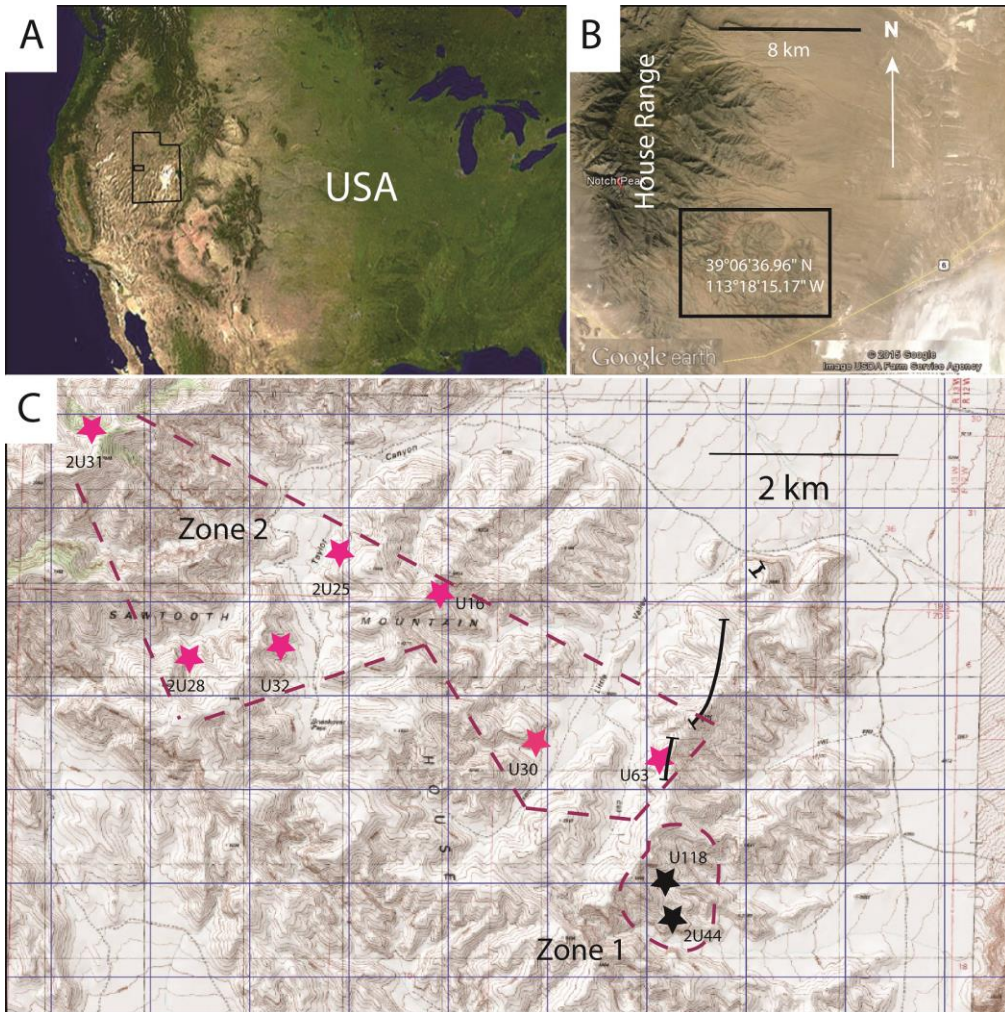


Fig. 1. Geological setting of research area. A) Satellite image of the USA showing state of Utah. Image Public Domain. Small black rectangle enlarged in B. B) Image adapted from Google Earth, USDA Farm Service Agency, showing research area (black rectangle enlarged in C). C) Image of research area provided by MyTopo indicating outcrop locations. Dotted lines approximately outline zones 1 and 2. Pink stars are outcrop locations in zone 2. Black stars are outcrop locations in zone 1. Outcrops and UTM coordinates are as follows from NW to SE: 2U31, 296590 4332862; 2U28, 297509 4330507; 2U25, 299088 4331582; U16, 299798 4331367; U30, 301002 4329694; U63, 302195 4329234; U118, 299154 4331613; 2U44, 302507 4327662. The type section constructed by Hintze et al. (1988, p. 21) runs through U63 (All 3 black lines).

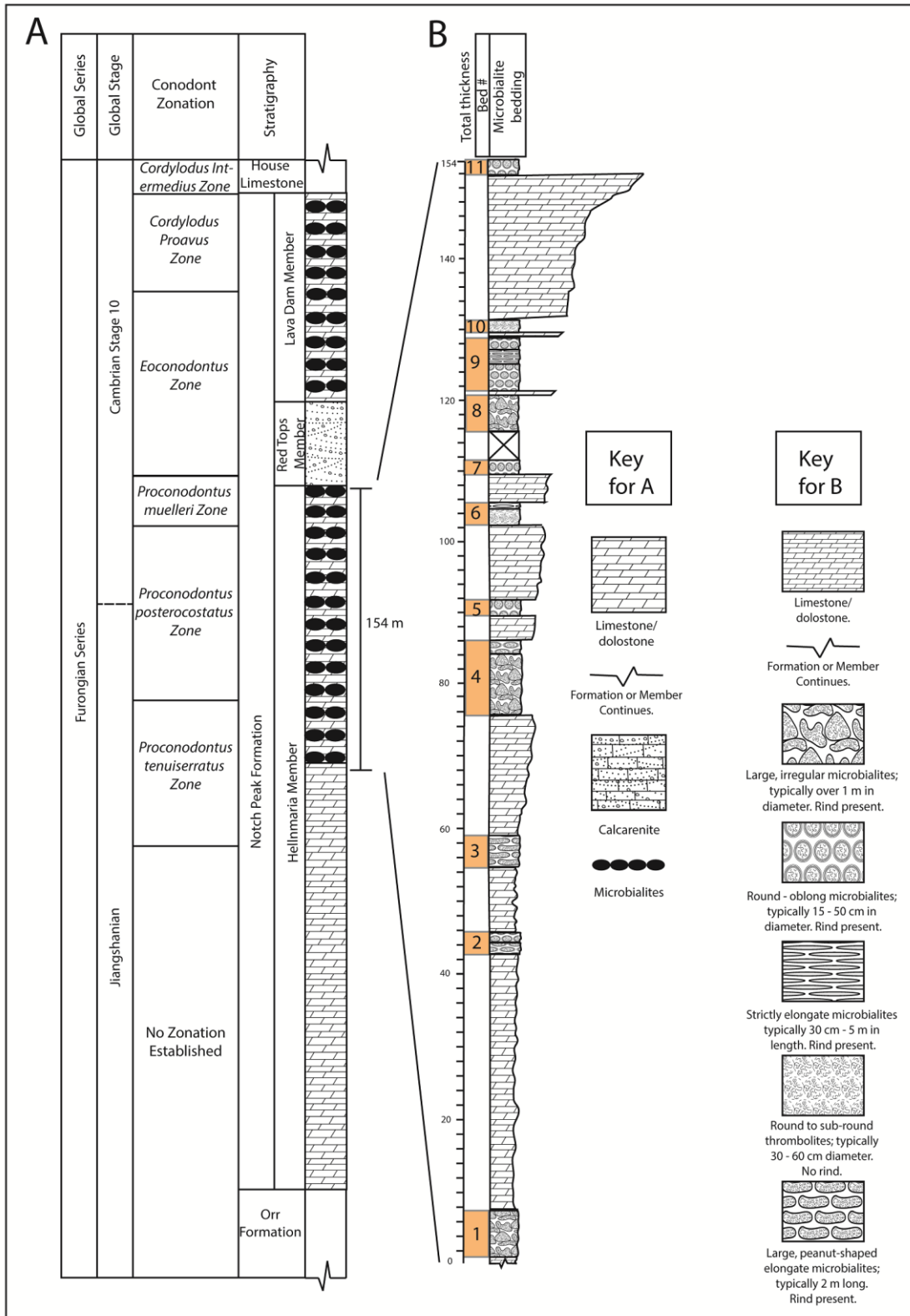


Fig. 2. Stratigraphy and biostratigraphy. A) Stratigraphic column of the Notch Peak Formation, adapted and simplified from Hintze et al. (1988), and conodont zonation adapted from Miller et al. (2003). Notice that in the Hellnmaria Member, microbialites are only found in the top 154 m. B) Stratigraphic column of the top 154 m of the Hellnmaria Member of the Notch Peak Formation measured at the type section (only beds 9,10 and 11 could be correlated across the research area. Bed thicknesses vary depending on outcrop) (see fig. 1C). Tapered limestone/dolostone sections communicate a general coarsening upward trend.

upwards succession is abruptly terminated by the Red Tops Lowstand (Miller et al., 2003, p. 27), where clean, largely homogeneous, fine to medium-grained limestones and dolostones are abruptly truncated by a coarse-grained calcarenite deposit

Methods

The microbialite bed pertinent to this paper was correlated over a large geographic area of about 20 km². Samples were sourced from nine outcrop locations (Fig 1C). Where rock samples could not be obtained easily, a gas powered Stihl drill fitted with a diamond studded 3.2 cm core bit, and a gas powered Shaw-backpack drill fitted with a diamond studded 5.1 cm core bit were used to obtain drill-core samples. Cores varied in length from 2 to 15 cm.

Forty five thin-sections were prepared from eleven different microbialites; six from zone 1 and five from zone 2 (Fig. 1C). Thin-sections and rock samples were analyzed using microscopy, and scanning electron microscopy (SEM). Larger samples sourced from various outcrops were lapped, polished and photographed.

Using microscopy, it was determined that the total area occupied by the sponges was about 50%. In order to quantify this, sponge spicule networks in three thin-sections, sourced from three separate zone 1 microbialites, were manually traced using the microscope and Illustrator CS6. These images were then filtered through ImageJ in order to obtain areal distribution of sponges as a percentage.

All rock samples are kept on campus at LLU in Risley Hall. All thin-sections are kept in the basement of Griggs Hall, room 10. Thin-sections are a combination of (n = 4) 2.5×4.5 cm, (n = 25) 5×7.5 cm, and (n = 16) 5×6.5 cm glass slides.

Results

Overview of Bed 11

Hintze et al. (1988) bundled all Hellnmaria microbialites into a single package of strata that spans the upper 154 m of the Hellnmaria Member (Fig. 2A). We re-measured this segment of the type section (Fig. 2B) being especially attentive to specific microbialite beds, bed thicknesses and general microbialite characteristics. We found eleven distinct microbialite-bearing beds separated by intervening wackestone-grainstone intervals that span the upper 154 m of the Hellnmaria Member (Fig. 2B). All eleven beds are morphologically unique, although substantial overlap does exist from one bed to the next. Bed 11 is a 1 to 3 m thick microbialite-bearing unit that contains a tightly packed field of round to sub-round microbialites covering a large geographic area of approximately 20 km². Microbialites within the bed are separated into two zones on the basis of some fundamental macro, meso and micro-scale differences (Fig. 1C). This zonation, however, is merely a useful artifact as the microbialites are contiguous across the entire bed.

Microbialites in zone 1 (Fig. 1C) are stromatolitic (Fig. 3A), have diameters of between 10 to 30 cm at their longer axes, and are typically 20 – 40 cm tall (Fig. 3B and C). Synoptic relief is about 10 – 20 cm. The interspace material is best described as an intra-bioclastic grainstone with some minor packstone domains (Fig. 4F). Allochems, predominantly composed of intraclasts ($\approx 50\%$) and trilobite bioclasts ($\approx 40\%$), average 0.5 – 4 mm in length, appear moderately sorted, sub-rounded, but generally are not spherical. Some trilobite bioclasts are over 1 cm long. These forms only have a small

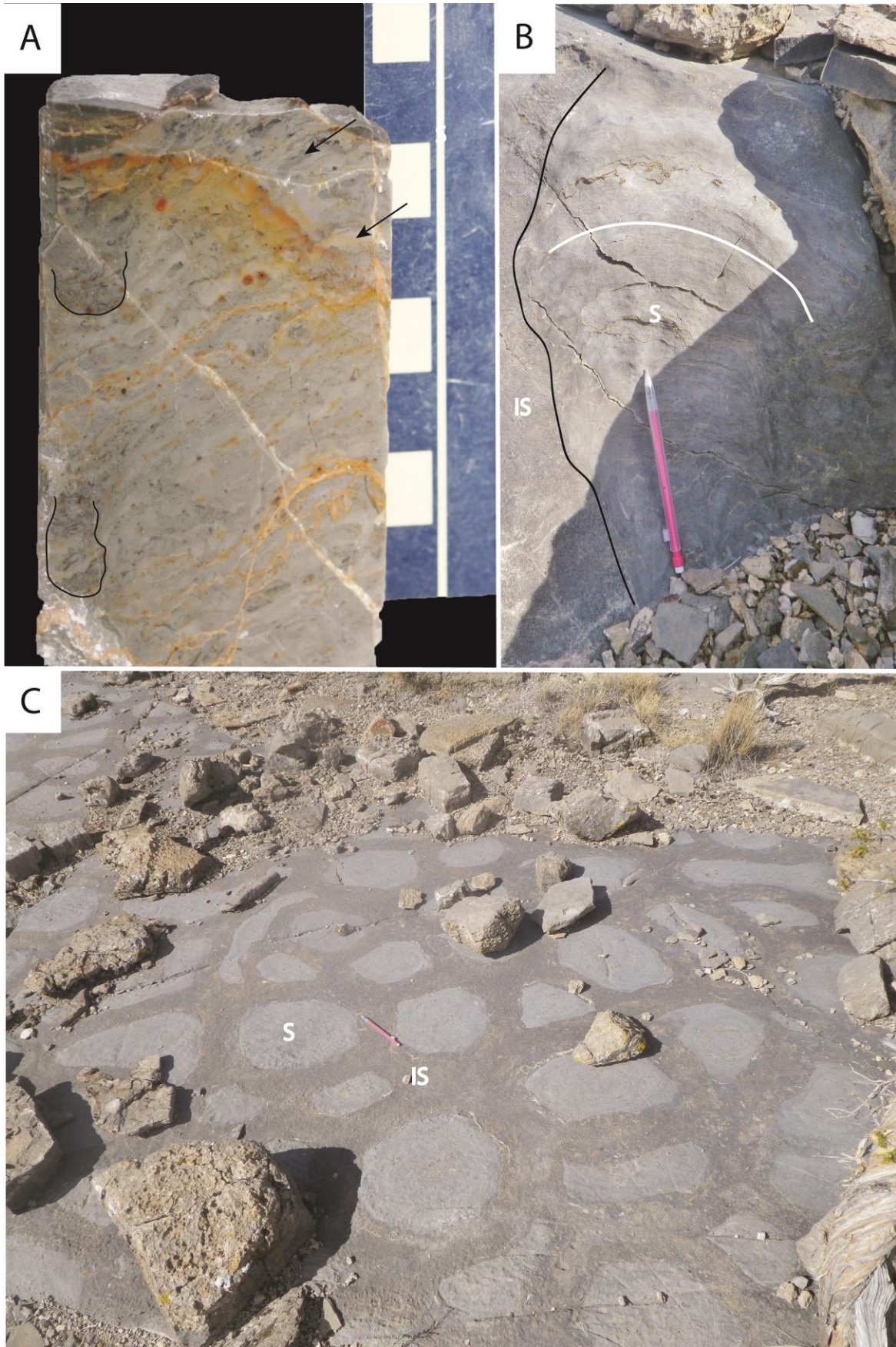


Fig. 3. Macro and meso-scale features of 'stromatolites' in zone 1. S = Stromatolite. IS = Interspace between macro forms. A) 5 cm diameter core, cut longitudinally, lapped and polished. Alternating sponge (darker color, top arrow) and micrite (lighter color, bottom arrow) forms crude, mm-scaled laminae. Pockets of bioclastic packstone are outlined in black. B) Cross-sectional image of a stromatolitic microbialite showing convex laminations (a single lamina outlined). C) Plan-view of microbialites. Cm scales. Pencil is 15 cm long. Sample numbers: A) 2U45B.

areal distribution of about 1 km² (Fig. 1C). Microbialites in zone 2 (Fig. 1C) are also stromatolitic, have diameters that vary from 40 to as great as 70 cm across their longer axes, with heights fluctuating from just a few dm to about 70 cm. These forms are differentiated from those in zone 1 by the presence of a central core composed of mini-stromatolites (Fig. 4A-E). Synoptic relief is about 10 – 20 cm. The interspace material is best described as an intra-bioclastic grainstone with some minor packstone domains. Allochems, predominantly composed of intraclasts (\approx 70%) and trilobite bioclasts (\approx 20%) average 0.5 – 2 mm in length, appear well-sorted, well-rounded and are sub-spherical. This form is laterally continuous across the majority of the bed, having a total areal distribution of about 20 km² (Fig. 1C).

Diagenetically, microbialites from zone 1 are rarely altered by dolomitic recrystallization. Those forms in zone 2 are often badly dolomitized within the mini-stromatolite-bearing core, with dolomitic recrystallization sometimes extending into the stromatolitic region of the microbialite proper.

Spicule Networks in Zone 1

Sponges are recognized as spicule networks that typically do not exceed a few cm in size, with many not exceeding 1 cm (Fig. 5A-D). With few exceptions, well preserved sponge spicule networks only occur within the microbialites of zone 1 (Fig. 6), and often grade into deteriorated spicule networks that vary in degree of preservation (Fig. 7A-F). Peloidal domains and voids seem to be the end members of the decay process (Fig. 7A and B). Spicule networks display various morphologies, taking on lamina-like, amoeboid, and varied lump-shaped forms, although the lamina-like form is the most

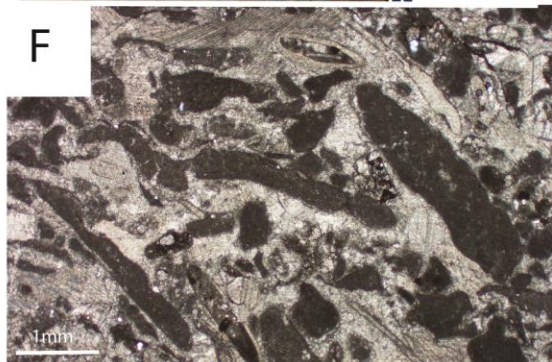
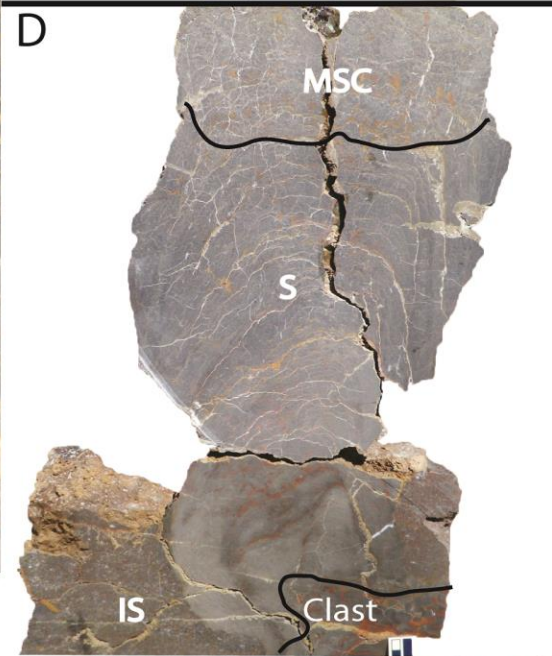
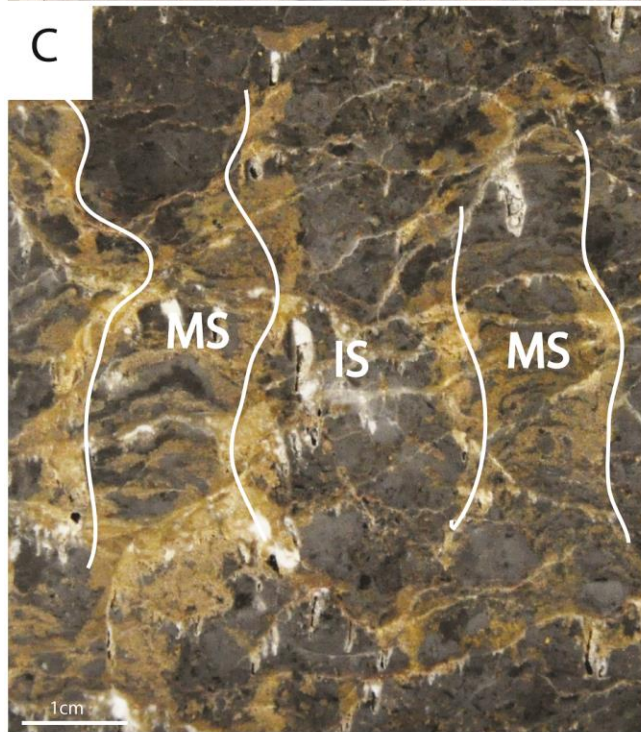
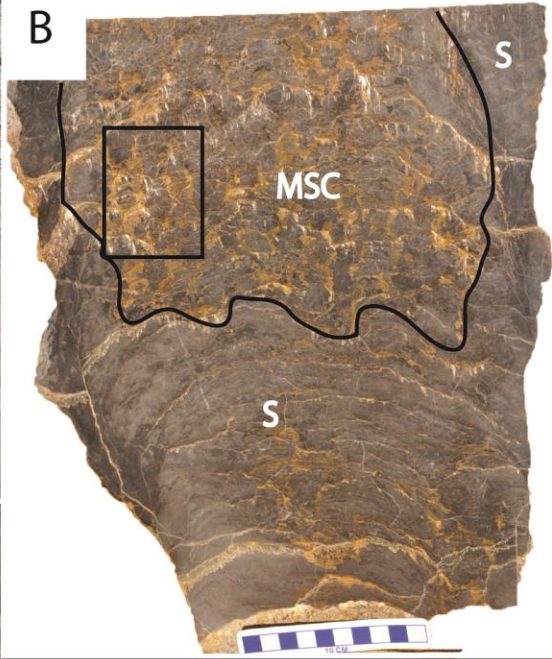
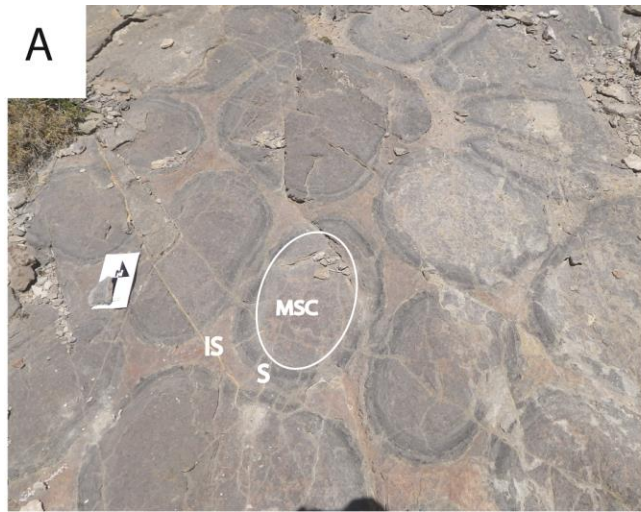


Fig. 4. Macro and meso-scale features of ‘stromatolites’ in zone 2. S = Stromatolite. IS = Interspace between macro and mini forms. MSC = Mini-stromatolite Core. MS = Mini-stromatolite. A) Plan-view of microbialites. B) A complete microbialite removed from outcrop, cut longitudinally through medial plane, lapped and polished. Mini-stromatolite core clearly marked off from stromatolite fabric below. Note the acute boundary. Rectangle enlarged in C. C) Enlarged from B showing two mini-stromatolites separated by packstone interspace. D) Second microbialite likewise cut longitudinally through medial plane. Specimen is not lapped or polished. Notice micritic clast (outlined) upon which this structure grew. White line separates stromatolite (below) from mini-stromatolite core (above). The boundary between both fabrics is also acute. E) Transverse cut through stromatolite in B reveals maze-like structures composed of mini-stromatolites and wackestone-packstone interspaces. F) Thin-section of intra-bioclastic grainstone from interspace between microbialites in figure 3C. Cm scales. Sample numbers: B) U110A. D) U101A. E) U110A_{top}.

common (Fig. 5). Cryptic habits are also observed (Fig. 6A). The cryptic specimens are chiefly associated with cm-scale pockets of bioclastic packstone that regularly appear throughout the microbialites (Fig. 3A).

Most of the megascleres have an overall length of between 200 and 500 μm (Fig. 6E-G). These desma-like tetraxons seem to fuse in patches, with many of the patches and/or individual megascleres ‘floating’ in what at one time may have been a fleshy matrix (Fig. 6E-G). Rounded and sometimes gnarled zygomes (Fig. 6E-G) average about 50 μm in diameter, and are attached to rays which themselves average 30 to 40 μm in diameter (Fig. 6F and G). The rays are often arcuate along their medial to distal axes (Fig. 6E-G), although some are straight (Fig. 6H). Some spicules exhibit an arcuate geometry that extends over the entire spicule structure. Zygomes in these spicules are typically diminished to non-existent (Fig. 6D). Using energy dispersive x-ray spectroscopy and microscopy, we determined that the formerly siliceous spicules are now preserved as drusy calcite, a diagenetic alteration that is typical for silica embedded in calcite.

After tracing out sponge spicule networks representative of three separate microbialites, we were able to determine that total areal sponge distribution was: $\approx 60\%$ (Fig. 5B), $\approx 49\%$ (Fig. 5C), and $\approx 46\%$ (Fig. 5D).

Homogenous micritic domains, often filled with monaxons that appear to be randomly distributed, are found at the center of some sponge spicule networks (Fig. 6B). The mm-thick micritic lenses crudely intercalated between the sponges tend to be homogenous, blotchy light to dark gray in color, and locally host abundant monaxons and less abundant bioclasts (Fig. 7G). Bioclasts are typically less than 2 mm in length, and

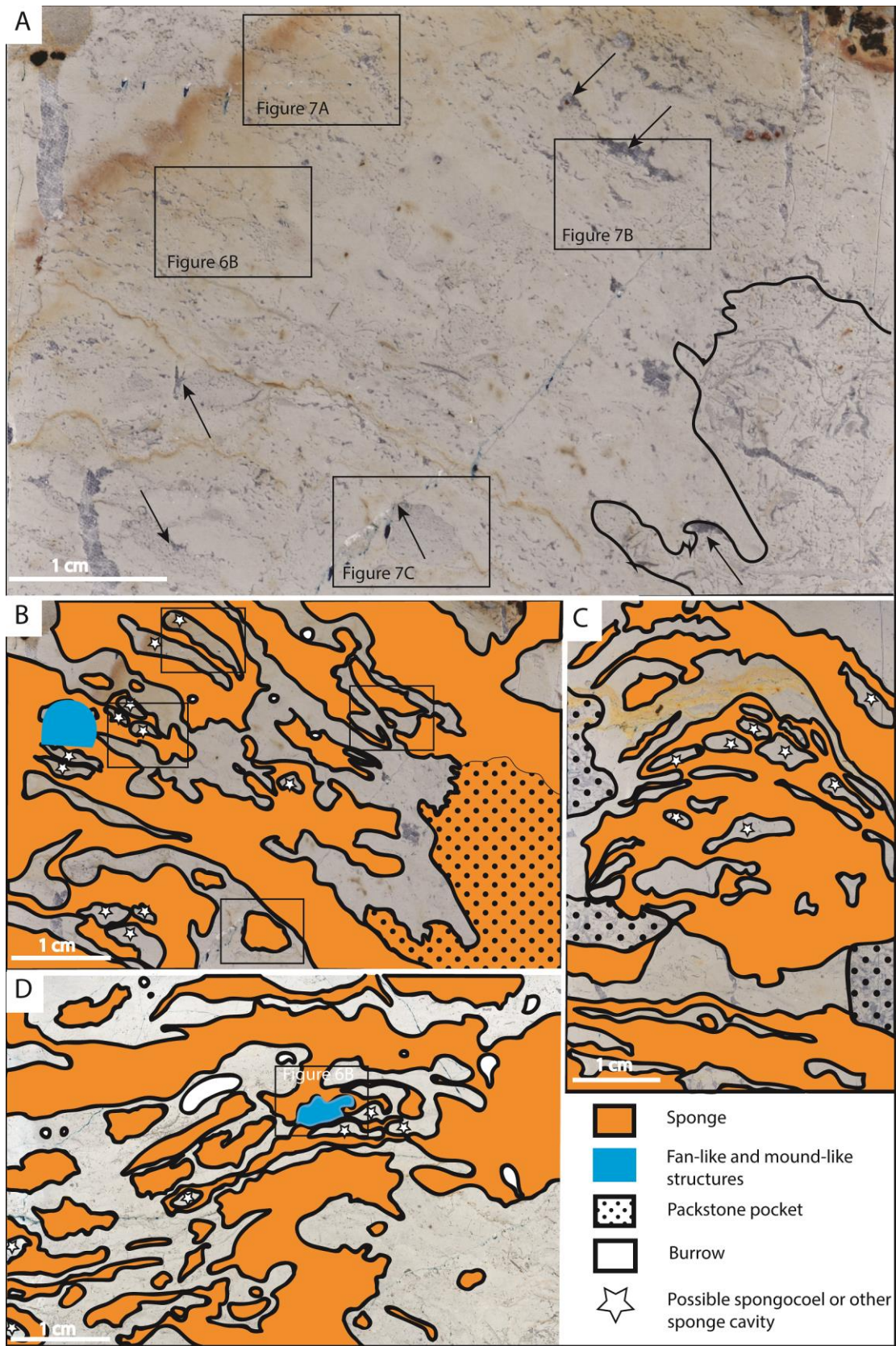


Fig. 5. Photographs of complete thin-sections showing areal sponge distribution and planar morphology. All images are in cross-section. A) Rock surface (A complete, prepared thin-section) showing lamina-like sponges (perforated gray fabric) encrusting micrite (solid gray fabric), producing crude, diagonal laminae (from top left to bottom right). Outlined area is a large bioclastic packstone pocket. Arrows point to deteriorated sponge spicule networks producing geopetal structures. B) Same image as in A with sponges outlined in orange, and having a sponge areal distribution of 60%. Sponges also encrust a micritic fan-like structure (in blue). Notice that the packstone pocket is filled with sponge spicule networks. C) Rock surface (A complete, prepared thin-section from another microbialite) showing sponges encrusting micrite producing crude, convex laminae. Sponge areal distribution is 49%. D) Rock surface (A complete, prepared thin-section from a third microbialite) showing sponges encrusting micrite producing diagonal laminae (from top right to bottom left). Rectangle enlarged in figure 7E, showing sponges encrusting a microbial mound-like structure. Sponge areal distribution of 46%.

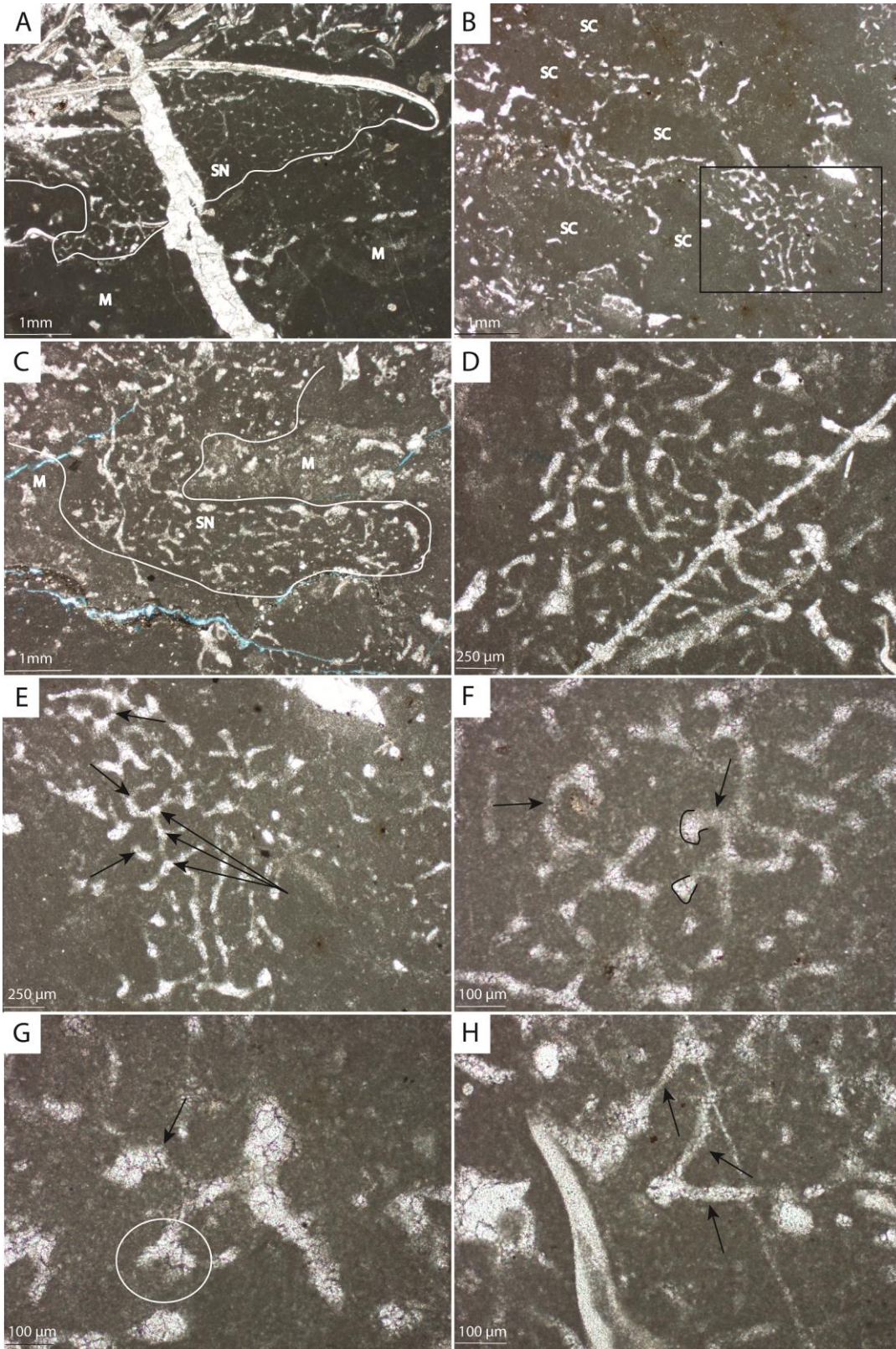


Fig. 6. Spicule networks from zone 1. All images are in cross-section. M = Micrite, S = Sponge, SC = Sponge cavity. A) Sponge is attached to the underside of a trilobite carapace displaying a cryptic habit. B) Spicule networks circumscribe possible sponge cavities. Note desma tetraxons enlarged in E. C) Sponge spicule network. D) Some spicules exhibit an arcuate geometry that extends to the entire spicule. Note the diminished to non-existent zygomeres. E) Desma-like spicules showing putative zygois (long arrows) and curved, arcuate rays (short arrows). F) Partial network showing bulbous zygomeres (outlined) and curved rays (arrows). G) Desma-like spicule showing possible gnarled zygomere (circled) and curved ray (arrow). H) Spicules showing straight rays.

occur sporadically in isolated, micro-scale wackestone patches. Very fine wavy, to horizontal micritic laminae, small convex micritic mound-like, and micritic fan-like structures are also randomly distributed throughout these micritic lenses (Fig. 7E and F). Most of these mm-thick micritic lenses, however, are structureless. Large, cm-scaled pockets of bioclastic packstone, often found truncating micritic lenses and sponges, can also be found embedded within the matrix (Fig. 3A). Calcimicrobes, typically identified on the basis of diagnostic genera such as *Epiphyton*, *Girvanella*, and *Renalcis*, are absent from our thin-sections.

Fenestral/Peloidal Networks in Zone 2

Microbialites in zone 2 contain fenestral/peloidal networks, very similar to the deteriorated spicule networks from forms located in zone 1 (Compare fig. 7 A-F with fig. 8A-G). Apart from some possible exceptions (Fig. 8A), spicule networks could only be clearly identified in the forms from zone 1, so at this stage we simply refer to the networks in the forms from zone 2 as fenestral or peloidal networks.

The microbialites in zone 2 are composed of a stromatolitic region at the base of the form that abruptly transitions into a central core composed of mini-stromatolites and chaotic stromatolitic fabric towards the middle/top of the microbialite proper (Fig. 4B). The mini-stromatolites are separated by interspaces filled with detrital, packstone fill (Fig. 4C). This central core is sometimes encased within the stromatolitic laminae of the larger microbialite structure. A transverse cut through the top of the microbialite proper presents an organization that looks somewhat maze-like (Fig. 4E), but should be

distinguished from the maceriate forms described by Shapiro and Awramik (2006) based on the absence of non-laminated meso-clots.

In cross-section, the basal, stromatolitic meso-fabric appears as alternating micrite-wackestone and fenestral/peloidal networks (Fig. 8G), similar to that found in zone 1. The micrite-wackestones are composed of homogeneous, blotchy light to dark gray micrites that contain ubiquitous, yet evenly distributed monaxons throughout. Some very fine laminae, small mound-like and fan-like structures can be found at random locations within the sediments. Small, less than 200 μm sized bioclasts are rarely found at this location within the larger microbialite form. The fenestral/peloidal networks often parallel the micrite-wackestone sediments, are about 1 – 3 mm thick, and are generally peloidal in character (Fig. 8G). Some of the peloids ‘float’ in blocky calcite, fenestral-filling cement (Fig. 8E-G). This same phenomenon is also found in the deteriorated spicule networks of zone 1 (Fig. 7A-F). Fenestral networks also display amoeboid, and varied lump-shaped forms, similar to the spicule networks in zone 1 (Fig. 8B-F). Importantly, we were able to determine that the initial micritic laminae budding from a micritic clast upon which one of the microbialites grew is free of fenestral networks. This means that the microbial communities, and not the alleged sponges seem to have been the initial constructors.

In the central, mini-stromatolite-bearing core of the microbialites, the wide, continuous laminations that are found at the stromatolitic base are replaced by 1 to 2 cm-wide, and up to 20 cm tall, mini-stromatolites (Fig. 4B and C). These structures are surrounded by inter-stromatolite bioclastic packstones, primarily composed of trilobite hash, peloids and intraclasts. Fine, convex, micritic laminations occur within the

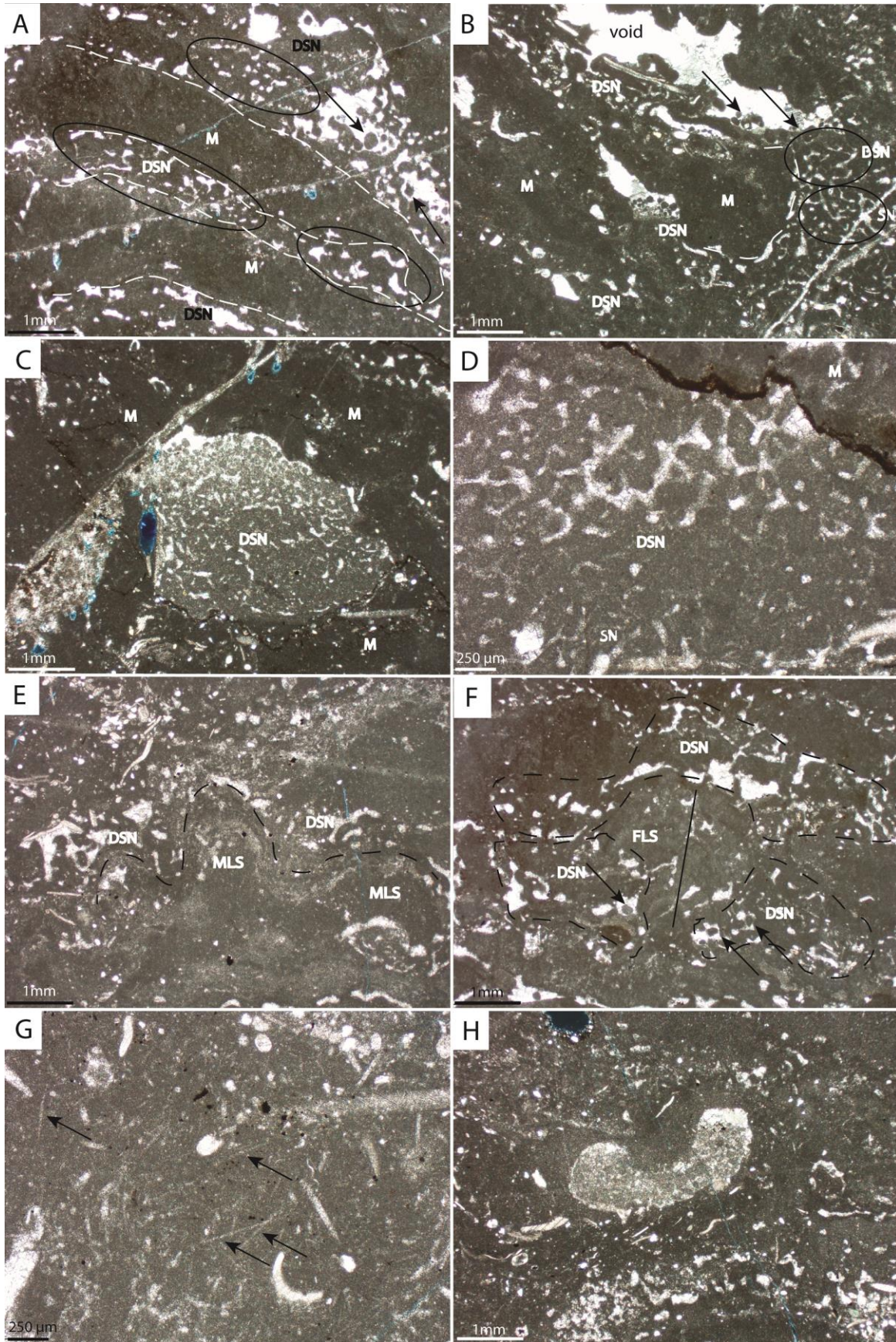


Fig. 7. Deteriorated spicule networks with associated micritic mound-like and fan-like structures from zone 1. All images are in cross-section. DSN = Deteriorated spicule network. FLS = Fan-like structure. MLS = Mound-like structure. M = Micrite. A) Deteriorated spicule networks circumscribe putative sponge cavities now preserved as micrite (outlined in dashed white lines. Note the pronounced boundary between networks and micritic domains). Networks show varying degrees of deterioration, with peloidal domains (arrows) presenting advanced decay (note 'floating' peloids). Less deteriorated domains (ellipses) contain filament-like cavities. B) Spicule network (lower ellipse. See figure 6D for enlargement) grades upwards into a deteriorated spicule network of filament-like cavities (upper ellipse), then into a peloidal domain (arrows), and finally into a void now preserved as drusy calcite. Dashed white line denotes a pronounced boundary between networks and adjacent micritic domain. C) Orb-shaped deteriorated spicule network consisting of filament-like cavities that grade into a peloidal domain. D) Reasonably well preserved spicule network grades upwards into a domain of filament-like cavities. E) Mound-like structure encrusted by sponges (now preserved as deteriorated spicule networks). F) Fan-like structure encrusted by sponges (now preserved as deteriorated spicule networks). Line runs through fan axial plane. Arrows show 'floating' peloids. G) Homogenous, monaxon rich (arrows) micrite intercalated between sponge spicule networks from zone 1. H) Faecal pellets (now preserved as peloids) fill a macroburrow. These structures can be differentiated from sponge-related deteriorated spicule networks.

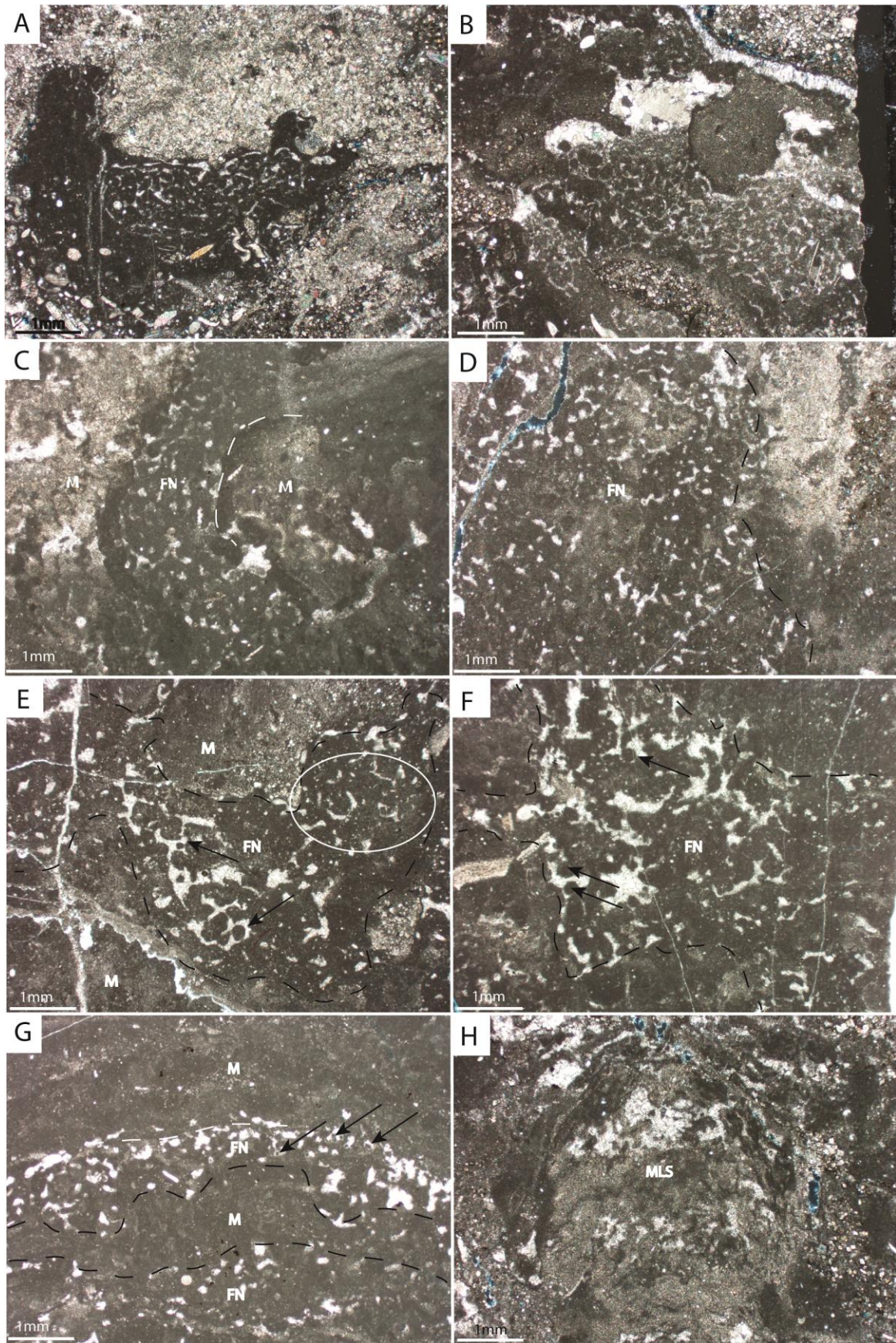


Fig. 8. Fenestral/peloidal networks from zone 2. FN = Fenestral network. M = Micrite. A – F) Networks are presented in a sequential series that display putative degrees of deterioration, going from best to worst. A) One of the rare, credible spicule networks from zone 2. B) Fenestral network composed of filament-like cavities that grade upward into a peloidal domain; very similar to the deteriorated spicule domains from zone 1. C) Automicrite vertically ‘encrusted’ by a fenestral network composed of filament-like cavities. Dashed lines delineate pronounced boundary between network and micritic domain. D) Fenestral network composed of less organized filament-like cavities. E) Fenestral network showing less organized filament-like cavities (ellipse), and peloidal domains (arrows). Note ‘floating’ peloids. F) Fenestral network composed of peloidal domains and voids. Note ‘floating’ peloids. G) Fenestral networks are oftentimes intercalated between automicritic sediments, similar to the spicule networks in zone 1. Arrows denote ‘floating’ peloids. H) Mound-like structure constructed of precipitated micritic clumps putatively derived from microbial activity.

mini-stromatolites, and alternate with fenestral/peloidal networks, similar to that found in the stromatolitic portion at the base of the structure. Larger, microbial mound-like structures are also found in the more chaotic regions of the mini-stromatolite-bearing cores (Fig. 8H).

Discussion

Microbial-sponge reef-building communities construct 'stromatolites.'

Based on the presence of well-washed, inter-columnar grainstones deposited between the microbialites of bed 11 (the entire bed), we suggest that these forms grew in a shallow, sub-tidal environment.

Microbial biofilms first colonized and stabilized the underlying substrate (or attached to already hard surfaces such as the clast in fig. 4D). As a result of continued microbial trapping and binding of lime mud and/or precipitation of micrite, the meso-fabric took on a stromatolitic texture. This initial rigid microbialite served as a suitable substrate for early sponge attachment (Kruse and Reitner, 2014; Adachi et al., 2015). It seems that both microbial and sponge communities then took on reciprocal encrusting roles, slowly immuring each other in a regular organization that eventually led to the construction of a columnar 'stromatolites' in both zones 1 and 2. We observed no criteria, however, to determine if this close relationship was mutualistic, commensalistic, or parasitic. Although wide laminae continued to characterize the forms in zone 1, a change in conditions initiated a diminutive growth phase in zone 2, whereby singular columnar 'stromatolites' branched into a grove of digitate, mini-'stromatolites.' We are not sure

what conditions changed, but this change must have been abrupt, as the boundary between the two different meso-fabrics is salient (Fig 4B).

Most Paleozoic reef experts agree that during the middle to late Cambrian, it was the microbial reef-building communities that played the most significant reef binding and constructing roles, with sponges taking on a secondary role (Riding and Zhuravlev, 1995; Adachi et al., 2011; Kruse and Reitner, 2014). We suggest that these microbial communities were responsible for the overall stromatolitic fabric, the convex laminations, and the overall columnar form. Sponges contributed to the overall macro-shape only by means of vertical inheritance, having a total areal sponge distribution of around 50%.

Although these sponges most commonly exhibit an encrusting habit, some sponges favored a cryptic habit and are found sheltered under bioclasts (Fig. 6A). This is important from a paleo-environmental perspective, since examples of sessile metazoan cryptobionts from the middle to late Cambrian are rare (Kobluk, 1988; Hong et al., 2014; Lee et al., 2014). This may, however, be an artifact based on the misidentification of sponges in many microbialite buildups (Luo and Reitner, 2015).

Metazoan reefs: Underrepresented or Overlooked?

Sponges closely resembling those described in this paper have also been described from middle Cambrian to Late Ordovician rocks in China and Korea (Hong et al., 2012, 2014; Chen et al., 2014; Lee et al., 2014; Park et al., 2015). Similarities include small-scale body sizes, irregular spicule networks, similar size and shape of megascleres, including the peculiar arcuate rays, similar reefal habits, and similar ecological zones. The absence of easily identifiable characters such as canal systems and rigid skeletons,

were also common features of these China/Korea associations. Typically, anthaspidellid sponge spicules fuse to form rigid frameworks of desmas easily identified as ladder-like trab networks (Rigby, 1983; Shapiro and Rigby, 2004; Adachi et al., 2013; Schuster et al., 2014; Hong et al., 2015). The desma-like spicules in the Notch Peak specimens however, seem to fuse in patches, with many of the patches and/or individual megascleres ‘floating’ in what at one time may have been a fleshy matrix (Fig. 6E-G). These observations may of course represent a taphonomic bias, but it may be that these isolated patches and/or individual megascleres were once attached to each other by spongin, a proteinaceous bundle of fibers that is rarely preserved (Narbonne and Dixon, 1984; de Freitas and Mayr, 1995; Warnke, 1995; Carrera and Botting, 2008; Luo and Reitner, 2014).

Although some of the spicule networks resemble the anastomosing filamentous structures of Luo and Reitner (2015) (Fig. 6D), we propose that the sponges connected with this study be affiliated with ‘Lithistida,’ a polyphyletic order of sponges that clusters around the presence of desma tetraxons (Pokorny, 1965; Rigby, 1983; Schuster et al., 2014) (Fig. 6F). Fused skeletons and larger, cone-shaped morphologies are often diagnostic of lithistids, but this is not always the case (Pokorny, 1965; Rigby, 1983; Schuster et al., 2014).

We suggest that these sponges, and others like them, shared a common morphological niche with microbial reef-building communities, but that this mutual role of construction has largely gone unnoticed for several reasons. First, weakly fused spicule networks are known to have a low preservation potential due to the absence of a robustly fused skeleton (Narbonne and Dixon, 1984; de Freitas and Mayr, 1995; Warnke, 1995;

Carrera and Botting, 2008). In order to achieve body rigidity, it has been suggested that ancient non-skeletonized sponges utilized spongin, much like many modern taxa (Carrera and Botting, 2008; Luo and Reitner, 2014). This rigidity can only be maintained, however, while the organism is alive. At death, bacterial decay will cause the sponge to disarticulate leaving disorganized spicule domains. The plentiful abundance of such a reef-building fauna in the Cambrian might explain the ubiquitous presence of spicules in reefal-type rocks that are at the same time often devoid of sponge fossils (de Freitas and Mayr, 1995; Carrera and Botting, 2008). de Freitas and Mayr (1995), discussing the presence of abundant spicules in an otherwise sponge-free Ordovician reefal environment, suggest the putative presence of what they call “fleshy, non-sclerotized” sponges. Carrera and Botting (2008, p. 131-133) recognize the presence of such a fauna in middle to late Cambrian environments, but acknowledge the rarity of such forms in the fossil record. This latest discovery, however, bridges a gap that associates an abundance of such a fauna with microbial reef-building communities.

Second, there is an important overlap that exists between spicule networks, deteriorated spicule networks and fenestral networks. The latter two kinds of networks are somewhat similar, and mainly differ in how closely they can be related to sponges. Most of the ambiguous fenestral networks are found in the microbialites from zone 2, and reflect different, yet unknown environmental conditions that reduced the preservation potential of the sponges. We therefore suggest that many of these fenestral networks are actually degraded spicule networks. This idea is not novel. Several authors have suggested that similar reticulate networks represent decayed and/or decaying sponge spicule networks (Klappa and James, 1980, p. 439; Pohler and James, 1989, p. 208;

Bourque and Boulvain, 1993, p. 613). Others propose that similar structures represent spaces originally occupied by cyanobacterial filament bundles (Flügel and Steiger, 1981, p. 393; Pratt, 1982, p. 1217; Monty, 1995, p. 20). Pratt (1982, p. 1218) did however, entertain the idea of a sponge presence. Luo and Reitner (2014, p. 474; 2015, p. 11), working with very similar, anastomosing filamentous microstructures from the Carboniferous and the Triassic, were convinced that this kind of fabric may represent the remains of 'keratose,' non-spicular sponges. They called into question a cyanobacterial possibility, appealing to a lack of examples where cyanobacterial filaments form these kinds of 3D networks. A non-spicular, 'keratose' sponge interpretation seemed most likely for similar microtubule domains according to Larmagnat and Neuweiler (2015, p. 179). Zhuravlev and Wood (1995, p. 457) discuss another possibility, attributing the presence of 100 – 500 μm tubular fenestrae to the activity of microburrowers. Microburrowers, however, excavate indiscriminately, and do not leave neat, linear boundaries between fenestral networks and adjacent micritic domains (Luo and Reitner, 2014; 2015) (Figs. 7A,B and 8C,G). Significantly, the reticulate structures from Klappa and James (1980, see fig. 23), Flügel and Steiger (1981, see fig. 21), Pratt (1982, see fig. 13), Bourque and Boulvain (1993, see fig. 10) and Monty (1995, see fig. 5), as well as the microtubule domains of Larmagnat and Neuweiler (2015, see fig. 10) look remarkably similar to some of the deteriorated spicule and fenestral networks found in our microbialites (Figs. 7 and 8).

Advanced deterioration of sponges ultimately produced unrecognizable peloidal domains followed by gravity collapse, and the formation of large voids now preserved as drusy calcite. The association of peloids with calcified sponge fossils is a well described

phenomenon (Pratt, 1982; Pohler and James, 1989; James and Gravestock, 1990; de Freitas and Mayr, 1995; Adachi et al., 2009, 2011; Hong et al., 2012, 2015; Luo and Reitner, 2014, 2015; Park et al., 2015). Warnke (1995) suggests that calcification of ancient sponge tissue through microbially induced processes such as ammonification and sulfate reduction, best explains the existence of calcified sponges in fossilized reefs. Reitner (1993) verified this process at work in modern sponges. Neuweiler et al. (2007) demonstrated that early calcification of modern sponges may actually result from necrosis of sponge collagen networks in still living organisms. Either way, it is clear that calcification of decaying sponge tissue is an important process in the formation of peloidal domains in carbonate sediments. Of course, the presence of a peloidal domain does not necessarily correlate to the prior presence of a sponge. The generation of peloid-rich domains can also be attributed to other factors; Riding and Tomás (2006) suggest that degradation of bacterial colonies are responsible for the formation of peloidal films encrusting Cretaceous stromatolites. Zhuravlev and Wood (1995) describe macroburrows filled with faecal pellets now preserved as peloids. Our specimens possess many macroburrow examples (Fig. 7H), and some microbial structures that although not containing peloids, do host microbially precipitated micritic clumps (Fig. 8H). These contextual references alleviate some of the ambiguity when deciding between sponge and non-sponge-related networks.

This latest discovery adds a significant element to these fenestral, filament-like and peloidal networks; many of the spicules of this as yet unclassified sponge are slightly curved to arcuate (Fig. 6D-G). Marginal decay and separation of calcified sponge tissue from around these spicules produced arcuate, 50 – 500 μm filament-like cavities that

obscured the former presence of spicules when viewed in cross-section (Fig. 7A-D). Further deterioration produced unrecognizable peloidal domains (Fig. 7A,B and E,F). These observations suggest that some vermiform, spongiform, and ‘algal’ microstructures, microtubule domains as well some peloidal domains described in the literature may actually characterize different stages of decay representative of sponges like the ones described in this study.

Third, these sponges cannot be seen in the field, and where they are preserved, can only be detected using microscopy. Unlike many coeval lithistid taxa, which typically had cm to dm-scale body-plans (Shapiro and Rigby, 2004; Johns et al., 2007; Kruse and Zhuravlev, 2008; Schuster et al., 2014; Luo and Reitner, 2015), the Notch Peak sponges only achieved mm to cm-scale dimensions. Such minuscule sponges are known from both modern (Reitner, 1993) and ancient environments (Luo and Reitner, 2015). Sponges closely resembling those described in this paper have also been described from middle Cambrian to Middle Ordovician rocks in China and Korea (Hong et al., 2012; Chen et al., 2014; Hong et al., 2014; Lee et al., 2014; Park et al., 2015). Most of these authors agreed that detection of this particular kind of sponge was almost impossible in the field.

Finally, this kind of sponge typically took a lamina-like form that encrusted both itself and locally associated microbial communities (Fig. 5). As such, the overall meso-scale fabric, although poorly laminated, is stromatolitic (Fig. 3A). This characteristic extends to the overall macro-scale morphology producing columnar ‘stromatolites (Fig. 4B and D).’ Up until recently, middle to late Cambrian stromatolitic microbialites were simply assumed to represent a microbial, non-metazoan reef-building community. As such, many microbialites, including thrombolitic and dendrolitic forms, may actually

contain remnants of metazoan reef-builders that have simply been overlooked. Luo and Reitner (2014; 2015) confirmed this observation when they found sponges in Carboniferous and Triassic ‘stromatolites’ that had previously been interpreted as metazoan-free microbial buildups. Taken together, these observations make it very easy to overlook this reef’s metazoan component, and by extension, may mean that other similar reefs have been overlooked at other localities around the world.

Conclusions

- I. Some lithistid sponge-microbial reef-building communities constructed laminated ‘stromatolites.’
- II. This particular kind of lithistid sponge can easily be overlooked in the fossil record for several reasons: 1) These sponges encrusted automicritic laminae using a similar lamina-like morphology that can easily be overlooked in microbial buildups. 2) These lithistid sponges are typically very small compared to other coeval forms. 3) These sponges have a low preservation potential compared with other coeval forms due to the absence of a fully fused skeleton. 4) These sponges possessed arcuate spicules and spicule rays. As the sponges calcified, the micritized sponge tissue around these geometric surfaces would naturally have possessed some curvature. Slight deterioration and marginal separation of calcified sponge tissue from these spicules produced filament-like fenestral and peloidal domains that obscured the former spicule networks when viewed in cross-section.

III. Some vermiform, spongiform, and 'algal' microstructures, microtubule domains as well some peloidal domains described in the literature may actually characterize different stages of decay representative of sponges like the ones described in this study.

References

- ADACHI, N., EZAKI, Y., LIU, J., and CAO, J., 2009, Early Ordovician reef construction in Anhui Province, South China: a geobiological transition from microbial to metazoan-dominant reefs: *Sedimentary Geology*, v. 220, p. 1–11.
- ADACHI, N., EZAKI, Y., and LIU, J., 2011, Early Ordovician shift in reef construction from microbial to metazoan reefs: *PALAIOS*, v. 26, p. 106–114.
- ADACHI, N., LIU, J., and EZAKI, Y., 2013, Early Ordovician reefs in South China (Chenjiache section, Hubei Province): deciphering the early evolution of skeletal-dominated reefs: *Facies*, v. 59, p. 451–466.
- ADACHI, N., KOTANI, A., EZAKI, Y., and LIU, J., 2015, Cambrian Series 3 lithistid sponge-microbial reefs in Shandong Province, North China: reef development after the disappearance of archaeocyaths: *Lethaia*, v. 48, p. 405–416.
- BOURQUE, P.-A., and BOULVAIN, F., 1993, A model for the origin and petrogenesis of the red stromatactis limestone of Paleozoic carbonate rocks: *Journal of Sedimentary Petrology*, v. 63, p. 607–619.
- BRUNTON, F.R., and DIXON, O.A., 1994, Siliceous sponge-microbe biotic associations and their recurrence through the Phanerozoic as reef mound constructors: *PALAIOS*, v. 9, p. 370–387.
- CARRERA, M.G., and BOTTING, J.P., 2008, Evolutionary history of Cambrian spiculate sponges: implications for the Cambrian evolutionary fauna: *PALAIOS*, v. 23, p. 124–138.
- CHEN, J., LEE, J.-H., and WOO, J., 2014, Formative mechanisms, depositional processes, and geological implications of Furongian (late Cambrian) reefs in the North China Platform: *Palaeogeography, Palaeoclimatology, Palaeoecology*, v. 414, p. 246–259.
- DE FREITAS, T., and MAYR, U., 1995, Kilometer-scale microbial buildups in a rimmed carbonate platform succession, Arctic Canada: new insight on Lower Ordovician reef facies: *Bulletin of Canadian Petroleum Geology*, v. 43, p. 407–432.
- FLÜGEL, E., and STEIGER, T., 1981, An Upper Jurassic sponge-algal buildup from the northern Frankenalb, West Germany, *in* Toomey, D.F., ed., *European Fossil Reef Models: Society of Economic Paleontologists and Mineralogists, Special Publication*, v. 30, p. 371–397.
- HINTZE, L. F., TAYLOR, M. E., and MILLER, J. F., 1988, Upper Cambrian—Lower Ordovician Notch Peak Formation in Western Utah: U.S. Geological Survey, Professional Paper, 1393, p. 1–29.

- HONG, J., CHO, S.-H., CHOH, S.-J., WOO, J., and LEE, D.-J., 2012, Middle Cambrian siliceous sponge–calcimicrobe buildups (Daegi Formation, Korea): Metazoan buildup constituents in the aftermath of the Early Cambrian extinction event: *Sedimentary Geology*, v. 253–254, p. 47–57.
- HONG, J., CHOH, S.-J., and LEE, D.-J., 2014, Tales from the crypt: Early adaptation of cryptobiontic sessile metazoans: *PALAIOS*, v. 29, p. 95–100.
- HONG, J., CHOH, S.-J., and LEE, D.-J., 2015, Untangling intricate microbial-sponge frameworks: The contributions of sponges to Early Ordovician reefs: *Sedimentary Geology*, v. 318, p. 75–84.
- JAMES, N.P., and GRAVESTOCK, D., 1990, Lower Cambrian shelf and shelf margin buildups, Flinders Ranges, South Australia: *Sedimentology*, v. 37, p. 455–480.
- JOHNS, R.A., DATTILO, B.F., and SPINCER, B., 2007, Neotype and redescription of the Upper Cambrian anthaspidellid sponge, *Wilbernicyathus donegani* Wilson, 1950: *Journal of Paleontology*, v. 81, p. 435–444.
- KLAPPA, C.F., and JAMES, N.P., 1980, Small lithistid sponge bioherms, early Middle Ordovician Table Head Group, western Newfoundland: *Bulletin of Canadian Petroleum Geology*, v. 28, p. 425–451.
- KOBLUK, D.R., 1988, Cryptic faunas in reefs: ecology and geologic importance: *PALAIOS*, v. 3, p. 379–390.
- KRUSE, P.D., and ZHURAVLEV, A.Y., 2008, Middle–Late Cambrian *Rankenella*–*Girvanella* reefs of the Mila Formation, northern Iran: *Canadian Journal of Earth Sciences*, v. 45, p. 619–639.
- KRUSE, P.D., and REITNER, J.R., 2014, Northern Australian microbial metazoan reefs after the mid-Cambrian mass extinction: *Memoirs of the Association of Australasian Paleontologists*, v. 45, p. 31–53.
- LARMAGNAT, S., and NEUWEILER, F., 2015, Taphonomic filtering in Ordovician bryozoan carbonate mounds, Trenton Group, Montmorency Falls, Quebec, Canada: *PALAIOS*, v. 30, p. 169–180.
- LEE, J.-H., CHEN, J., CHOH, S.-J., LEE, D.-J., HAN, Z., and CHOUGH, S.K., 2014, Furongian (late Cambrian) sponge-microbial maze-like reefs in the North China Platform: *PALAIOS*, v. 29, p. 27–37.
- LI, Q., LI, Y., and KIESSLING, W., 2015, Early Ordovician lithistid sponge-*Calathium* reefs on the Yangtze Platform and their paleoceanographic implications: *Palaeogeography, Palaeoclimatology, Palaeoecology*, v. 425, p. 84–96.

- LUO, C., and REITNER, J., 2014, First report of fossil "keratose" demosponges in Phanerozoic carbonates: preservation and 3-D reconstruction: *Naturwissenschaften*, v. 101, p. 467–477.
- LUO, C., and REITNER, J., 2015, 'Stromatolites' built by sponges and microbes –a new type of Phanerozoic bioconstruction: *Lethaia*, Doi: 10.1111/let.12166.
- MILLER, J. F., EVANS, K. R., LOCH, J.D., ETHINGTON, R. L., STITT, J. H., HOLMER, L., and POPOV, L. E., 2003, Stratigraphy of the Sauk III interval (Cambrian-Ordovician) in the Ibex area, western Millard County, Utah and central Texas: *Brigham Young University Geology Studies*, v. 47, p. 23–118.
- MONTY, C.L.V., 1995, The rise and nature of carbonate mud-mounds: an introductory actualistic approach, *in* Monty, C.L.V., Bosence, D.W.J., Bridges, P.H., and Pratt, B.R, eds., *Carbonate Mud-Mounds: Their Origin and Evolution: International Association of Sedimentologists, Special Publication*, v. 23, p. 11–48.
- NARBONNE, G.M., and DIXON, O.A., 1984, Upper Silurian lithistid sponge reefs on Somerset Island, Arctic Canada: *Sedimentology*, v. 31, p. 25–50.
- NEUWEILER, F., DAOUST, I., BOURQUE, P.A., and BURDIGE, D.J., 2007, Degradative calcification of a modern siliceous sponge from the Great Bahama Bank, The Bahamas: A guide for interpretation of ancient sponge-bearing limestones: *Journal of Sedimentary Research*, v. 77, p. 552–563.
- PALMER, A.R., 1981, Subdivision of the Sauk Sequence, *in* Taylor, M.E., ed., *Short Papers for the Second Symposium on the Cambrian System: U.S. Geological Survey Open-File Report 81-743*, p. 160–162.
- PARK, J., LEE, J.-H., HONG, J., CHOH, S.-J., LEE, D.-C., and LEE, D.-J., 2015, An Upper Ordovician sponge-bearing micritic limestone and implication for early Paleozoic carbonate successions: *Sedimentary Geology*, v. 319, p. 124–133.
- POHLER, S.M., and JAMES, N.P., 1989, Reconstruction of a Lower/Middle Ordovician carbonate shelf marine: Cow Head Group, Western Newfoundland: *Facies*, v. 21, p. 189–262.
- POKORNY, V., 1965, *Principles of Zoological Micropaleontology*, Pergamon Press, Oxford, New York, 455 p.
- PRATT, B.R., 1982, Stromatolitic framework of carbonate mud-mounds: *Journal of Sedimentary Petrology*, v. 52, p. 1203–1227.
- REITNER, J., 1993, Modern cryptic microbialite/metazoan facies from Lizard Island (Great Barrier Reef, Australia) formation and concepts: *Facies*, v. 29, p. 3–40.

- RIDING, P., and TOMÁS, S., 2006, Stromatolite reef crusts, Early Cretaceous, Spain: bacterial origin of in situ-precipitated peloid microspar? *Sedimentology*, v. 53, p. 23–34.
- RIDING, R., and ZHURAVLEV, A.Y., 1995, Structure and diversity of oldest sponge-microbe reefs: Lower Cambrian, Aldan River, Siberia: *Geology*, v. 23, p. 649–652.
- RIGBY, J.K., 1983, Fossil Demospongia, in Broadhead, T.W., ed., *Sponges and Spongiomorphs: Notes for a Short Course*: University of Tennessee, Department of Geological Sciences, Knoxville, Tennessee. *Studies in Geology*, v. 7, p. 12–39.
- SCHUSTER, A., ERPENBECK, D., PISERA, A., HOOPER, J., BRYCE, M., FROMONT, J., and WORHEIDE, G., 2014, Deceptive desmas: Molecular phylogenetics suggests a new classification and uncovers convergent evolution of lithistid demosponges: *Plos One*, doi: 10.1371/journal.pone.0116038.
- SHAPIRO, R.S., and AWRAMIK, S.M., 2006, *Favosamaceria cooperi* new group and form: A widely dispersed, time-restricted thrombolite: *Journal of Paleontology*, v. 80, p. 411–422.
- SHAPIRO, R.S., and RIGBY, J.K., 2004, First occurrence of an in situ Anthaspidellid sponge in a dendrolite mound (Upper Cambrian; Great Basin, USA): *Journal of Paleontology*, v. 78, p. 645–650.
- WARNKE, K., 1995, Calcification processes of siliceous sponges in Visean limestones (counties Sligo and Leitrim, Northwestern Ireland): *Facies*, v. 33, p. 215–228.
- ZHURAVLEV, A.Y., 1995, Lower Cambrian reefal cryptic communities: *Palaentology*, v. 38, p. 443–470.

CHAPTER FOUR

CONCLUSIONS

Excellent exposures within the uplifted mountains of southwestern Utah present geologists with a unique opportunity to study upper Cambrian microbialite reef environments and ecologies. The upper Hellnmaria Member of the Notch Peak Formation located in the northern House Range of southwestern Utah contains over 40 meters of in-situ microbialites separated into at least 11 microbialite-bearing beds. Most of these beds, although sharing the same geographic location, differ substantially with regard to their paleoenvironmental and paleoecological constituents. Two of these beds were chosen for the purpose of studying some of these components, and then applying our results to both ancient and modern analogues.

In one bed, the existence of a uniquely preserved suite of microbialite morphologies capturing many phases of elongate-related processes in vertical succession, serves as a useful case study from which to compare strongly elongate microbialites found in other ancient, as well as modern environments. This example demonstrates that coalescence is the most effective mechanism for constructing strongly elongate microbialites, parallel to flow, in deep-subtidal or wave restricted settings where intertidal scouring processes are weak. Other elongate-related processes do create strongly elongate structures, but in these cases the elongate forms are intertidal or very shallow subtidal structures that owe their primary morphology to a combination of sheet-like microbial growth combined with intertidal mechanical wave scour. Although not a new discovery, this example also confirms that elongate morphologies, according to both modern and ancient analogues, are always formed in the presence of directional

hydrodynamics where the long axes parallel the direction of flow, irrespective of whether those forms are constructed in a subtidal, intertidal or supratidal setting. The hypothesis put forward by Mariotti et al. (2014) as well as the example discussed by Shapiro (1990) are exceptions. If, as in the latter case, elongate microbialites are found to have formed perpendicular to flow, then this might indicate some kind of substrate control that overprinted the hydrodynamic component. This study also shows that a close-packing relationship is important for elongation by means of coalescence to occur. Since most Proterozoic and early Paleozoic microbialites are closely packed, this factor, in conjunction with coalescence may provide a good explanation for the presence of strongly elongate forms in the fossil record. Finally, extremely narrow interspaces demonstrate that modern examples of sculpting by mechanical, intertidal wave scour, are not good analogues from which to interpret some ancient examples. Extremely narrow and consistent interspaces found in the Notch Peak growth series are best explained by abrasion related to the propagation of less turbulent internal wave bores which entrain smaller, less abrasive detrital grains than do intertidal surface waves propagating across siliciclastic beach zones.

In bed 11, the presence of microbial-sponge reef-building communities that constructed laminated 'stromatolites' reflects a new kind of bio-structure that up till now has only been described from the Carboniferous and Triassic. This particular kind of lithistid sponge has most likely been overlooked in the fossil record for several reasons:

- 1) These sponges encrusted automicritic laminae using a similar lamina-like morphology that can easily be overlooked in microbial buildups.
- 2) These lithistid sponges are typically very small compared to other coeval forms.
- 3) These sponges have a low

preservation potential compared with other coeval forms due to the absence of a fully fused skeleton. 4) These sponges possessed arcuate rays. As the sponges calcified, the micritized sponge tissue around the rays would naturally have possessed some curvature. Slight deterioration and marginal separation of calcified sponge tissue from these spicules produced filamentous and peloidal domains that obscured the former spicule networks in several sponges. This means that vermiform, spongiform, and 'algal' microstructures, as well as microtubule domains and perhaps some other carbonate microstructures described in the literature may actually represent poorly preserved sponge spicule networks.

APPENDIX A

WACKESTONE—GRAINSTONE INTERVAL

I also measured the wackestone-grainstone interval located between beds 10 and 11 (Fig 2B, p. 71) at seven different locations along an 8 km northwest-southeast transect that runs through the research area. I found that this interval generally thickens in a northwesterly direction from 22 m at outcrop 2U44 to about 30 m at outcrop 2U31 (Fig. 1). I drew a line connecting these two outcrops and then superimposed the remaining five outcrops onto that line. This trend may indicate a relative deepening towards the northwest, perhaps signifying a mini carbonate ramp that dipped down into what was left of the middle Cambrian HRE trough.

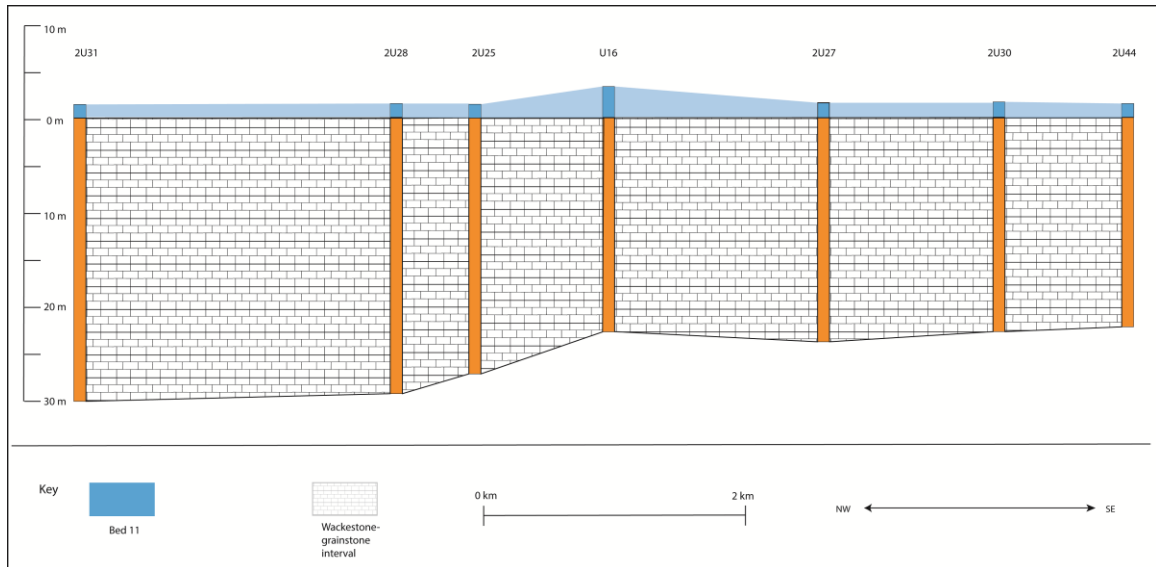


Fig. 1. Wackestone-grainstone interval located between beds 10 and 11 (Fig 2B, p. 71). Notice general thickening of the interval towards the northwest. Datum set at the base of bed 11. Blue color is bed 11.

APPENDIX B

ADDITIONAL METHODS

All microbialite-related insoluble residues came from drill core samples sourced from a single outcrop. Cores were drilled in the interspatial zones as well as within the microbialites themselves, and spaced so as to obtain data from most of the discrete morphologies. Each sample was weighed, placed into a 500 mL beaker and then left to dissolve overnight in about 100 mL of 6N HCL. Acid was tested for strength the next day, and more acid added to the sample/acid mixture if the chemical reaction was poor. Once samples were completely dissolved, the sample/acid mixture was added to two 50 mL test tubes and placed in a Beckman, Coulter Allegra X-30R Centrifuge for 15 minutes at 3000 RPMs. After 15 minutes, test tubes were decanted leaving only the sediment plug behind. Deionized water was then added to the test tubes which were then thoroughly shaken and placed back in the centrifuge for an identical run. After test tubes were drained off for the second time, more deionized water was added, the tubes were then shaken vigorously, and their contents filtered. Filter paper was weighed both prior to filtering and after the filter, combined with insoluble residue, had completely dried. The difference was then recorded as a percent value.

Thin-section samples were likewise sourced from a single outcrop, although four extra samples were obtained from the interspace zones of the strongly elongate layer at four other locations. Most of our thin sections were prepared at LLU using a Pelcon Automatic thin section machine. SEM and EDS data were obtained at LLU using a Tescan Vega II instrument interconnected to a Noran EDS device utilizing NORAN system SIX spectral imaging software. In order to qualitatively determine particle size

and composition of insoluble residues, a small portion of the sample was placed on a 1 cm diameter aluminum stub, and then completely disaggregated by thoroughly mixing the sample with acetone while on the stub. This process moved heavier particles to the stub center, while smaller particles formed a thin film at the stub circumference. We were then able to closely examine the stub qualitatively to determine average clast sizes and composition. XRD analysis was performed at LLU using a Bruker, D8 Advance machine and then interpreted using JADE software.

APPENDIX C

CROSS-BEDDING

Very fine cross-bedding is present to a small degree at the bottom of the wackestone interval intercalated between beds 10 and 11 (Fig 2B, p. 71 and Fig. 2A below). One-half m thick cross-beds, composed of a very well sorted, coarse-grained ooid grainstone were correlated for about 100 m at the top of the same interval at the U16 outcrop location (Fig. 2B and C below). This cross-bedded grainstone bed was also found at another location about 3 km away (Fig. 2D below). In both cases the bed is located 0.5 m to 1 m below bed 11 (Fig. 2B below), but we are not sure if the bed is connected with the U16 location. Similarly, we were unable to detect the presence of tidal channels at either site, but it seems likely that this herring-bone cross-stratification reflects bi-directionality associated with tidal channels. In all three cases, dip directions favor paleocurrent flowing from the northwest and southeast.

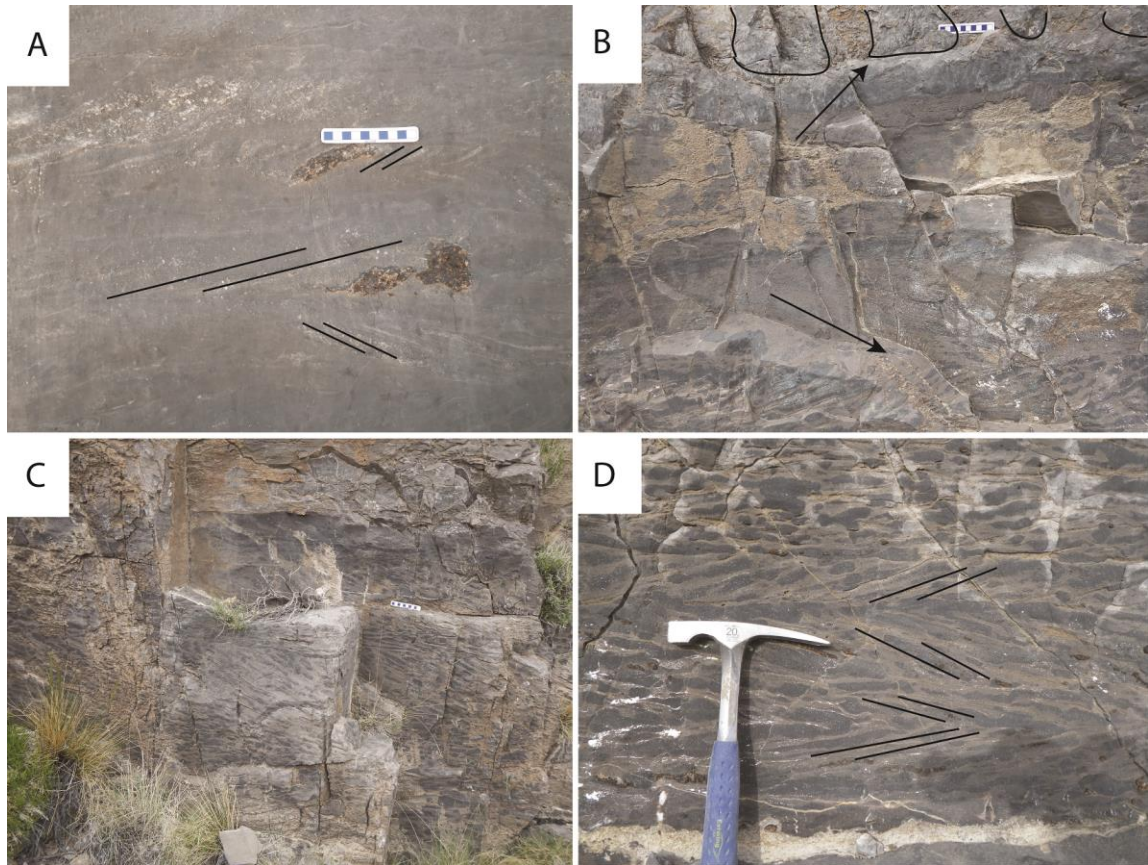


Fig. 2. Cross-beds located at the bottom and top of wackestone-grainstone interval between beds 10 and 11. A) Very finely cross-bedded layer located just above bed 10 at the U16 outcrop (sense of cross-beds outlined). B) 0.5 m to 1 m coarse-grained, yet laminar to massive layer intercalated between cross-bedded layer (bottom arrow) and stromatolites of bed 11 (top arrow) (base of some stromatolites outlined). C) Cross-bedded layer located at the U16 outcrop. D) Cross-bedded layer located about 3 km to the west of U16 (sense of cross-beds outlined). All cross-bed dip directions favor paleocurrent flowing from the northwest and southeast.

APPENDIX D

SEM IMAGES OF INSOLUBLE RESIDUES

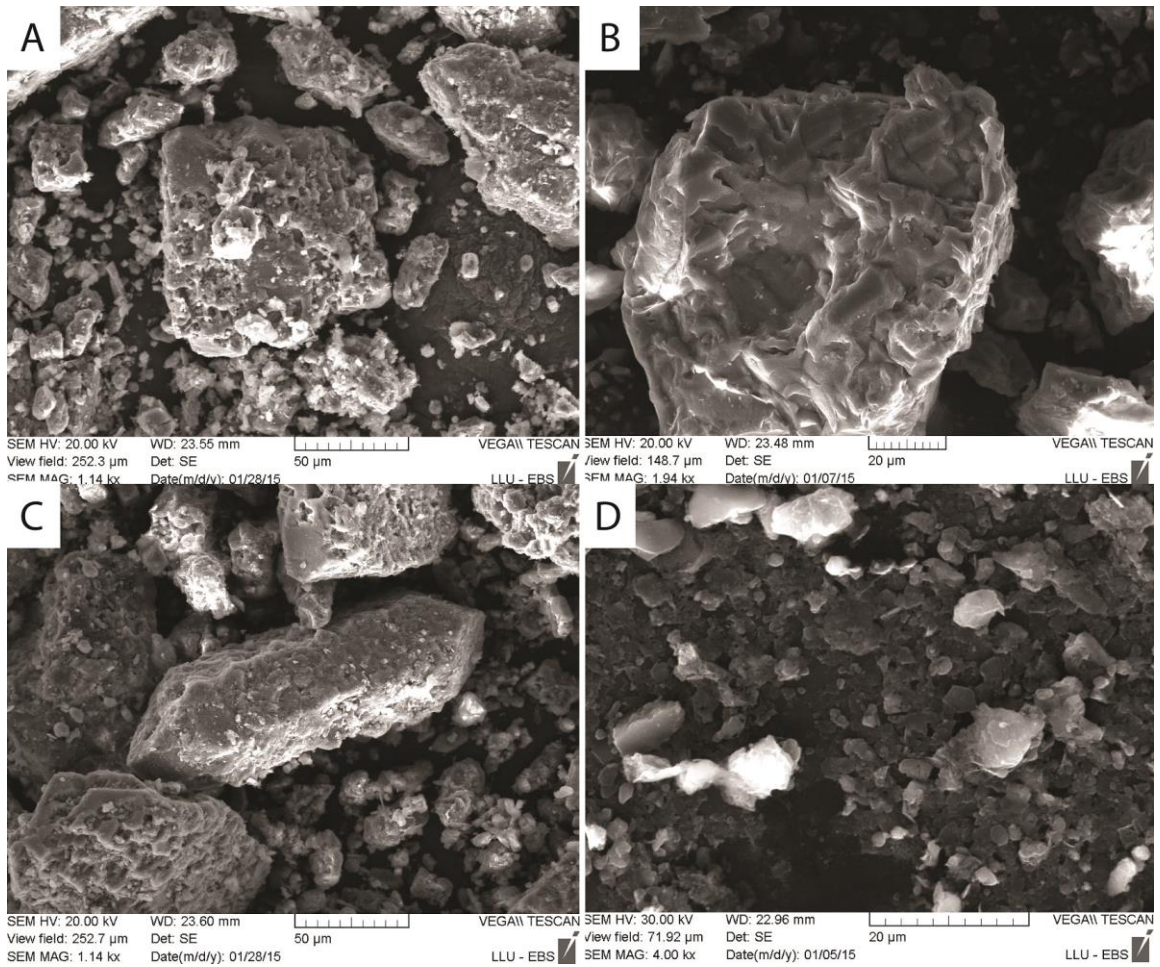


Fig. 4. SEM images of insoluble residues. A) Potassium feldspar showing signs of decay. B) Detrital quartz. C) Authigenic quartz (notice euhedral crystal center of image). D) Putative detrital chlorite or muscovite.

APPENDIX E

HYDRODYNAMICS AFFECTS MORPHOLOGY

Fossilized elongate microbialites, although lacking the actualistic advantage of modern day analogues, seem to strengthen the assumption that directional hydrodynamics are extremely important for elongation. Hoffman (1967; 1976) determined that the subtidal, elongate stromatolites of the lower Proterozoic Pethei Formation in Northwest Territories (NWT), Canada, owed their directional growth and primary orientation to the hydrodynamic flow regime. He was even able to show that over-steepened, laterally linked stromatolites accreted laminae and thickened in the up-current direction. Campbell and Cecile (1975) duplicated these findings for subtidal, stromatolitic, elongate mounds, 30 m long, 10 m wide and about 3 m high, found in the Precambrian Goulburn Group, also in NWT, Canada. Upper Proterozoic, subtidal, stromatolitic mounds, several tens of m long and a few m high, found on Victoria Island, northwestern Canada, are considered by Young and Long (1976) to have been influenced by long-shore currents, with long axes both parallel to current direction and shoreline. In this example, the mound edges contain discrete, elongate stromatolites that are likewise thought to be shaped by the same long-shore currents. Individual stromatolites are arranged in horizontal beds stacked one upon the other, and are about 25 cm high and about 2 – 15 cm in diameter for round forms. In plan-view, these individual stromatolites exhibit a change in morphology from circular at the center of the mound to strongly elongate at the mound edge, with the long axes parallel to that of the mound (Fig. 4). Each mound is separated by a channel from a few cm to about 50 cm in width which acted as a conduit for water flow. Since channelized-flow is more likely to intensify flow velocity at mound margins, it is not

surprising that Young (1973) and Young and Long (1976) suggest a strong correlation between current flow and acute elongation at these margins. Mounds of similar dimensions have also been found in the lower Proterozoic Pretoria Group in South Africa, and likewise are interpreted to have grown in a subtidal environment where the long axes paralleled the hydrodynamic flow regime (Button and Vos, 1977). Although Button and Vos (1977) do not discuss processes related to elongation, they nevertheless imply a direct correlation between long axes direction and hydrodynamic flow.

According to Eriksson (1977), elongate stromatolitic mounds that average 10 m wide and about 40 m long from the related Chuniespoort and Chaap Groups in South Africa, likewise formed as a result of directional hydrodynamics in a subtidal environment. He documents clear instances of mechanical scour, trapping, binding, and over-steepening of laminae in the up-current direction.

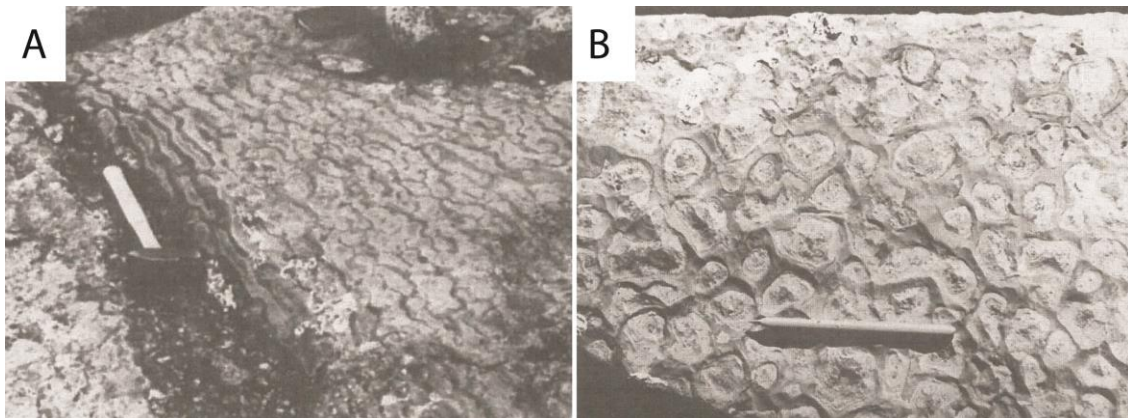


Fig. 4. Round to elongate transition of small microbialites found in the same elongate mound. A) Elongate microbialites at the margin of a large, elongate mound. The hammer is sitting in the inter-mound zone. Many of these individual forms are coalesced. B) Round microbialites from the center of the same mound in A. Photos courtesy G. Young, [http://dx.doi.org/10.1016/0301-9268\(74\)90015-1](http://dx.doi.org/10.1016/0301-9268(74)90015-1), license number 3702150483903. Cropped for detail.

APPENDIX F

NUTRIENT DIFFUSION

Petroff et al. (2010) have successfully tested a hypothesis that explains consistent, uniform, centimeter scale spacing for coniform microbialites growing in Yellowstone National Park (YNP). They predicted that narrow, uniform interspaces reflect the creation of a nutrient gradient due to the photosynthetic activities of microbes. Essentially, over a 12 hour period, cyanobacteria harvest their nutrients more rapidly than the nutrients are able to move through the liquid media. This produces a diffusion gradient that exists over a length scale of about 1 cm (0.5 cm away from each microbialite). If this gap closes to less than 1 cm, then microbes from one microbialite will begin competing with microbes from a neighboring microbialite for nutrients. In order to limit competition, the cyanobacteria therefore maintain this regular 1 cm spacing which in turn produces a highly uniform centimeter scaled interspace between individual forms. They tested their hypothesis by growing mats under a range of day-night cycles that varied from 3 to 48 hours. They confirmed that the 1 cm spacing between conical aggregates was a direct function of microbial communities limiting competition for nutrients. This 1 cm spacing between forms also holds true for ridge-like microbialites that are growing in YNP. During unidirectional flow, molecular diffusion in the direction of flow is of course negligible, but still occurs when transporting the required nutrients to the cyanobacteria perpendicular to flow. As a result, long ridges with consistent, 1 cm wide interspaces, develop.

Extreme caution must of course be used when applying this data to the *Hellnmaria* forms. It must be kept in mind that the microbialites growing in YNP are

freshwater examples forming in the absence of sedimentation and are many orders of magnitude smaller. Secondly, and I think most importantly, their model only works for 1 cm wide interspace gaps. It is true that the *Hellnmaria* elongate microbialites exhibit narrow interspaces of between 3 and 8 cm, but that is still a far cry from 1 cm. Since Petroff et al. do try to apply their model to the fossil record (Petroff et al., 2010, p. 9960), they proposed some modifications that may help explain the much larger interspace gaps found in fossilized forms. They hypothesized that competition for nutrients might continue to influence interspace gaps, but on a larger scale, given the role of molecular diffusion *in concert* with moving water and advection (Petroff et al., 2010, p. 9959).

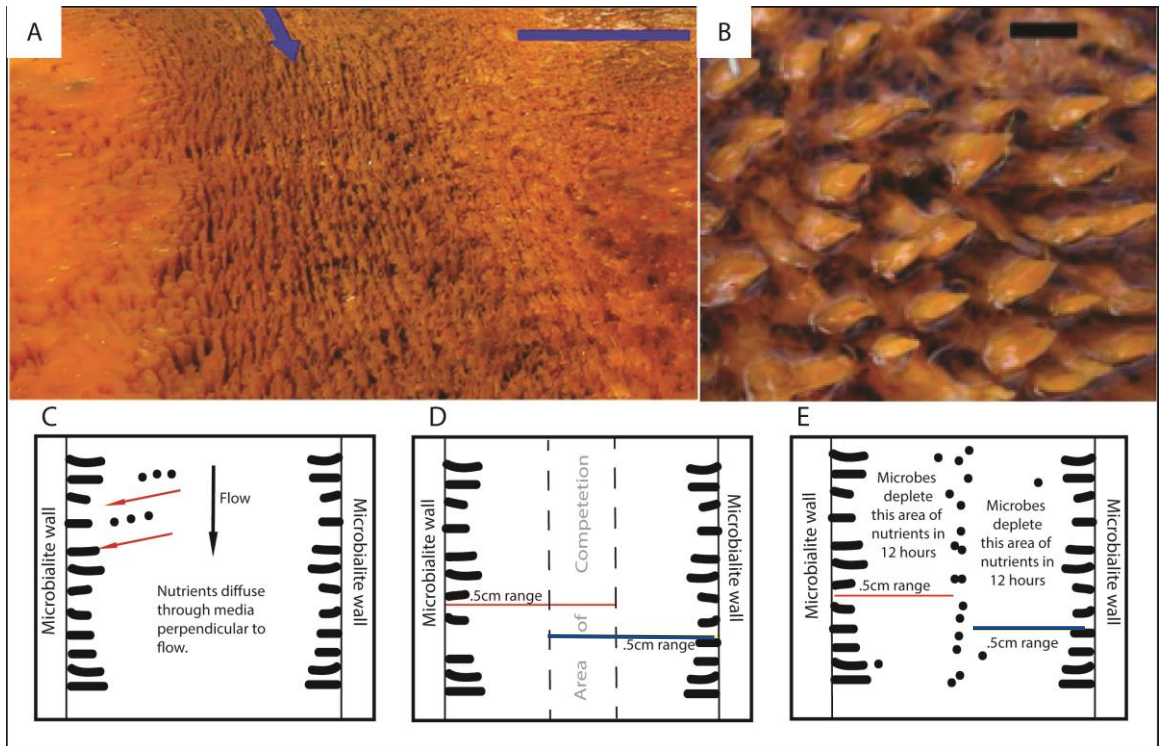


Fig. 5. Interpretation from Petroff et al. (2010) explaining microbial nutrient gradients. A) Elongate ridges formed in the presence of unidirectional, laminar flow (arrow shows flow direction) from YNP. Scale = 30 cm. B) Cones formed in the presence of standing water. Scale = 1 cm. C) Diffusion of nutrients is perpendicular to flow. Dots represent nutrients. Squiggles represent microbes attached to the sides of adjacent microbialites. D) Red and blue lines represent the range in which microbes deplete the water column therefore setting up a diffusion gradient. If microbes are too close to each other, as in this frame, an area of competition is generated (between dotted lines). This is not favorable for optimal microbial metabolism. E) A distance of 1cm separating microbes produces a favorable metabolic scenario. Microbes therefore maintain this distance. Image in A courtesy of Petroff, A. P., Sim, M. S., Maslov, A., Krupenin, M., Rothman, D. H., and Bosak, T., 2010. Biophysical basis for the geometry of conical microbialites. *Proc. Natl. Acad. of Sci. U. S. A.* 107, 9956-9961. Image in B courtesy of the Geological Survey of Western Australia, Department of Mines and Petroleum. © State of Western Australia 2015.

References

- BUTTON, A., and VOS, R., 1977, Subtidal and intertidal clastic and carbonate sedimentation in a macrotidal environment: an example from the lower Proterozoic of South Africa: *Sedimentary Geology*, v. 18, p. 175 – 200.
- CAMPBELL, F.H.A., and CECILE, M.P., 1975, Report on the geology of the Kilohigok Basin, Goulburn Group, Bathhurst Inlet: N. W. T. Geological Survey of Canada, Paper, 75-1, p. 297 – 306.
- ERIKSSON, K.A., 1977, Tidal flat and subtidal sedimentation in the 2250 M. Y. Malmani Dolomite, Transvall, South Africa: *Sedimentary Geology*, v. 18, p. 223 – 244.
- HOFFMAN, P., 1967, Algal microbialites: use in stratigraphic correlation and paleocurrent determination: *Science*, v. 157, p. 1043 – 1045.
- HOFFMAN, P., 1976, Stromatolite morphogenesis in Shark Bay, Western Australia, *in* Walter, M. R., ed., *Developments in Sedimentology: Stromatolites*, Vol 20. Elsevier, Amsterdam, pp. 261 – 271.
- PETROFF, A.P., SIM, M.S., MASLOV, A., KRUPENIN, M., ROTHMAN, D.H., and BOSAK, T., 2010, Biophysical basis for the geometry of conical microbialites: *Proceedings of the National Academy of Science, U. S. A.*, v. 107, p. 9956-9961.
- YOUNG, G.M., 1973, Stratigraphy, paleocurrents and stromatolites of Hadrynian (Upper Cambrian) rocks of Victoria Island, Artic Archipelago, Canada: *Precambrian Research*, v. 1, p. 13 – 41.
- YOUNG, G.M., and LONG, D.G.F., 1976, Microbialites and basin analysis: an example from the upper Proterozoic of northwestern Canada. *Palaeogeography, Palaeoclimatology, Palaeoecology*, v. 19, p. 303 – 318.